Vehicle restraint system crash test modelling – Application to steel-wood structures

Clément Goubel

N° d'ordre Année 2012

THESE DE L'UNIVERSITE DE LYON

Délivrée par

L'UNIVERSITE CLAUDE BERNARD LYON 1

ECOLE DOCTORALE
MEGA (Mécanique, Energétique, Génie civil, Acoustique)

DIPLOME DE DOCTORAT

(arrêté du 7 août 2006)

soutenue publiquement le 13/12/2012

par

M GOUBEL Clément

TITRE :
Modélisation d'essais de choc sur dispositifs de retenue de véhicules
-
Application aux dispositifs mixtes acier-bois

Directeurs de thèse :
M MASSENZIO Michel
Mme RONEL Sylvie

JURY :
M ANGHILERI Marco
M MARKIEWICZ Eric
M ICHCHOU Mohamed
M DI PASQUALE Edmondo
M BLOCH Jean

University Claude Bernard Lyon 1 – Ecole doctorale MEGA, INSA de Lyon
Thesis reference number: XXX – 2012

PhD THESIS

Vehicle restraint system crash test modelling
–
Application to steel-wood structures

Presented and defended publicy on 13/12/2012 at IUT Lyon 1 – Site Gratte-Ciel

A Dissertation submitted in partial fulfilment of the requirements for the degree of

Doctor of University Claude Bernard – Lyon 1
(Department of Mechanical Engineering)
by

Clément GOUBEL

Graduate Committee

Reviewers:
Professor M. Anghileri, Polytecnico di Milano, Italia
Professor E. Markiewicz, Université de Valenciennes, France

Advisors:
Professor M. Massenzio, Université Claude Bernard Lyon 1, France
Professor S. Ronel, Université Claude Bernard Lyon 1, France

Examiners:
Professor M. Ichchou, Ecole Centrale de Lyon, France
PhD E. Di Pasquale, Université de Valenciennes, France
PhD J. Bloch, LIER, France

Biomehanics and Impact Mechanics laboratory
UMR_T 9406

Inrets Road Equipment Laboratory

Modélisation d'essais de choc sur dispositifs de retenue de véhicules

-

Application aux dispositifs mixtes acier-bois

Préambule

Cette thèse a été financée par le LIER (Laboratoire INRETS Equipements de la Route) dans le cadre d'un contrat CIFRE avec l'ANRT (Association Nationale de la Recherche et de la Technologie) et le LBMC (Laboratoire de Biomécanique et de Mécanique des Chocs – UMR_T9406), unité mixte de recherche entre l'IFSTTAR (Institut Français des Sciences et Technologies des Transports, de l'aménagement et des Réseaux) et l'Université Claude Bernard Lyon1. Les travaux qui ont été menés s'inscrivent dans un contexte normatif européen. En particulier, les validations des modèles numériques s'appuient sur des critères définis par le groupe CEN (Comité Européen de Normalisation) TC226 (Equipements de la route) WG1 (Barrière de sécurité, glissières, garde-corps et parapets) TG5 (Simulation Numérique) auquel le LIER participe activement.
Le rapport de thèse a donc été rédigé en anglais afin d'élargir le champ des lecteurs et afin de pouvoir intégrer des personnes non francophones dans le comité de jury. Un résumé en français se trouve à la fin du document.

Vehicle restraint system crash test modelling

-

Application to steel-wood structures

Foreword

This PhD was funded by LIER (INRETS Road Equipment Laboratory) under a CIFRE contract with ANRT (National Research and Technology Association) and LBMC (Laboratory of Biomechanics and Impact Mechanics), research unit with IFSTTAR (French Institute of science and technology for transport, development and networks) and Claude Bernard Lyon1 University. The research work presented in this document is linked to a European normative context. In particular, validations of numerical models presented in the document are based on criteria defined by CEN (European Committee for Standardization) TC226 (Road Equipment) WG1 (Crash barriers, safety fences, guard rails and bridge parapet) TG5 (Computational Mechanics) to which LIER actively participates.
Thus, this PhD report has been written in English in order to broaden the spectrum of readers and allow non French-speakers to join the PhD committee. A French summary can be found at the end of the document.

Modélisations d’essais de choc sur dispositifs de retenue de véhicules - Application aux dispositifs mixtes acier-bois

---

En France, un tiers des personnes tuées sur la route le sont lors d’un accident sur un obstacle fixe. Dans 90% des cas, ces accidents surviennent après une perte de contrôle du véhicule. Les dispositifs de retenue de véhicule ont pour but de maintenir les véhicules en perdition sur la chaussée en limitant la sévérité de l’impact.
Ces dispositifs doivent subir des essais de chocs normatifs afin de pouvoir être installés sur le bord des routes européennes et d’évaluer leurs performances en termes de sévérité et de déflexion.
Les tolérances existantes sur les paramètres d’essai (véhicule, masse du véhicule, vitesse, angle et point d’impact …) et les incertitudes sur les caractéristiques mécaniques des matériaux constituant le dispositif ont un effet sur les performances de ce dispositifs et doivent être prises en compte lors des calculs
Les dispositifs mixtes (acier-bois) présentent une difficulté supplémentaire en raison de l’hétérogénéité du matériau et de sa sensibilité aux variables d’environnement telles que la température et l’humidité.
Afin de prendre en compte cette variabilité et d’évaluer son impact sur les performances d’un dispositif, des essais dynamiques sur des échantillons de structure ont été réalisés et modélisés numériquement.
Enfin, un modèle complet d’un dispositif de retenue de véhicule a été effectué et corrélé sur un essai de choc réel à l’aide d’une méthode prenant en compte la variation de paramètres physiques liés à l’apparition des modes de ruine de la structure. Une fois corrélé, le modèle a été utilisé afin d’évaluer l’incidence de la modification des caractéristiques mécaniques du bois liée aux variations des conditions environnementales.

Mots clefs
Simulation numérique d’essai de choc, Dispositifs de Retenue de Véhicule, Validation de modèles éléments finis, Etudes paramétriques, Modes de ruine, Bois

---

DISCIPLINE
Mécanique

INTITULE ET ADRESSE DE L'U.F.R. OU DU LABORATOIRE :
Laboratoire de Biomécanique et de Mécanique des Chocs - UMR_T 9406 – Ifsttar/UCB Lyon1
Institut Universitaire de Technologie Lyon 1 – Site Gratte Ciel - Département Génie Mécanique Productique.
17, rue de France 69627 Villeurbanne Cedex

In France, one third of the people dying on the roads are killed after impacting against a hazard. In 90% of the reported cases, these accidents result from loss of control. Vehicle Restraint Systems (VRS) are specially designed to restrain an errant vehicle and to limit impact severity.
Before being installed on the roadsides, these devices have to be crash-tested according to standards in order to evaluate their safety and deflexion performances.
Tolerances exist on impact parameters (vehicle, vehicle mass, impact speed, impact angle, impact point …) and material's mechanical characteristic uncertainties have an effect towards device performances and have to be taken into account during numerical simulations.
Steel-wood structures present an additional numerical challenge due to wood heterogeneity and its sensibility to environment variables such as temperature and moisture content.
In order to assess the effect of this variability toward safety performances, three point bending dynamic experiments on structural samples are performed and modelled.
Finally, a complete model of a vehicle restraint system is built and validated according to real crash test results thanks to a parametric method. This method takes into account the variability of the parameters associated to the failure modes of the structure. Once validated the model is used to assess the effect of wood mechanical properties modifications due to environment variable variations.

Keywords
Crash test simulation, Vehicle Restraint System, Finite element model validation, Parametric studies, Failure modes, Wood

Acknowledgments

I would like to thank Jean-Pierre Verriest for welcoming me at the Laboratory of Biomechanics and Impact Mechanics and Philippe Vezin, current director of the laboratory, for his patience and trust along these past years.

My thanks also go to my PhD advisors Michel Massenzio and Sylvie Ronel for their persistent help and useful experience, as well as for their kindness and availability and for all the good moments we have shared over the last four years and, hopefully for many more years of further cooperation to come.

I am indebted to Professor Marco Anghileri who kindly accepted to review my work. His selfless involvement in the field of Roadside safety and his open minded attitude will remain an example for me all along my career.

I would like to express my gratitude towards Professor Markiewicz for accepting the review of my work as well as to Professor Ichchou for taking part in the jury committee.

Edmondo Di Pasquale has become much more than a professional relation. Most of the work presented here would not have been performed without his contribution. I would like to thank him for his friendship and for the long hours he spent listening to my various puzzlements.

Last but not least, let me thank my colleagues at LIER, especially Jean Bloch who let me start this PhD adventure, Martin Bourbon, Antonin Chalmel-Teulade and Fabien Berthet who all have to endure my moods during the completion of this thesis and took charge of the daily studies of the simulation department at LIER.
My thanks go also to my Ifsttar colleagues including people from Unex without whom no experiment would have been possible.

Table of content

List of Figures

List of Tables

Introduction

Context

In France, one third of the people dying on the roads are killed after impacting against an hazard (2010). In 90% of the reported cases, these accidents result from a loss of control. Vehicle Restraint Systems (VRS) are specially designed to restrain an errant vehicle (stopping it from drifting away of the road).

Roadside safety research started around 50 years ago when traffic grew and when the first highways appeared. In those days, development of structures aiming to restrain an errant vehicle used to be made using common sense, engineering judgement and many crash tests. All French "generic" devices dating from that time seem to be difficult to optimize.
Nowadays, the rules for crash testing are well defined in Europe. EN1317 norm defines the crash conditions and mainly classifies the tested devices as a function of severity indices and working width. Manufacturers of such devices intend to develop more efficient devices reducing both criteria.
In addition to crash testing and engineering observations, the development of a numerical tool became obvious at the same time as the computational resources were growing.
One issue of VRS crash simulations is the number of parameters which can vary and affect the interaction Vehicle/VRS and the VRS performances: Among other things, the tolerances on the crash conditions (Vehicle, Vehicle mass, impact point, impact angle, impact speed, …) and the characteristics of the VRS itself (e.g. the mechanical properties of the materials).
In fact, the variations of mechanical properties could modify the sequence of events (Failure modes) that characterize the behaviour of the structure during the impact of a vehicle and affect the performances of the VRS.
In contrast to conventional design, considering crash loading, the use of safety coefficients is meaningless (in most cases the components are loaded beyond the elastic domain and some until failure point) and analyst must take into account these variations if he wants to be predictive.

Some VRS are structures composed of steel and wood. Currently praised in locations where infrastructure has to be discreet (mountains, countryside), this kind of structure has to pass the same crash tests as other kind of devices. However, this choice of device remains sadly a question of aesthetic more than performances.
The modelling of such structures is even more complex because of wood itself. In fact, wood is sensitive to environment variables (Temperature and Moisture Content) leading to a spread of mechanical characteristics. Furthermore, heterogeneity of the material (growing conditions, defect localization, …) brings some modelling challenge.

Problematic

Some questions arise from this context analysis:

- Is it satisfactory to limit the VRS evaluation to one single test configuration considering impact conditions and mechanical properties variability?
- What is the aim of wood in a steel-wood structure?

The aim of this work is twofold:
A first aim is to develop an efficient numerical tool capable of simulating steel-wood structures under crash loading in order to understand and optimize the use of wood in roadside equipment.
A second aim is to propose a method which integrates the stochastic variations of the parameters linked to the failure modes of the structure in order to obtain a correlated model

matching real crash test results. This correlated model will be used to assess the variability of the mechanical properties of wood and their effect towards VRS performances.

Methodology

Figure 1-1illustrates the steps needed to achieve the defined goals. The assessment of wood variability effect toward VRS performances can be accurately performed only on a correlated numerical model and after assessment of the variability.

As briefly introduced above, a large number of parameters can affect the vehicle/VRS interaction. In order to fulfil the requirements of model correlation as defined in the literature, a method based on failure mode analysis which takes into account the stochastic variation of related physical parameters is proposed.

Few data concerning wood behaviour under impact loading is available in literature.

Therefore, in order to assess the wood variability, some experiments are required and allow on the one hand to assess wood variability and to validate a wood material constitutive law available in the literature. On the other hand, experimental data, thanks to the simplicity of the test configuration, brings needful data to improve the modelling techniques.

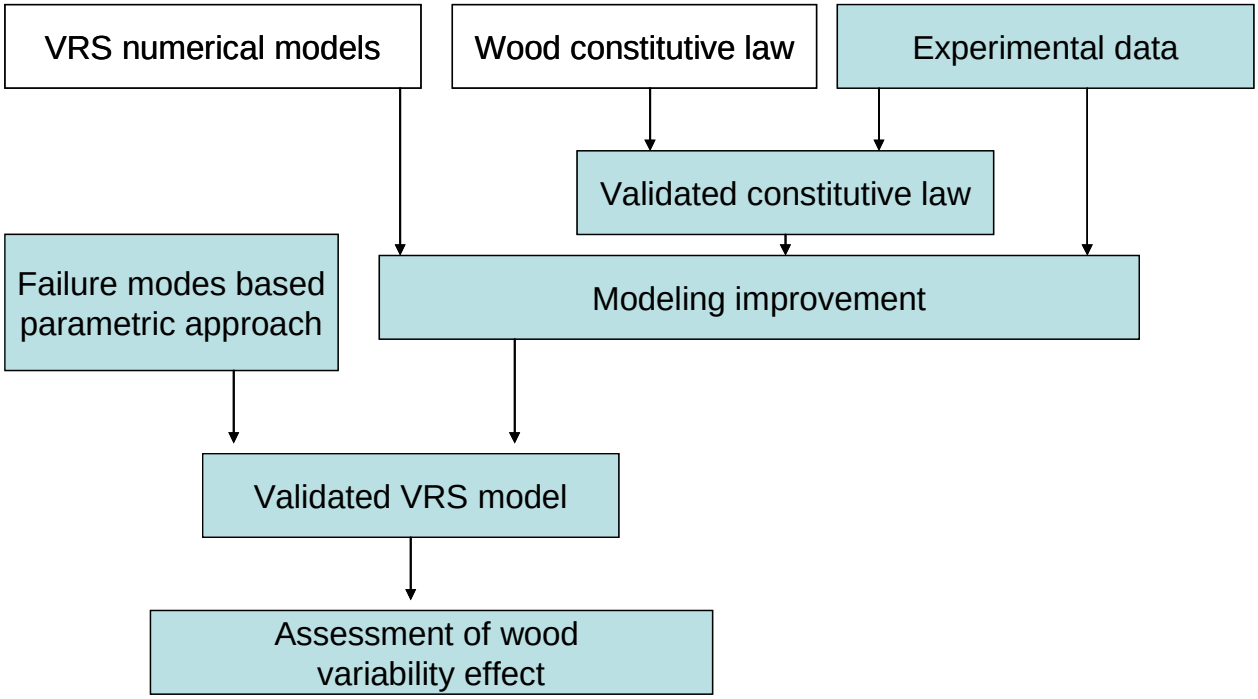

Figure 1-1: Contribution

In blue: present contribution

Document organisation

First, a review of literature is realised in order to set-up the context. Some historical facts about French infrastructure development are presented before introducing the current normative context. After that, a state of the art concerning VRS modelling, computational mechanics use and model validation is described.

Then, dynamic three point bending tests on wood and steel-wood structure samples are described in a second chapter and give useful information concerning the wood mechanical properties range of variation.

In a third chapter a model of the three point bending dynamic tests is set-up and used to test several numerical parameters, to improve the steel-wood coupling model and to evaluate the material constitutive law.

Finally, a full model of a VRS is built and correlated thanks to a parametric method based on structural failure modes analysis.
Once the correlation is reached, a new parametric study based on wood mechanical properties variation is performed and the results in term of VRS performances are presented.

Chapter 1 State of the art

1.1. Vehicle Restraint Systems

1.1.1. Some historical facts

Crash testing is commonly associated to the development of new vehicles and to their evaluation in view of obtaining Euro-NCAP stars. Most people, (at least French people as will be explained hereafter), imagining that there is a whole industry and researchers at trying to improve Vehicle Restraint Systems (VRS) is unconceivable.
Such a state of mind is mainly due to two facts:

- A Vehicle Restraint Systems seems to be a very simple structure. We will see that a VRS is not as simple as it may appear at first glance specifically when talking about behaviour under dynamic conditions.
- In France, people are used to see the "Generic" VRS developed from the 60's onwards by the technical services of the French state [BLO11].

Back then, the French administration performed a large number of crash tests. Around 700 crash tests(1) were performed by ONSER association (Organisation Nationale de la SEcurité Routière – the French National Organisation for roadside safety). The method used then was almost entirely experimental, the aim of the first step being to avoid the crossing, the roll or the too severe redirection of the vehicle.
Once this step was completed, devices were optimized (always following engineering judgment and performing crash tests) trying to minimize deflection and looking forward to determining the best condition for devices' implantation following NF requirements. Considerable effort was made to understand the mechanical phenomenon involved and to optimize the behaviour of different types of VRS.
In 1976 ONSER became INRETS (Institut National de recherché sur les transports et leur sécurité – National Institute for transport and safety research) and, 7 years later, INRETS decided to transfer the test installations to a subsidiary company called LIER (Laboratoire INRETS Equipements de la Route – INRETS Laboratory for Road Equipment). This decision was made as the activity started to turn more to tests production rather than research work for developing French devices and thus, got outside the focus of INRETS.
In 1988 [CIR88] the French administration published some reference documents defining "generic" French devices and their conditions of use. Thus, a trade developed in order to produce the generic devices and to install them along French roads.
NF requirements were replaced by European Norm 1317, which will be detailed in the following section. The introduction of CE marking forced French manufacturers to setup their own crash tests and they obviously seized this opportunity to implement modifications on the generic devices in view of their optimization.
Nowadays, as regards Western Europe, the activity concerning crash testing of current section VRS is much lower due to the market itself (we are not building new kilometres of highways every day) and also to fierce competition. Furthermore industrials, who already dispose of an existing range of products, are reluctant to invest in costly and haphazard tests.

(1) from LIER archives

Nevertheless, in France, the lack of VRS in some areas should be a greater preoccupation for the road authorities. Actually, in 2010 alone, 38% of the casualties resulted from an impact against a hazard (VRS included). When impacting a VRS, the risk of death is divided by two. [ONI11]
Between 2000 and 2008, the number of people killed on French roads was halved, mainly thanks to a political effort concerning the speed automatic control and financial repression (see figure 1) [ONI01] [ONI09].
Since then, the number of people killed remains more or less constant highlighting the limit of such action. It is worth to notice that the same trend has taken place as regards casualties against fixed hazards around 40% of total deaths [ONI10], [ONI11].
A study, [MAR97] confirms that the level of equipment on highways is correlated with the severity of an accident (and with the number of fatalities).
Therefore, improving the level of road side equipment would reduce the number of people dying on the roads.
Figure 1-1 highlights the fact that the number of people killed after an impact against a VRS is very low.

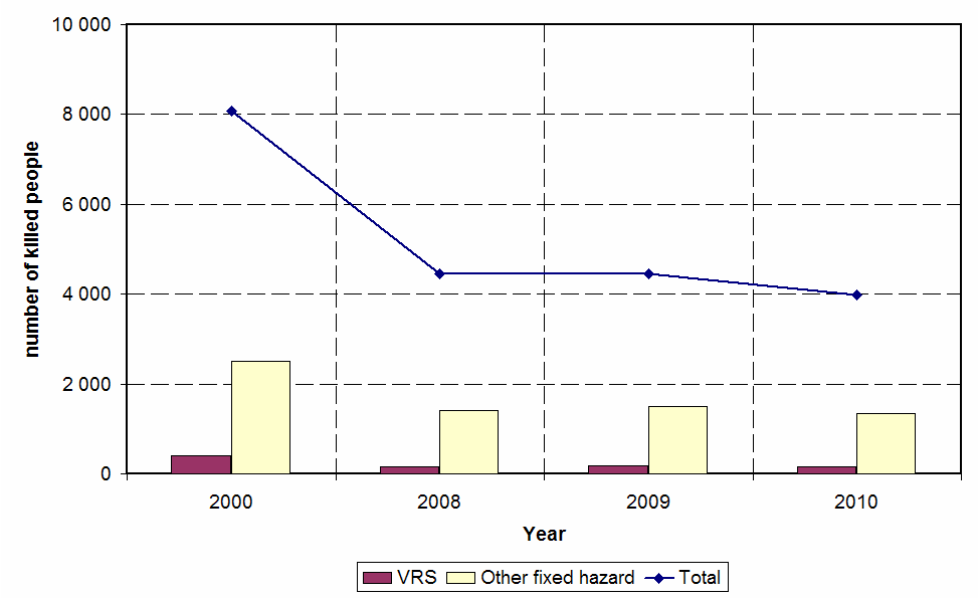

Figure 1-1: Evolution of killed people on French roads

Thus, the installation of VRS must be a priority as well as development of VRS with better performances.
In this context, the use of numerical tools to gain an in-depth analysis of the crash phenomenon and to maximize the chances of success of the crash test became obvious.
To assist its customers in their development, LIER decided to start a new activity of Computational Mechanics (CM) in 2005 whose role in the framework of roadside safety will be detailed in the following section.

1.1.2. Aim of a VRS

Basically, a road barrier is called Vehicle Restraint System because it aims firstly to restrain – or to contain – an errant vehicle that has lost control of its trajectory.

Different types of VRS exist with distinct goals. The French administration [CIR88] divided them in three main categories:

- Hard shoulder metallic devices
- Hard shoulder concrete devices
- Frontal devices

This categorization is interesting because of its strong link with the structure behaviour under impact loading.
Hard shoulders devices aim to contain and redirect the vehicle while frontal devices are designed to contain and stop the vehicle. The French administration distinguishes the Hard shoulder devices depending on their constitutive materials. Another classification could be done in terms of conditions of use:

- Temporary devices: Used for working area protection, in which are to be found plastic units filled with sand or water, reinforced-concrete units or steel units. These devices mainly use the inertia properties of the units to apply a load to the vehicle and redirect it smoothly.
- Permanent soft devices, when the risk of VRS crossing is considered acceptable and when the space behind the VRS is compatible with its working width. In this range of products, steel devices are the most common and steel-wood products are preferred because of their aesthetic interest. For this kind of devices, a soft post is linked to a rail thanks to a fusible connection which leads to more complex failure modes of the structures.
- Permanent rigid devices, preferred when the deflection of the device (when impacted by a vehicle) has to be minimized e.g. bridges or highways median strip. These kinds of VRS usually consist of concrete or strong steel structures which are able to restrain buses and/or heavy trucks. They are implemented in locations where minimum deformation is required. Therefore, such devices are usually characterized by high severity indices and exit speed.

One common statement is to say that a VRS must “dissipate” the impact energy which is not always the case.
Frontal devices are designed to absorb all the impact energy stopping the vehicles and converting all the kinetic energy in deformation. For hard shoulder devices, the aim is to redirect the vehicle. Obviously, a certain amount of energy, depending on the VRS and on the impact conditions is dissipated via distinct types of mechanisms such as plastic deformation, fusible breaking, or contact friction but this dissipation can be considered as negligible with respect to initial impact energy. Indeed, in theory, one can consider a perfectly elastic material with very good friction properties (close to zero friction coefficients) which could re-direct the vehicle in the good direction without any change in speed.

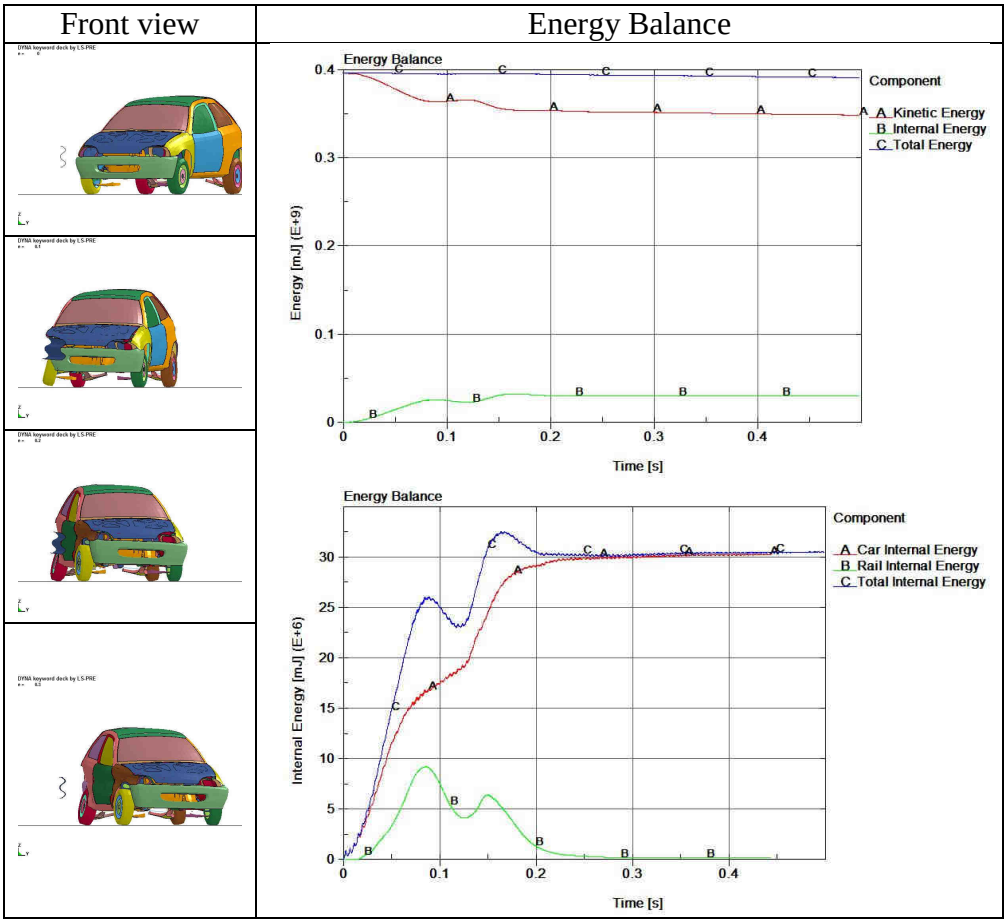

Figure 1-2: Perfectly elastic VRS kinematics

Figure 1-2 (right) illustrates the good redirection of a car obtained with a height meter length rail (with a boundary condition at each end) for which a perfectly elastic property is applied.
It's worth noticing that the global internal energy is the algebraic sum of Car Internal Energy and rail internal energy (Figure 1-2 top left) on one hand. On the other hand, the decrease of kinetic energy is equivalent to the increase of internal energy (Figure 1-2.bottom left). Finally, concerning the rail deformation, one can notice that the peak value of internal energy is one third of the total internal energy (i.e. there is twice more energy "absorbed" by the car deformation") and the decrease of kinetic energy is not significant (less than 10%). Furthermore, as far as the rail is modelled elastically, there is no energy dissipation in the rail (the internal energy returns to zero).

However, as far as frontal devices are concerned, the things are strictly different.
For the purpose illustration, a 5m honey-comb structure has been modelled. The aim being to stop the vehicle, all the impact energy has to be converted from kinetic energy to internal energy as shown in Figure 1-3.
In this case the amount of internal energy is obviously higher than in the rail case. Three quarter are absorbed by the Honey Comb and the last one by the car.

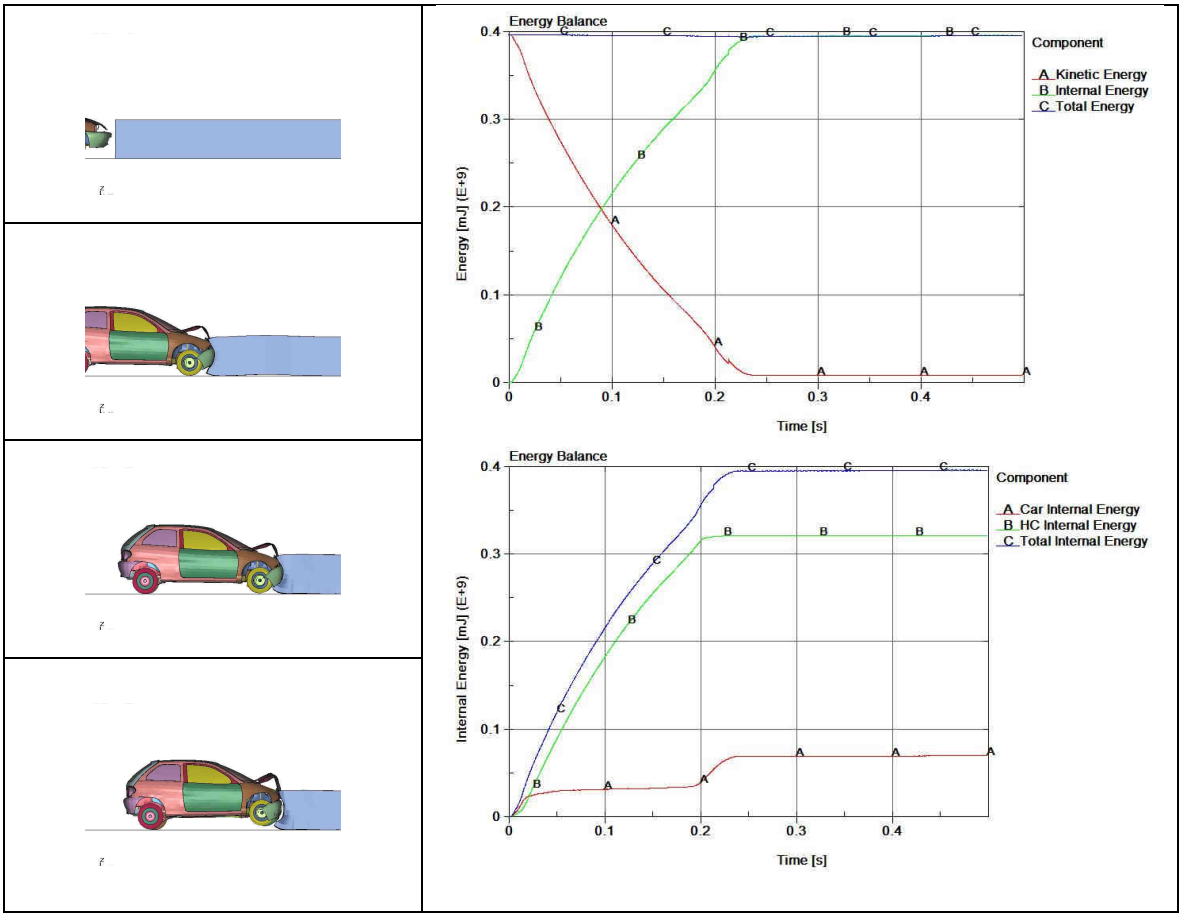

Figure 1-3: Theoretical frontal device

In order to achieve its goal of either restraining or stopping a vehicle, each device may not operate in the same way. This fact has been illustrated by the different types of energy balance.
This has brought about the introduction of structure's failure modes concept.

1.1.3. Failure modes

A failure mode is an ordered sequence of events (not necessarily failures) which will characterize the operation of a device.
Most of VRS are fairly simple structures, made of few components and can be characterized by a simple sequence of events.
Figure 1-4 & Figure 1-5 present the sequence of events leading to the expected behaviour of respectively simple rail and double rail metallic devices as described in [CIR88].

Figure 1-4: Operation of simple rail metallic devices from NF P98-410

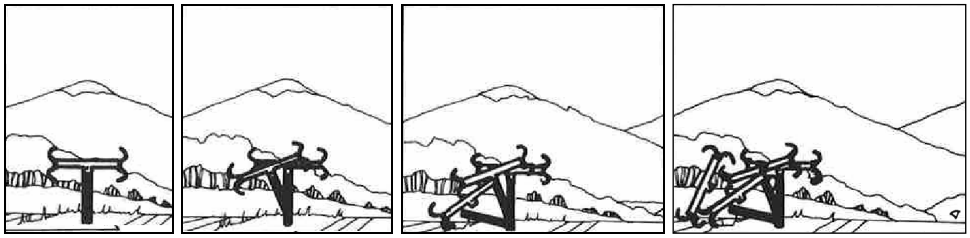

Figure 1-5: Operation of double rail metallic devices from NF P98-410

In both cases, the correct behaviour is obtained by the disconnection between the rail (or rails assembly) from the post allowing the rail (or rails assembly) to remain at a proper height for a good interaction with the vehicle.

This main mechanism can be divided in three sub events:

- Yield of the rail under vehicle contact pressure and transfer of contact forces to the surrounding posts.
- Bending of the post (formation of a plastic hinge at the post base)
- Disconnection of post-rail link. This fusible link could be obtained by different ways:
- Bolt failure (double rail device)
- Bolt pulled out (single rail device)

To achieve this proper behaviour the following points must be respected in order to prevent unexpected failure modes:

- Continuity of strength under longitudinal forces due to vehicle impact loading
- Correct height of the rails
- Good anchorage of posts

Nevertheless, the activation of each mechanism is linked to, at least, one physical parameter itself subject to important variation.
For each of the above events, at least one physical parameter and a relating range of variations are associated in Table 1-1.

Failure modes	Physical parameters	Range of variation
Yield of the rail	Rail steel yield and/or Section thickness	>235 MPa 3mm
Post bending	Post steel yield and/or Section thickness	>235 MPa 5mm
Fusible link	Spacer steel yield and/or Section thickness and/or Bolt strength	>235 MPa 5mm (4.6 class)

Table 1-1 ; Failure modes and variation range

Table 1-1 illustrates one issue of VRS design.
Most of materials used are not premium materials, and quite too often the lower values only are defined. Yet experience has shown that significantly higher values than those displayed may occur. For S235 steel, the yield point minimum value is 235MPa. Nevertheless, steel certificate analysis from VRS producers frequently shows values higher than 330 MPa.
Therefore, the designer of a VRS has to deal with these uncertainties and must ensure that the global sequence of the impact will not be changed.

Every kind of device, before being installed on the road, has to be crash tested in accordance with the EN1317 standard which will presented in the next section. Real crash tests provide a view of the failure modes of the device with one set of parameters. In the framework of CE marking process, some material analyses are performed but are not totaly reliable because only one test is performed on one sample of each component.

Furthermore, one cannot know how robust the design is because the repetition of a crash test is economically not viable and also because the mechanical properties cannot be controlled.
Numerical tools allow the evaluation of the robustness of a design taking into account all these variations.
Within a certain range, the failure modes of the structure will remain comparable and “just” the performances of the device will be affected. The widths of these ranges characterize the robustness of the design.
Beyond the limits of these ranges, the failure modes may change and the global behaviour may be different. For instance, if the fusible link does not appear due to a too strong blot, the rail may remain attached to the bended post and the car could run over the device.

1.2. Normative context

1.2.1. Testing aims and limitations

Full scale impact testing has been and will continue to be the most common method of evaluating the safety performance of every kind of road features. Because of the multiplication of test houses in Europe and in the United states, there is an increasing need for uniformity in the procedures and criteria used to evaluate roadside safety features.

The purpose of these procedures is to promote uniform in-service evaluation so that road engineers may confidently compare the safety performances of different designs (even if designs are tested in different agencies). The real life condition of installation of road equipment is innumerable and impractical if impossible to replicate in a reasonable number of standardized tests. Hence, the approach to normalized test conditions is described below:
Straight longitudinal barriers are tested although curved installations exist; flat ground is recommended even though installations are sometimes situated on sloped shoulders and /or behind curbs; soil conditions may vary a lot (sand, stabilized, asphalt, concrete sockets…) and could affect the behaviour of devices under vehicle impact loading conditions.
Also test vehicles and impact conditions, meant to give an in-service evaluation of roadside safety features performances, may not represent the entire real life impact conditions but are harmonized in order to compare and classify safety performances.
ROBUST (Road Barrier Upgrade of Standards) [ROB06-1] European project has demonstrated that a crash test configuration can be repeated in two different test houses with highly comparable results but with a high level of control of input parameters (Car model and age, impact conditions…)

1.2.2. European approach – US approach

Two main approaches co-exist and will be briefly described hereafter: European Norm EN1317 [NFE10-1&2] and NCHRP (National Cooperative Highway Research Program) report 350 [NCH93] for the United States of America progressively being replaced by the MASH (Manual for Assessing Safety Hardware from the AASHTO (American Association of State Highway and Transportation).
Both documents provide guidelines as regards crash testing conditions and criteria for the evaluation of roadside safety features: Longitudinal Barriers, Terminals, Crash Cushions, Support Structures (NCHRP Report 350 only, in Europe these items are evaluated in the framework of EN12767) and Truck-Mounted Attenuators (NCHRP Report 350 only it will be included in a future part of EN1317).

	Containment levels	Acceptance test	Impact Conditions			
			Vehicle Type	Impact Mass [kg]	Impact Speed [km/h]	Impact angle [°]
Low	T1	TB 21	Car	1 300	80	8
	T2	TB 22	Car	1 300	80	15
	T3	TB 21 TB 41	Car SUVT[1]	1 300 10 000	80 70	20 8
Normal	N1	TB 31	Car	1 500	80	20
	N2	TB11 TB32	Small Car Car	900 1 500	100 110	20 20
Higher	H1	TB 11 TB 42	Small Car SUVT[1]	900 10 000	100 70	20 15
	H2	TB 11 TB 51	Small Car Bus	900 13 000	100 70	20 20
	H3	TB 11 TB 61	Small Car SUVT[1]	900 16 000	100 80	20 20
Very high	H4a	TB 11 TB 71	Small Car SUVT[1]	900 30 000	100 65	20 20
	H4b	TB 11 TB 81	Small Car T/VT[2]	900 38 000	100 65	20 20

Table 1-2: EN1317 Containment level definition

Test Level	Test Designation	Impact Conditions			
		Vehicle Type	Impact Mass [kg]	Nominal Speed [km/h]	Nominal Angle [°]
1	1-10	Small Car	895 / 1175	50	20 / 25
	S1-10	Small Car	775	50	20 / 25
	1-11	Pickup Truck	2000 / 2270	50	25
2	2-10	Small Car	895 / 1175	70	20 / 25
	S2-10	Small Car	775	70	20 / 25
	2-11	Pickup Truck	2000 / 2270	70	25
3 Basic Level	3-10	Small Car	895 / 1175	100	20 / 25
	S3-10	Small Car	775	100	20 / 25
	3-11	Pickup Truck	2000 / 2270	100	25
4	4-10	Small Car	895 / 1175	100	20 / 25
	S4-10	Small Car	775	100	20 / 25
	4-11	Pickup Truck	2000 / 2270	100	25
	4-12	SUVT[1]	8000 / 10 000	80 / 90	15
5	5-10	Small Car	895 / 1175	100	20 / 25
	S5-10	Small Car	775	100	20 / 25
	5-11	Pickup Truck	2000 / 2270	100	25
	5-12	T/VT[2]	36000	80	15
6	6-10	Small Car	895	100	20 / 25
	S6-10	Small Car	775	100	20 / 25
	6-11	Pickup Truck	2000 / 2270	100	25
	6-12	T/TT[3]	36000	80	15

Table 1-3: NCHRP Report 350 Test matrix for longitudinal barriers (Length of Need) / Mash modifications

[1]: Single-Unit Van Truck
[2]: Tractor/Van Trailer
[3]: Tractor/Tank Trailer

If one focuses on the VRS, similarities are to be found between the two approaches. First, the test matrices (Table 1-2 and Table 1-3), present different containment levels in which two crash tests are needed for a VRS evaluation: one light vehicle used to assess the severity of the device and one heavy vehicle, whose weight depends on the restraint level, to assess the containment capabilities of a device.
By example the “normal” N2 level of EN1317 and the “basic” level 3 of NCHRP Report 350 both present a small car impact at 100 km/h and 20°. Nevertheless, the second test is more severe for NCHRP report in terms of mass (2000 kg instead of 1500 kg) and angle (25° instead of 20°).

In both approaches, three main assessment factors are presented:

- Structural adequacy
- Occupant risk
- After collision trajectory

The next paragraphs will detail the criteria of both American and European approaches dividing them into two main classes: Qualitative and Quantitative criteria.

1.2.3. Qualitative criteria

The mail goal of a VRS is to contain and redirect an impacting vehicle. Table 1-4 summarizes the qualitative criteria assessed during the test which allows to evaluate the effectiveness of a proper redirection.

Evaluation factor	NCHRP R350 Evaluation Criteria	EN1317 Evaluation Criteria
Structural adequacy	Test article should contain and redirect the vehicle ; the vehicle should not penetrate, underride or override the installation although controlled lateral deflection of the test article is acceptable	Test article should contain and redirect the vehicle. Lateral deflection are measured and detailed in the quantitative criteria.
Occupant risk	Detached elements, fragments or other debris from test article should not penetrate or show potential for penetrating the occupant compartment, or present an undue hazard to other traffic, pedestrian or personnel in work zone. Deformation of, or intrusion into, the occupant compartment that could cause serious injuries should not be permited.	No ejection of a “main” part of the VRS must be observed during the impact.
	The vehicle should remain upright during and after collision although moderate roll, pitching and yawing are acceptable.	No rollover of the vehicle on the test zone may occur
Vehicle Trajectory	After collision it is preferable that the vehicle’s trajectory not intrude into adjacent traffic lanes	The redirection of the car must comply with the “CEN box” criteria : 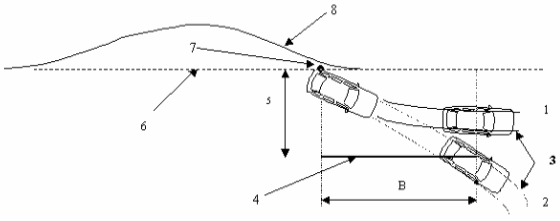 1: passed 2: Failled 3: wheel tracks

Table 1-4: Qualitative criteria

1.2.4. Quantitative criteria

If the qualitative criteria are satisfied, quantitative criteria are calculated in order to assess the performances of the VRS in term of severity and/or deflexion.

1.2.4.a. EN1317 Severity indices

The Acceleration Severity Index (ASI) is intended to give a measure of the severity of the motion for a person within a vehicle during an impact with a road restraint system. It's a non dimensional quantity computed using the following equation 1:

$$ASI = \max\left(\sqrt{\left(\frac{\bar{a}_x(t)}{12}\right)^2 + \left(\frac{\bar{a}_y(t)}{9}\right)^2 + \left(\frac{\bar{a}_z(t)}{10}\right)^2}\right)$$

Equation 1

Where

$$\bar{a}_{x,y,z} = \frac{1}{\delta}\int_t^{t+\delta} a_{x,y,z}\,dt$$

Equation 2

Equation 2 represents the 3 components of the vehicle acceleration averaged over a moving time interval δ=0.05s.

Theoretical Head Impact Velocity (THIV) which concept has been developed for assessing occupant impact severity for vehicles involved in collisions with road restraint systems. The occupant is considered to be a freely moving object (head) that, as the vehicle changes its speed during contact with the vehicle restraint system, continues moving until it strikes a surface within the interior of the vehicle. The magnitude of the velocity of the theoretical head impact is considered to be a measure of the vehicle restraint system impact severity.

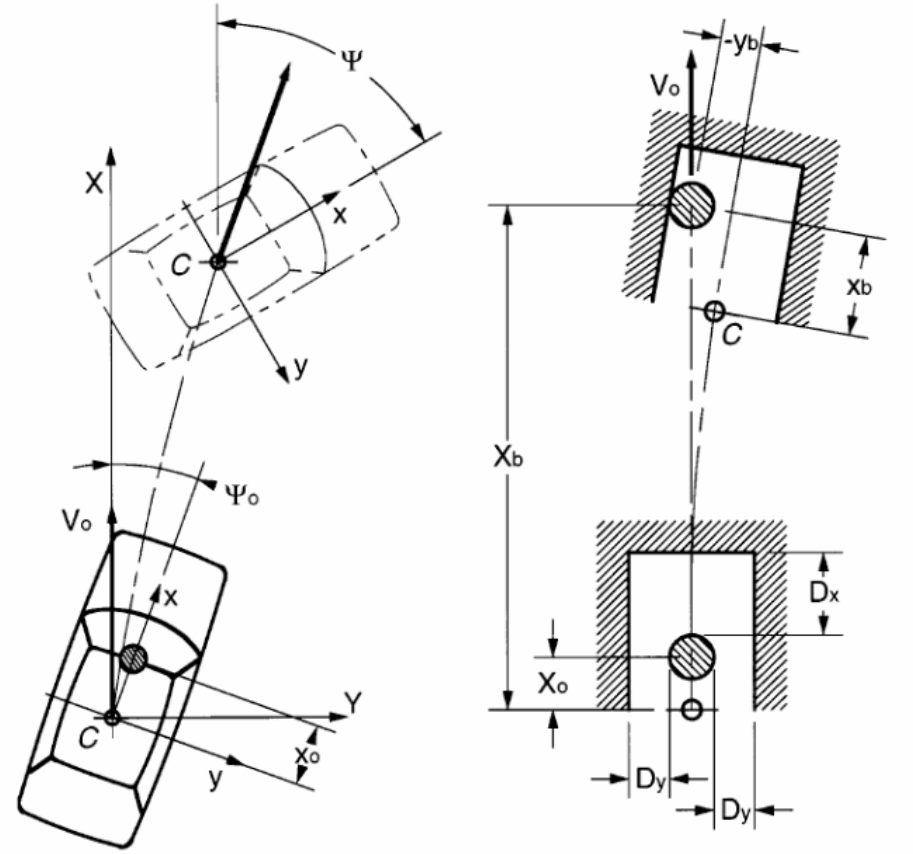

Figure 1-6: THIV - left: reference frames - right: Theoretical Head left impact

1.2.4.b. NCHRP 350 severity indices

Occupant impact velocities should satisfy the following:

Occupant Impact Velocity Limits (m/s)		
Component	Preferred	Maximum
Longitudinal and Lateral	9	12
Longitudinal	3	5

Occupant Ridedown accelerations should satisfy the following:

Occupant Ridedown Acceleration Limits (G's)		
Component	Preferred	Maximum
Longitudinal and Lateral	15	20

1.2.4.c. Deflexion measurement

In the framework of NCHRP report 350 a lateral displacement is accepted but not measured while EN1317 distinguish between two values:

- The Working width (W) is the distance between the traffic face of the restraint system and the maximum dynamic lateral position of any major part of the system.
- Dm: Dynamic deflexion is the maximum lateral dynamic displacement of the side facing the traffic of the restraint system

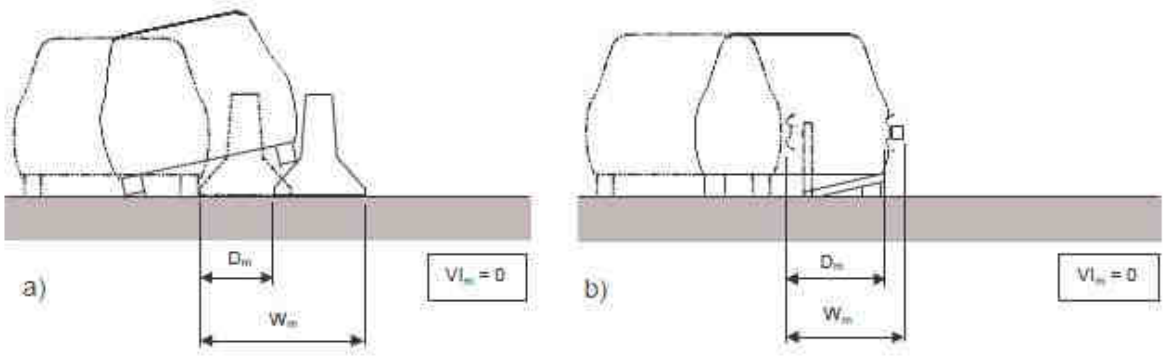

Figure 1-7: Working width and Dynamic Deflection

The difference between dynamic deflection and working width is illustrated on the above Figure 1-7. The W value represents the space needed for the VRS to work properly. It is expected that in real life installation this space remain free of hazards and thus, it is important to reduce this value.
In the revision dated 2010 of EN1317, which will be implemented in early 2013, these values will be normalized taking into account the theoretical speed and the actual test impact speed.

1.2.5. Discussion

Both approaches aim to define testing condition for VRS that are comparable.
Nevertheless testing conditions are related to specific vehicle fleet. One main difference between NCRP report 350 and EN1317 in the comparison of normal level of the EN1317 (N2) and the related basic level of NCHRP report 350. The latter is significantly more severe

(+50% of momentum). In the updated conditions of MASH, the mass of the vehicle is increased and almost all the impact angles are at 25° leading to more severe testing conditions.
[HUB12] compares NCHRP 350, MASH and EN1317 test levels in term of kinetic energy.

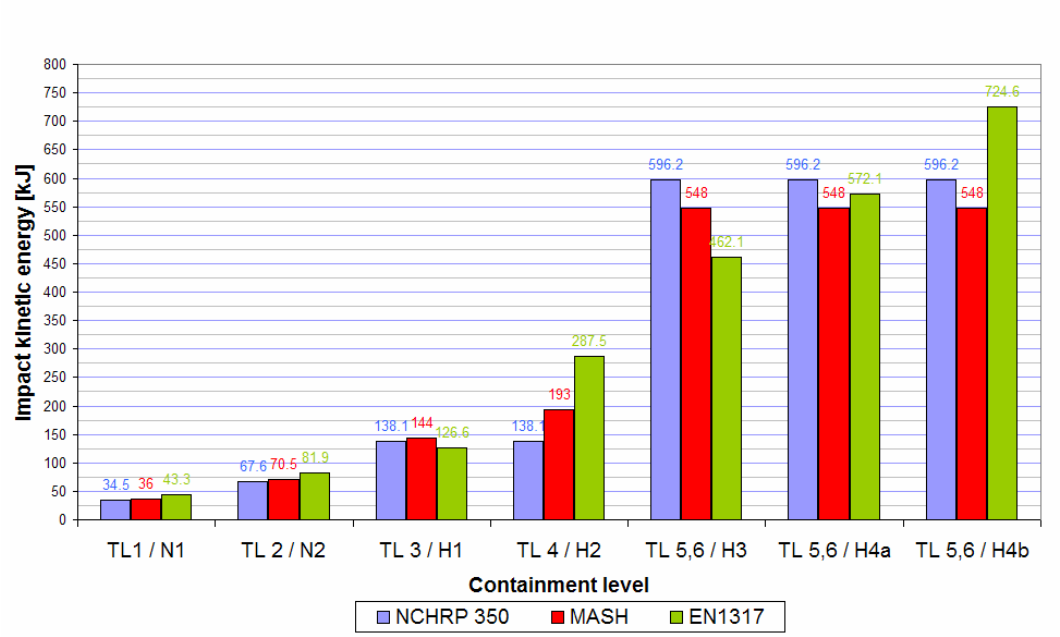

Figure 1-8: Kinetic energy comparison

When considering impact phenomena, it is preferable to consider momentum instead of kinetic energy. Nevertheless, Figure 1-8 presents the interest of showing that, in spite of slight differences, orders of magnitude are comparable.
One noticeable difference between the two approaches lies in the quantitative criterion.
EN1317 defines ASI whereas NCHRP report analyses both in plane components separately. Both approaches deal with occupant velocity but in a different way. EN1317 defines THIV where movement is considered in plane while NCRH also neglect the yaw angle. This difference may be balanced when one takes into consideration that THIV value (and maybe the same for OV) usually appears at an early stage of the impact at a time when yaw angle may be neglected.
Finally, NCRRP report defines some acceptance limits (and also preferred value even if one does not really know how to deal with) while EN1317 provides a classification of a VRS performances which depends on the results of the three qualitative criteria presented in the previous paragraph. From ASI and THIV values, the severity class is obtained following the Table 1-5 below:

Severity class	criteria		
A	ASI ≤ 1,0		THIV ≤ 33 km/h
B	ASI ≤ 1,4	And	
C	ASI ≤ 1,9		

Table 1-5: EN1317 severity class

The Working width values are also distributed in various classes as presented in the following Table 1-6:

W classes	Value (m)
W1	$W \leq 0,6$
W2	$W \leq 0,8$
W3	$W \leq 1,0$
W4	$W \leq 1,3$
W5	$W \leq 1,7$
W6	$W \leq 2,1$
W7	$W \leq 2,5$
W8	$W \leq 3,5$

Table 1-6: EN1317 Working width class

The global performance of a VRS is presented as a compilation of restraint level (which gives the information about the passed crash tests), W class and Severity class (e.g. N2 – W3 – A)

The replacement of NCHRP report by MASH was based primarily on changes in the American vehicle fleet. Vehicles have increased in size and light truck bumper heights have risen since the NCHRP report 350 criteria were adopted in 1993.
It's worth noticing that MASH states that any vehicle older than 6 years cannot be used while no restriction is set in the EN1317.
The MASH is an AASHTO publication (not an NCHRP document). AASHTO is controlled by the various states and not by the federal government. As a result, each Department of Transportation (DOT) is allowed to set its own MASH implementation date and its own MASH/NCHRP 350 implementation criteria. As long as the States do not require MASH products and agree on the use of NCHRP 350 products, there will be low motivation for manufacturers to develop new products.

1.3. VRS crash test modelling

1.3.1. Context

Computational Mechanics (CM) has been used for a long time. [RAY97] reports the first uses of CM in the early sixties and concludes that great deal of progress has been achieved into the roadside hardware design process thanks to non-linear finite element analysis.
In its early stage, simple analytical models using beams, masses and springs were developed to examine vehicle dynamics while impacting a road barrier.
Several years later, following codes and computer development, more advanced models emerged but still looked like soap boxes (Figure 1-9)

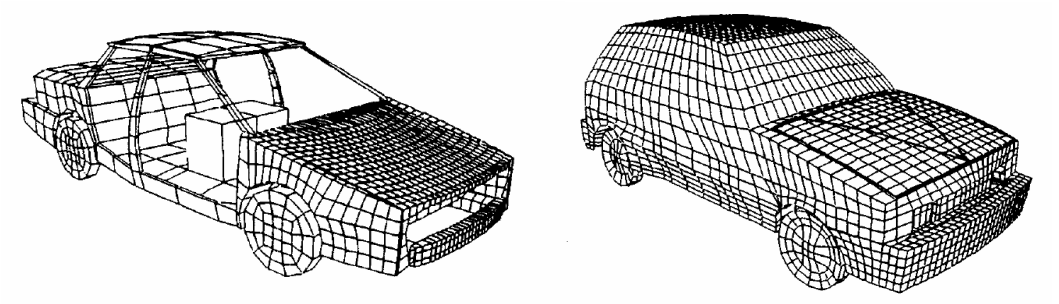

Figure 1-9: Model of 1991 GM Saturn and 1995 Ford fiesta

These vehicle models were never intended to be representative of the real vehicle geometry nor to include all parts and joints. The intent was to have simple models that had correct inertia properties (such as good centre of gravity) in order to obtain time histories that could be compared to those from real crash tests.

Nowadays, the use of Computational Mechanics in the field of road side safety covers two main applications:

- Development of new design or optimisation of existing ones
- Certification of modified products

In both cases, numerical models are expected to be predictive, in the first case, to increase the probability of success (mainly for economical purposes - avoiding failed crash tests), in the second case for safety reasons as certified modified devices are bound to be installed on the roads.

Predictability concerns then mainly the capability to represent the global behaviour of the vehicle during the impact and to evaluate the EN1317 criteria (severity indices, deflection measurements).

This predictability of a model is often challenged since a multitude of parameters may have an effect on the performances of a device.
First of all, it exists tolerances for tests conditions (Vehicle mass, impact speed, impact angle) see Figure 1-10.

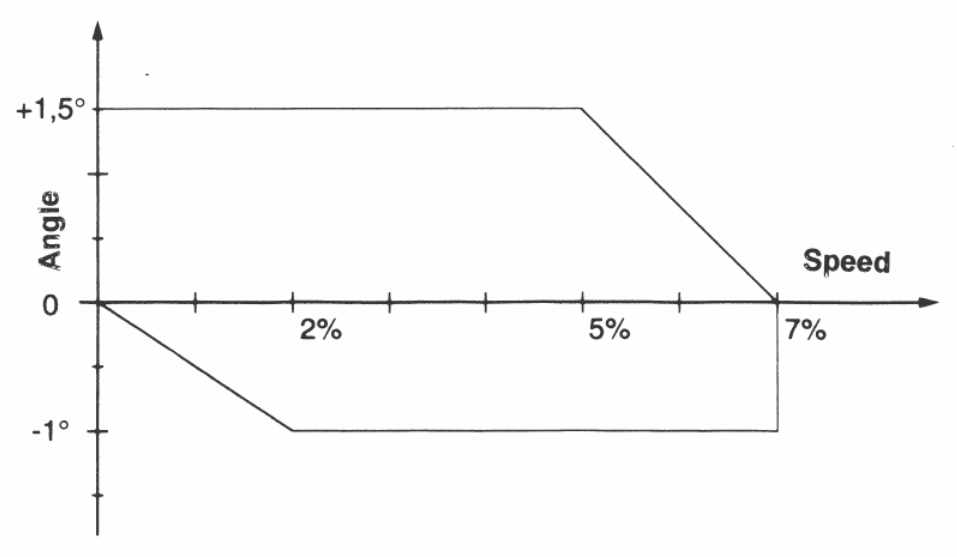

Figure 1-10:EN1317 impact angle and impact speed tolerances

Secondly, depending on the device design, when one focuses on the VRS structure behaviour under impact loading, the failure modes of the structures are usually driven by a very high number of parameters subjected to stochastic variation. In the set up of a numerical model, one is often led to use standardized data, such as steel yield point and ultimate strength, which may differ greatly from actual values.

Thus, it becomes obvious that a single result is surely not sufficient to predict the expected result of a future crash test insofar the tolerances of crash test conditions suffice to modify slightly the performances of a device.
While trying to reproduce a passed test, test conditions are known but a time consuming iteration work is needed in order to find a set of parameters which allows reproducing in an accurate way the behaviour of the crash configuration.

Moreover, in addition to physical parameters, F.E. models for restraint systems present numerical issues.
First of all, the total length of the VRS models (usually around 100 meters) and the total duration of this kind of crashes (between 1 and 2 seconds) imply a constant quest for the optimized mesh which will permit to obtain good results in a shorter time.
Furthermore the models definition itself (VRS and/or vehicle, boundary conditions, …) can determine the output.
The benefit of the numerical tool is to take into account the greatest part of the variability:

- On the one hand to predict better the performances of a design before real crash testing (providing a range for expected results instead of a single result)
- On the other hand to assess the robustness of a modification (is the modification as safe as the original one?).

The use of Computational Mechanics is increasing and its interest is obvious when one wants to evaluate device performances within the norm's conditions, to develop or to optimize it and, finally, to understand the phenomenon involved in the impact. However, in contrast to physical test results, the results of a simulation are always questioned. Taking into account all the variations of the parameters listed above is almost impossible and meaningless. The question is how far can we trust a numerical model, and if real tests exist, how can we compare the results of a simulation to those of a test?

1.3.2. Vehicle models

National Crash Analysis Center (NCAC) is a main actor in the field of road side safety modelling. Vehicle and some VRS models are available for free download on their web page [http://www.ncac.gwu.edu/vml/models.html].

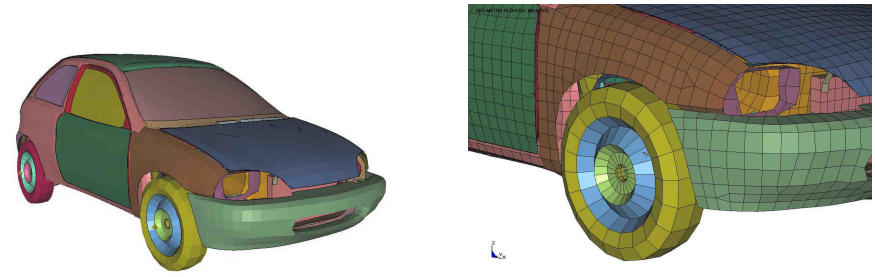

Figure 1-11: Geometro FE model

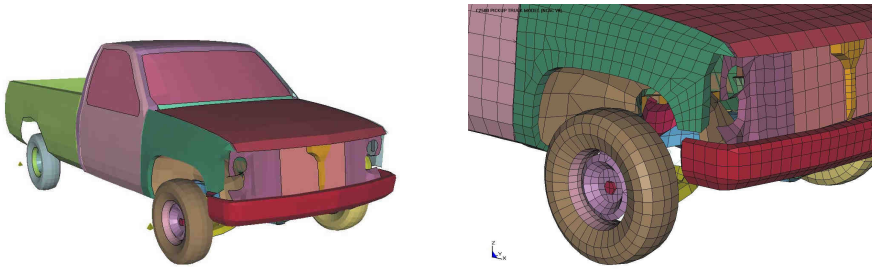

Figure 1-12: C2500 pick-up FE model

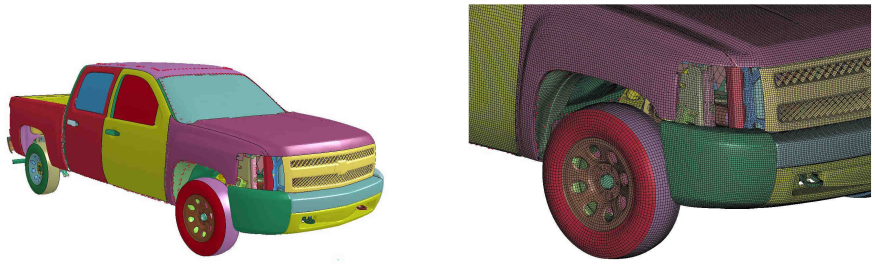

Figure 1-13: Chevy Silverado FE model

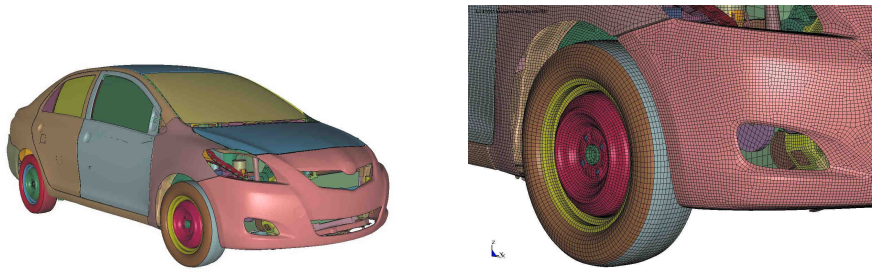

Figure 1-14: Toyota Yaris FE model

Figure 1-11 to Figure 1-14 illustrate the evolution of vehicle models over the past 10 years. Geometro and C2500 models dated 2000 are respectively 16 126 and 10 518 Finite elements. 10 years later, the Chevy Silverado (dated 2007) and Toyota Yaris (dated 2010) are respectively 929134 and 984 383 Finite Elements.

These very good looking vehicle models can be downloaded for free and come with a reports illustrating the correlation obtained in respect of NCAP test configurations. Some examples are shown in Figure 1-15 and Figure 1-16.

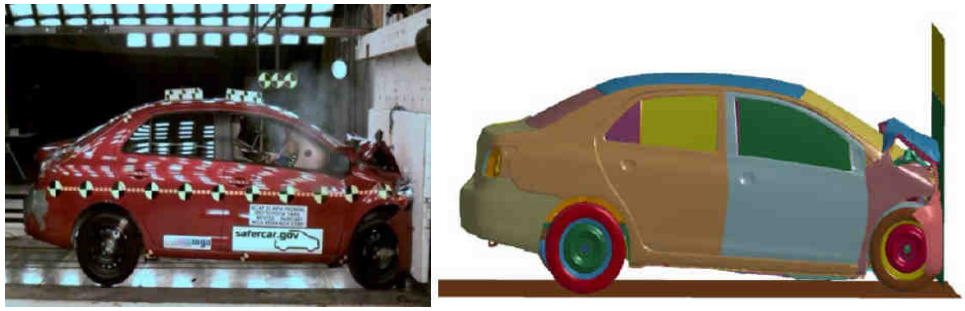

Figure 1-15: Toyota yaris comparison between NCAP test and simulation result

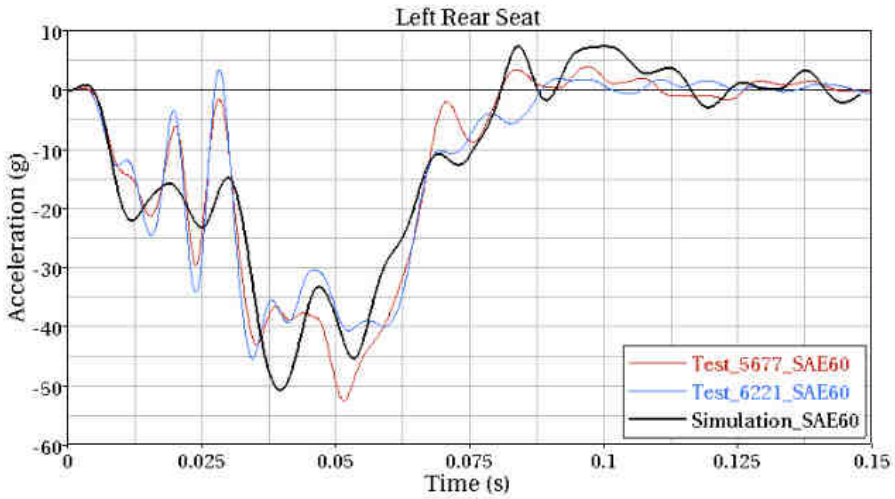

Figure 1-16: Toyota Yaris Acceleration signals comparison

Nevertheless, these models, due to high number of elements involved, are cost-intensive and the results very difficult to use in a parametric approach for roadside equipment crash simulations. In fact these models are mainly developed for NCAP applications where frontal impacts against deformable barriers are considered. These impacts involve mainly the car model and last around 150 milliseconds.

Within the Technical group 5 of CEN TC226/WG1, some experts of Computational Mechanics (CM) are collaborating to provide guidelines concerning the use of CM in the specific field of roadside safety [CEN12-1]. Vehicle models have been developed (mainly by Politecnico di Milano) to represent EN1317 vehicles (from 900 kg small car to 38 tonnes articulated truck) and are also available on the NCAP web page (see Figure 1-17). The ultimate aim in doing so was to have numerical models fine enough to be able to receive acceleration signals comparable to those obtained during real testing but coarse enough to allow their use with a 100m length VRS FE model for a simulation of a 2 seconds impact. Furthermore, in these models, a particular effort was made on the representation of a correct kinematics of suspensions and direction systems which is fundamental when one tries to represent a non frontal impact configuration involving redirection (i.e. rotation) of the vehicle. Therefore all these models meet the requirements defined in [CEN12-2].

Figure 1-17: CM-E vehicle FE models

The average size of these models is around 40 000 FE. As a result, the CPU time is reduced by almost 25 and makes it possible to run parametric studies within a reasonable computational time.

It is with a similar objective that LIER developed its own model of 1500 kg car with a total of 21 304 FE (Figure 1-18).

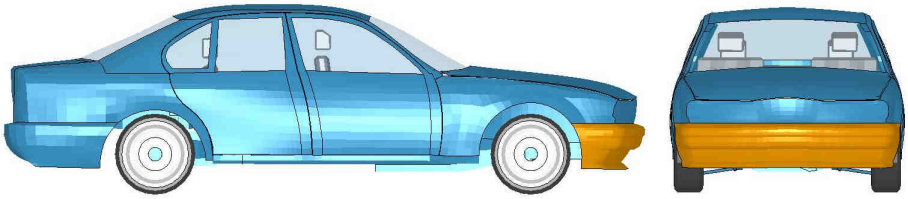

Figure 1-18: LIER BMW FE model for TB32 simulations

Like the CM-E models, this model is a compromise. Unlike the first FE models, the intention here is to match a real vehicle. Experience has shown that some geometrical characteristics have to be adjusted when one wants to reproduce a crash test (or be predictive before a crash test). Nevertheless, all components are not modelled and the intention is not to be an “exact” replication for that “exact” replication has a mean.

1.3.3. VRS models

The interest for using computational mechanics for roadside safety features has been demonstrated by the large amount of papers available in specialised literature.
The applications cover a large field.

- Development or optimization of products
- Three publications of the NCAC [NCA09] and [NCA10-1&2] concern the development of a new end treatment for a steel-backed timber guardrail. In this work numerical simulations were used to evaluate conceptual design and select the design which presents the best chance of success for real crash testing. In the last report, crash test results are presented and seem to fit the model prediction.

- [REI00] CM is used to modify a design of a bullnose guardrail system starting from a failed test, analysing the phenomenon (validation of model based exclusively on failure modes of the structure) and leading to successful crash test on the modified design.
- Research purpose
- [YON05] presents a model of portable traffic barrier to compare different concrete constitutive laws.

- [REI98] analysis of energy dissipation in order to optimize guardrail terminals

- [ANG09] use of CM tool to propose an upgrade of standard procedures.

Numerous research papers can be found relating to road equipment modelling either in the USA (related to NCHRP report 350 test conditions) or in Europe (related to EN1317 crash test conditions). Most of them follow a very efficient roadmap:

- Subcomponent test and model
- Device and model description
- VRS model validation
- VRS evaluation under different impact conditions or design modification performances assessment
- Crash test to consolidate results obtained from FEA study

1.3.3.a. Local models

Local models are often used to focus on the modelling in link to specific phenomena. Their relative small size, in contrast with global models, allows the use of much finer meshes and the study of phenomena which have to be idealized at a higher scale.
For instance, [TAB00_1] presents local analysis related to following topics:

- Post/soil
- Bolt pull out
- Effect of ends

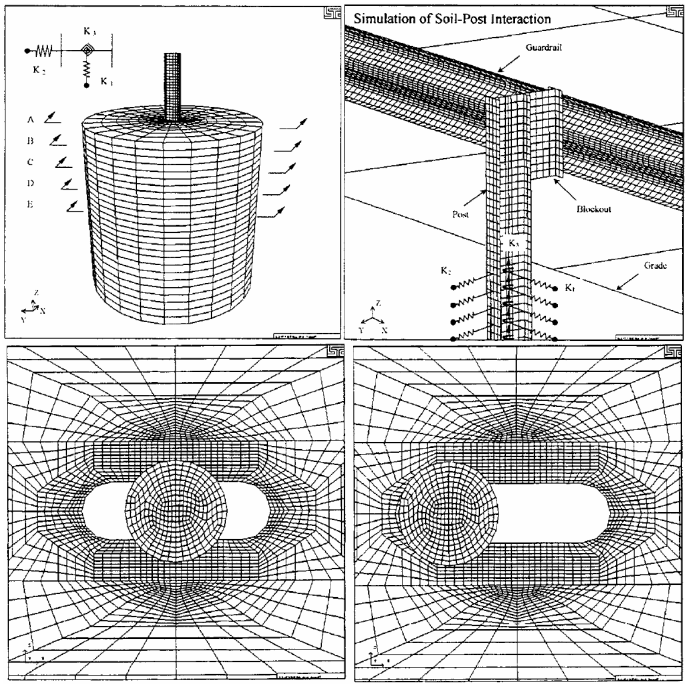

Figure 1-19: Local analysis [TAB00]

Figure 1-19 illustrates on top left the component simulation of a post/soil interaction in order to extract values for non linear springs used to model the soil in a global configuration (displayed top right). Bottom pictures shows two extreme cases of bolt location which were used to define a non linear spring load curve used for the rail/post model. It is stated that the bolt localisation has an effect which is not quantified in the paper.
[PLA03], on the same issue present some real component test and various sizes models which represent the pull-out phenomenon and conclude to a force variation between 18.0kN (one beam layer with centred bolt) and 64.7kN (two layers of W beam non centred bolt). Table 1-7 summaries the results obtained which illustrate on the one hand the variability between tests and on the other hand the effect of the bolt location.

Maximum force kN			
Test case	Test 1	Test 2	Average test max.
Single layer – bolt centred	16.8	19.1	18.0
Single layer – bolt non centred	26.7	30.7	28.7
Two layers – bolt centred	40.6	41.1	41.0
Two layers – bolt non centred	62.1	67.3	64.7

Table 1-7: Post-bolt connection failure from laboratory tests [PLA03]

[CHA01] explored the pull-out phenomenon which is the main failure modes of French generic device GS2/4 in a local model with different meshes and boundary conditions.

Model	Boundary Conditions	Pull-out force [kN]
Rear Face (Rm=500MPa)	all edges with 6DOF constrained	28
Rear Face (Rm 500 MPa)	top and bottom edges with 6DOF constrained	30
Rear Face (Rm=360MPa)	top and bottom edges with 6DOF constrained	20
Complete spacer	boundary condition on spacer front face (3 translations constrained)	30.3
Complete spacer and post	boundary condition on spacer front face (3 translations constrained)	~30

Table 1-8: Pull out force for post-spacer connection [CHA01]

For the first four cases, a velocity is applied to the bolt, modelled rigid, and the force is recorded within the rigid body. For the last case, bolt and nut are modelled and a flexion moment is applied to the post.
The results presented in Table 1-8 are comparable in term of magnitude to those obtained in the laboratory tests reported by [CHA03] for one single layer of steel.
It is worth noticing that the steel grade, which variation is evaluated here, seems to be a first order parameter.

[SEC05] focuses on post anchorage conditions in the soil. Two kinds of posts (steel and wood) were tested with a bogie vehicle impact and served as a basis for local model validation. In a second step a mow trip pavement is added.

Logically, when trying to model a steel VRS, shell elements are commonly used to represent the membrane behaviour of the distinct steel components.
Analysis of literature thereto reveals two main issues concerning the FE modelling of VRS which could affect heavily the answers provided by the FE models:

- Modelling of soil

Modelling technique	Advantages	Disadvantages
Boundary Condition	CPU	No possibility of post extraction
Non linear springs	CPU	Push-pull tests needed for solution setting-up
3d model – Lagrangian mesh	realistic	CPU cost Subjected to mesh distortion
3d model – Eulerian mesh	realistic	CPU cost

- Modelling of bolted connection

Modelling technique	Advantages	Disadvantages
Merged nodes	CPU	No representation of failure
Non linear springs	CPU	To be tuned
3d rigid model with non linear springs	realistic	CPU – to be tuned

In all cases, these very sensitive components should be modelled with great care and have to be tuned according to component tests or according to prior experience.

For instance, [TAB00] intended to implement a method to decrease the needed length of numerical models replacing the rails by a spring assuming that the rails out of the impact pocket should remain in the elastic domain and thus may present a global stiffness in accordance with Equation 3:

$$K = \frac{EA}{L}$$

Equation 3

Nevertheless, this approach was abandoned due to significant differences between forces recorded in these springs and forces recorded in global models. The author blamed the bolt sliding and the post/soil interaction which are not taken into account in the linear spring model.
This illustrates the limitations of local models. Local models are very useful in order to try different modelling techniques, validate failure modes according to local tests and to assess the range of variation of several parameters but they can not substitute for a global analysis.

1.3.3.b. Global models

A significant model which appears quite often in the literature is the American G4 (1S) Device.
[TAB00] presents a model of “the most common guardrail system in the USA”
[WHI04], [MAR07] and other related reports from NCAC [NCA07-1 to 3] are also related to this device and to the evaluation of several of its modifications.

The guardrail system is composed of standard w-beams of 3.807m length supported by W150x12.6 steel posts of 1830mm length embedded 1100mm deep into the ground every 1.905 m. Routed wood spacers are placed between the posts and the W-beam rails and have dimensions of 150x200x360mm.
The total system is 53.3m long and is anchored at both ends.

A detailed finite element model is presented. In particular, a very fine mesh is used for six rails located at the middle of the entire guardrail system while the remaining rails are modelled using coarser mesh. The connection between fine meshed rails is performed by means of 8 bolts which are fully meshed (see Figure 1-20 top right image). In order to reduce computational time (since very small elements are needed to capture the bolt geometry) the material formulation chosen is rigid and thus, will not control the time step. A spring is placed between the bolt head and the nut to represent the stiffness of the bolt.

As regards the long bolts used to connect the rails to the posts through the wooden spacer, they are modelled using beam elements; null-shell elements are tied to the beam nodes to represent the external geometry of the bolt and for contact purposes.
Another advantage of this model is the modelling of the soil represented by a cylindrical block of 2.7meters in diameter and 2.02m in height. The soil is meshed with eight node hexahedral solid elements and the outer boundary is constrained using a non-reflection boundary constraint option used to model infinite domain and thus to avoid stress wave reflection. Finally, a contact is defined between the post and soil meshes.
This model is definitively the most complete one, compiling benefits of previous works.

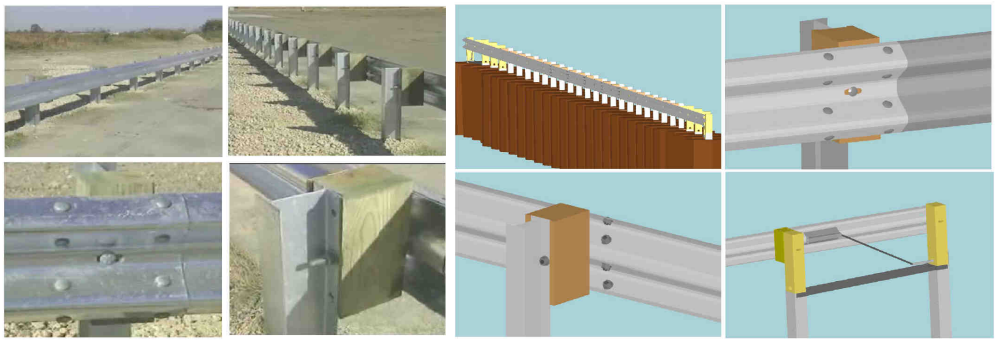

Figure 1-20: Typical standard W-beam guardrail and its related model from NCAC

[UDD99] presents a model of a three-wave guardrail quite close to G4(1S) device except the fact that the rail consists of three waves instead of the original two. This model is older and less detailed. For instance, most of the connections are modelled via merged nodes which prevent the representation of disconnection of jointed elements.

[WU04] uses a Swedish W-beam guardrail EU4 model consisting of a W-beam connected to a sigma profile post. In the FE model, non-linear springs are used to model soil and beam layers connections (Figure 1-21). The “post to beam” connection is modelled via a set of spot-welds.

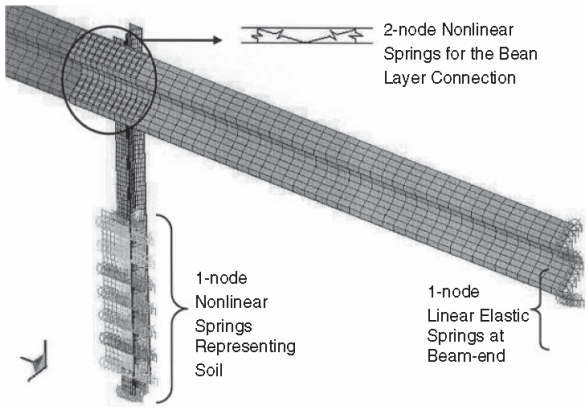

Figure 1-21: EU4 model [WU04]

Within ROBUST European project, a Work Package is dedicated to Computational mechanics [ROB06-2]. Round robin simulations were performed among several European test houses, universities and simulation agencies which set the bases of the CM-E which provides some recommendations concerning the VRS modelling techniques [CEN12-3].

1.3.3.c. VRS performances

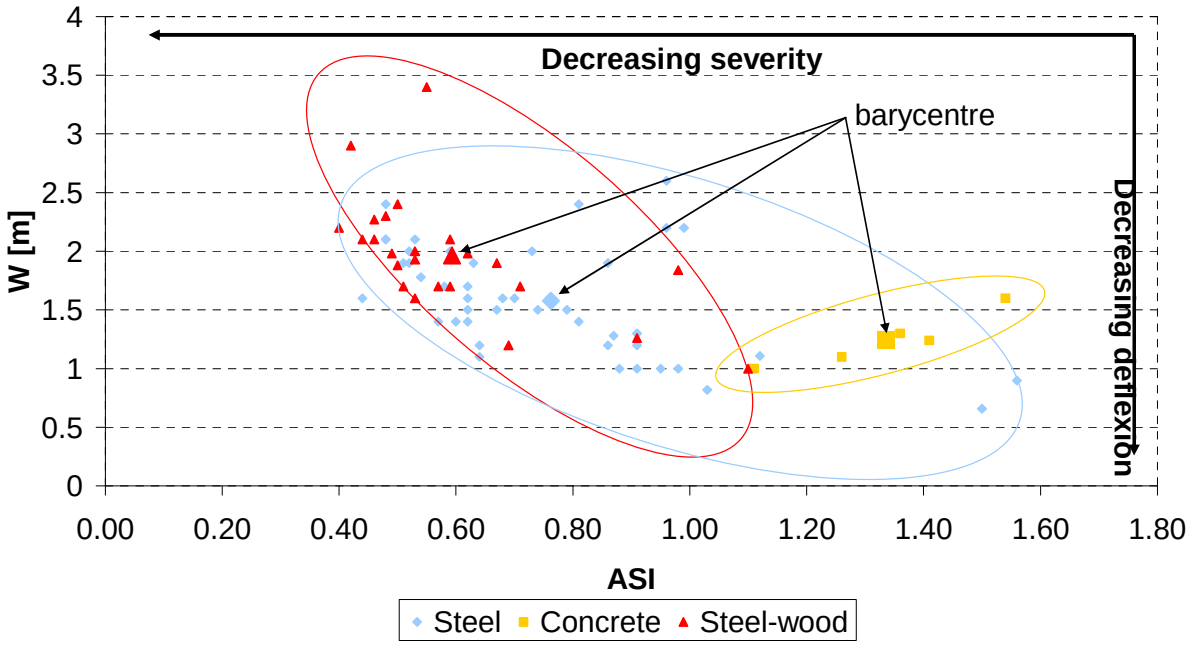

Figure 1-22: N2 test results from LIER database

The Figure 1-22, based on LIER test database concerning EN1317 N2 restraint level devices illustrates the performances of some devices, divided in three main classes: Steel devices, Reinforced concrete devices and steel-wood products.
Few results are displayed for concrete devices as far as these kinds of devices are commonly found at higher containment level.
Nevertheless, concrete devices are characterized by low working width and high severity which appears logical for this kind of stiff devices.
Steel devices usually provide a significantly lower severity. A quite important spread can be observed, due to the fact that some devices to be installed on bridges are much stiffer (and close to concrete devices) while some others are much lighter and characterized by higher working width and lower value of severity indices (softer devices).
The same conclusions can be applied to steel-wood devices. Nevertheless, on average, the steel wood devices offer significantly higher working width and lower severity indices.
Furthermore, in terms of optimisation, as far as class A of severity indices concerns ASI values from 0 to 1.0, the interest of a decrease of severity indices is limited. By contrast, an increase of the working width is highly detrimental. This confirms the need of an efficient numerical tool in order to develop optimized steel-wood products.
[CHA01] is the only study found explicitly relating to steel-wood VRS modelling. An important work is reported concerning the modelling of VRS structures under vehicle impact loading. Unfortunately this work suffers of lack of knowledge concerning VRS testing and results leading to poor correlations.
Steel-wood VRS are never found along highways because of they relative high cost and also because one consider that wood aging and mechanical properties variation, resulting from environment variables can affect the safety performance of the products.
One aim of this work will be to quantify the variability of wood and to evaluate its impact towards one VRS performances.

1.3.3.d. Validation procedures

In the publications detailed in the previous section, the capabilities of F.E. models to reproduce real crash configurations are demonstrated. Nevertheless, the relevance of the correlation is not homogeneous.

Generally speaking, the papers demonstrating subcomponent tests provide a fairly good agreement between test and simulation acceleration time histories. For Instance, Figure 1-23 shows the comparison of longitudinal acceleration signals related to bogie real test against a steel post and the related signal from a FE model. This figure illustrates the good agreement of the acceleration signals for both global trend and peak value.

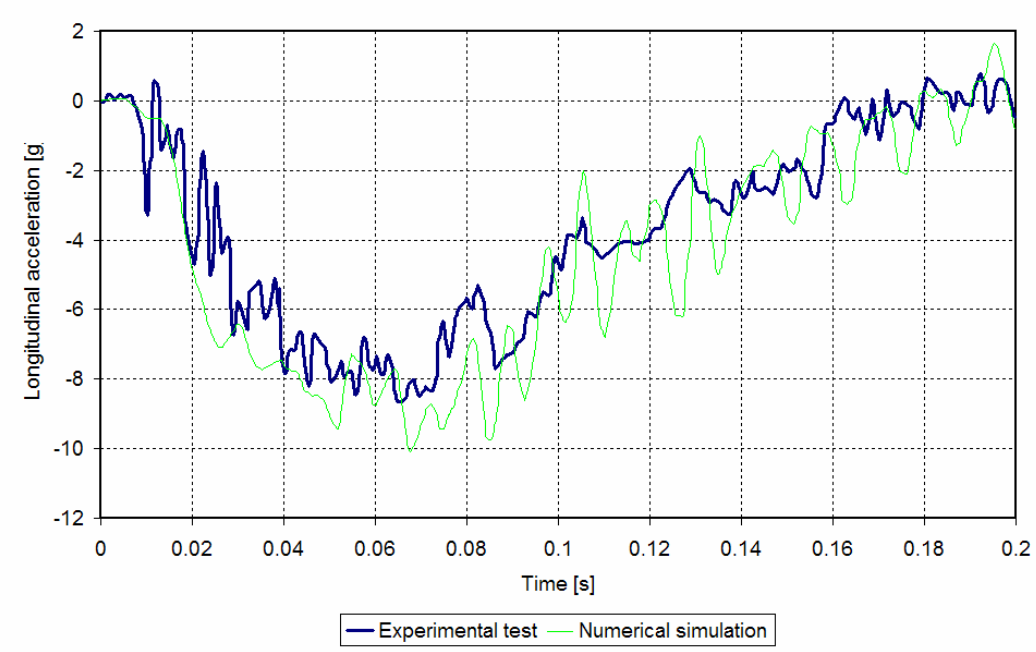

Figure 1-23: [SEC05] Bogie test acceleration signals comparison

At the next level, full scale crash test simulation, the correlations presented are usually limited to criteria calculation (peak values), pictures are taken from high speed cameras and compared to snap shots from the simulations and angle time histories comparison (Figure 1-24).

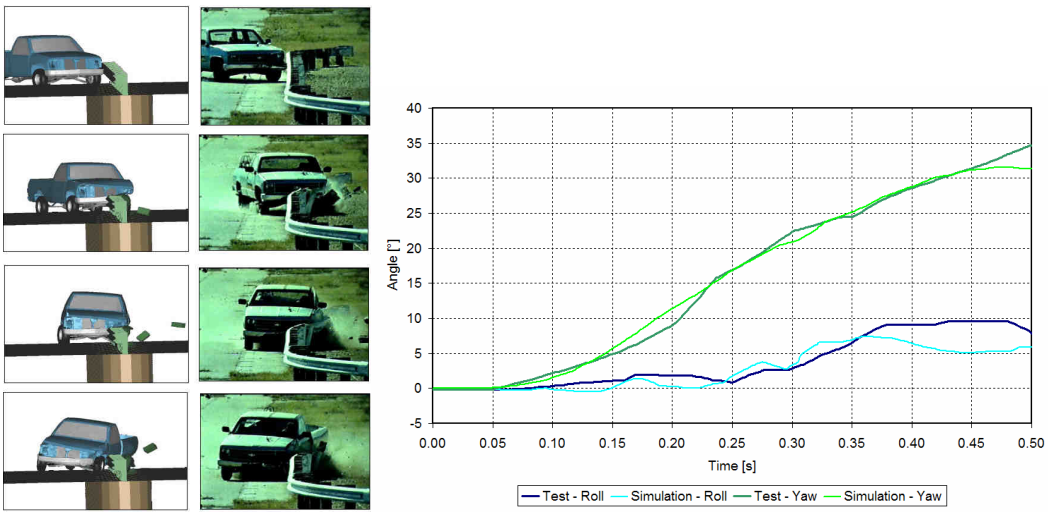

Figure 1-24: Typical correlation process [NCA07-3]

In very few cases authors give velocity time histories and even fewer authors authorize themselves to present acceleration time histories. In the later case, the agreement between

time histories is rarely quantified and the agreement is qualified by the author of “reasonable” or “fairly similar” (see Figure 1-25).

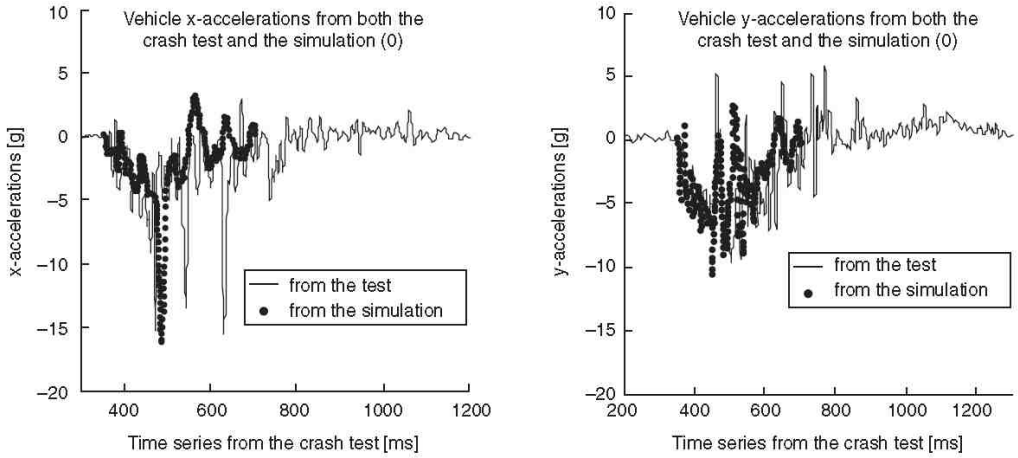

Figure 1-25: Fairly similar acceleration time histories [WU04]

[RAY96] proposes to apply statistic methods to compare two time histories and quantify the differences. If two time histories are sampled at the same rate, filtered at the same frequency and start at the same time; then, one proposed method is to measure the residual between each pair of data point (the difference at each time step between the two data points). Consequently, the author presents statistical method to quantify the differences between two curves.
The limitations of these methods are that they are (highly) sensitive to the time shift and that the signals are usually (very) noisy.
Furthermore, to analyse the results of a paired two-tailed t-test criterion, one would need to know the variability of the test data which is unknown.
This point highlights a major limitation of the validation process which is often limited to a point-to-point comparison as far as usually only one crash test configuration is concerned and serves as a validation basis without any idea of device robustness.

[TAB00] presents the NARD validation procedure, based on the theory of signal processing and analysis, which consists of both time domain and frequency domain analyses. In the paper, the time-domain validation is presented and three measures are presented:

Relative Moment Difference
The n^{th} moment of test signal f(t) and its corresponding simulation output are defined as

$$M_n(f(t)) = \int_0^T t^n f(t)dt$$

Equation 4

$$M_n(g(t)) = \int_0^T t^n g(t)dt$$

Equation 5

Root Mean Square (RMS) log measure of difference between two signals is then defined as:

$$r_d = \sqrt{\int_0^T \left[10\log\left(\frac{f^2(t)}{g^2(t)}\right)\right]^2 dt}$$

Equation 6

The RMS log average of the two signals is defined by the following equation:

$$r_d = \sqrt{\frac{\int_0^T \left\{ \left[10\log(f^2(t))\right]^2 + \left[10\log(g^2(t))\right]^2 \right\} dt}{2}}$$

Equation 7

The energy measure of the correlation between two signals is given by the following equation:

$$R[f(t), g(t)] = \frac{\int_0^T f(t)g(t)dt}{\sqrt{\left(\int_0^T f^2(t)dt\right)\left(\int_0^T g^2(t)dt\right)}}$$

Equation 8

All these measurements are applied to comparison of acceleration signals from a test and its simulation (Figure 1-26) and results are presented in Table 1-9.

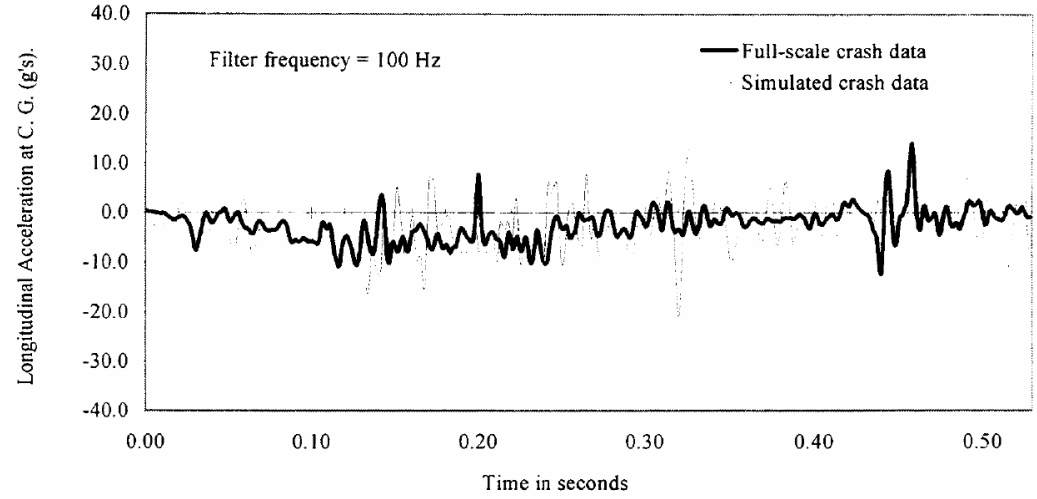

Figure 1-26: Longitudinal Acceleration at centre of Gravity [TAB00]

Acceleration Validation	
Zero Moment	0.126
1st Moment	0.095
2nd Moment	0.102
3rd Moment	0.118
4th Moment	0.132
5th Moment	0.146
r_d	10.1
r_a	9.35
r_d / r_a	1.08
Correlation Measure	0.50

Table 1-9: Metrics for acceleration signals validation

In the end, the question of whether these values are acceptable or not remains subjective but offers the benefit of quantifying the correlation obtained.

[PER09] and [GOU09] use the residual methods, based on resultant velocity time history, which was under discussion at this time within the CEN TC226/WG1/TG1/CM-E (Computational Mechanics-Europe) group.

Recently, CM-E has become an official Technical Group of CEN TC226. TG5 group brought about a technical document summarizing validation procedure issued from the CM-E group. This document aims to become an appendix of EN1317-5 which deals with CE marking of modified products.
First of all a comparative table (Table 1-10) has to be completed. A "yes" meaning that there is agreement between test and simulation.

Critical behaviour	type	Comparison: Yes / No
Containment	Required	Yes/no
Rollover	Required	Yes/no
Exit box for barrier	Required	Yes/no
Wheel trajectory	Required	Yes/no
Redirection zone for crash cushion and terminals	Required	Yes/no
Suspension failure	Informative	Yes/no
Failure of longitudinal elements	Required	Yes/no
Dynamic deflection for barrier	Required	Yes/no
Vehicle intrusion	Required	Yes/no
Lateral displacements for crash cushion and terminals	Required	Yes/no
Penetration of parts inside the vehicle.	Required	Yes/no
comparison between final shapes of test article	Informative	Yes/no

Table 1-10: Comparison table

Tolerances are defined as regards measurement of deflection (Dynamic Deflection, Working width and Vehicle intrusion) and the difference has to be inferior to the value calculated thanks to Equation 9:

$$d < \pm\left(0.05m + 0.1 \times Measure\right)$$

Equation 9

In addition, final shapes and failure modes should be compared.

Here after is another table for severity indices and time histories comparison (Table 1-11):

Criteria	Type	Comparison: Yes / No
ASI	Required	Yes/no
THIV	Required	Yes/no
Time histories	Required	Yes/no

Table 1-11: Additional comparison table

Tolerances for ASI and THIV values are respectively ±0.1 and ±3 km/h for peak values and a tolerance of ±0.05s is accepted as regards the time of these peaks.
The group of experts decided to compare velocity time histories. The comparison is based on longitudinal and transversal components (related to the test article) of the vehicle's velocity in plane motion and on the yaw rate.

The numerical simulation is considered validated when the following requirements are met:

- The numerical components of the vehicle velocity remain inside a window built around the physical velocity components until the farthest in time amongst the max ASI time and the time of flight is reached. When the validation is requested for a modified product, the numerical velocity time history must remain inside the window

until the vehicles have loaded the modified components. The variation limits for the window are: ±4% of the initial velocity and ±.01s in time.

- The numerical yaw rate of the vehicle remains within a window built around the physical yaw rate until the farthest in time amongst the max ASI time and the time of flight is reached. When validation is requested for a modified product, the numerical velocity time history must remain within the window until the vehicles have loaded the modified components. The variation limits for the window are: ±4% of the maximum yaw rate and ±.01s in time
- More details concerning the European validation procedures can be found [ANG12] ad [CEN12-4].

1.3.4. Discussion

All authors agree that a lot of parameters could affect the behaviour of a VRS. This is usually demonstrated by means of local models with very nice meshes which allow to present very good correlation between experimental and simulation acceleration time histories.
Unfortunately, at a global scale, the variations revealed by the local observation are not evaluated (or at least not reported).
In most cases, the correlation between a crash test configuration and a simulation is limited to one simulation case with comparison of snap shots and vehicle angle time histories. Some authors have tried to use statistic analysis to quantify the curves comparison but, in the end, the result remains poor because of the limitation of a point-to-point comparison.
The main interest for using numerical tool is to allow the evaluation of some parameters effects which are not possible to assess in the real life either because of crash test costs or because some parameters can not be easily controlled).
In the light of the parameters that may affect the VRS performances, reporting of one simulation results is a scientific aberration.
In chapter 4 a method for numerical model validation using a parametric study based on structure's failure modes analysis and on the related physical parameter variations will be described aiming to fin out a set of parameters compliant with requirements for model validation defined within the CEN TC226/WG1/TG5.

1.4. Conclusion

The use of Computational Mechanics has been adopted in the field of roadside safety and is more and more necessary in a complex economical and normative context.
To be reliable, models have to represent the failure modes of the structures. When crash tests exist failure mode models can be tuned to capture the behaviour observed in the test.
When crash test does not exist, the model has to be able to predict the apparition of distinct failure modes.
Literature analysis has illustrated that an infinite number of parameters drive the failure modes of this kind of structures and that it is impossible to master them all.
Ranges of variation for some topological parameters have been reported but the effect of this range of variation upon device's performances has never been studied.
The modelling of steel-wood VRS requires an accurate model of wood material which is, by nature, also subject to sensibility of environment variables.
Our approach is to start with local testing to assess a range of variations of wood mechanical properties and to validate the failure modes of a steel-wood beam.
Next, the wood model available in Ls-Dyna will be evaluated.
Finally, a global model of the VRS will be created and validated upon real crash test results using a parametric approach based on failure mode analysis and using the range of variation of each related physical parameter.
In a last phase, the effect of wood mechanical properties variation upon VRS performances will be assessed.

Chapter 2 Dynamic three point bending experimental tests

2.1. Material and methods

Wood structures responses under dynamic loading have not been investigated a lot yet. A large amount of data concerning wood elastic characteristics is available in the literature. [GUI]
In order to enhance the accuracy of our finite element model, experimental test were required. Our objective is to have a simple test configuration with energy level comparable to those observed during a real crash test with wooden sample with identical geometrical and mechanical characteristics.
It was decided to test two kinds of structure, wood and an assembly of steel and wood in order to validate also the assembly modelling and to have indication of the aim of each component.

2.1.1. Samples

A total of 20 wood beams were received from a French roadside safety system producer (SOLOSAR). The samples were supposed to be in standard conditions of use for roadside safety purpose.

2.1.1.a. Dimensions

The wood beams consisted in cylinders of 200mm in diameter cylinders by a length of two meters length. The rear side is machined in order to get a plane face of 110mm height.
This face was used for steel-wood tests to fix a steel reinforcement of 100x5x2000mm by the means of two M16 bolts positioned at 275mm from either extremity.
The same machining was performed on 300mm at the each side of the bottom face for the height positioning of the beam.

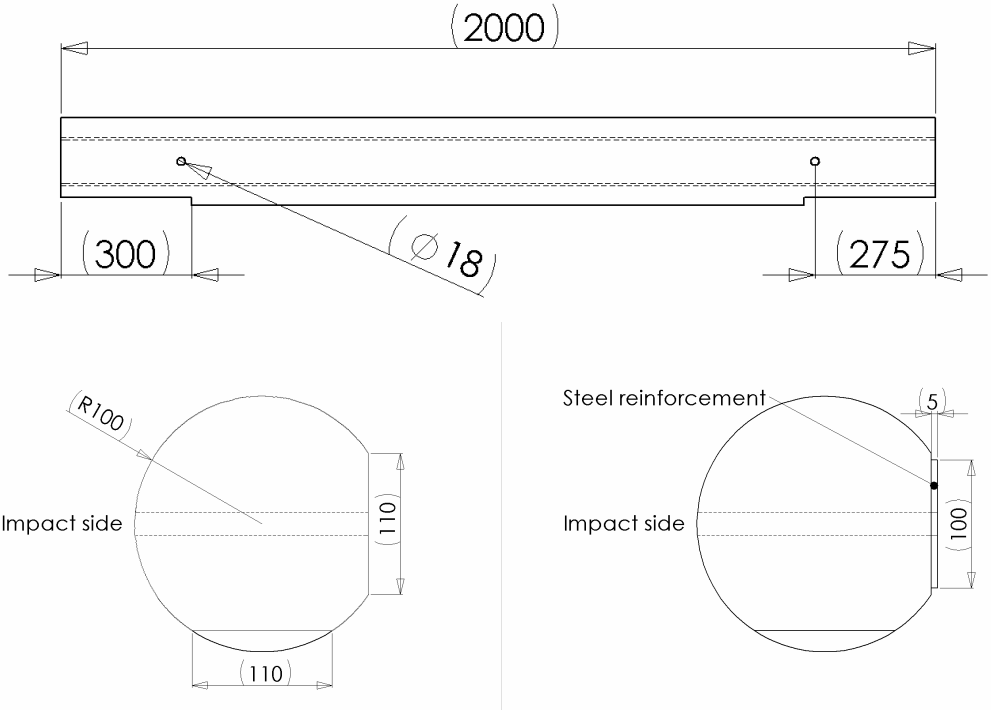

Figure 2-1 Samples dimensions

2.1.1.b. Mass and moisture content

Samples were weighted several times. All the samples were weighted at reception and, after that, on every morning of experimentation day and finally, just before testing.

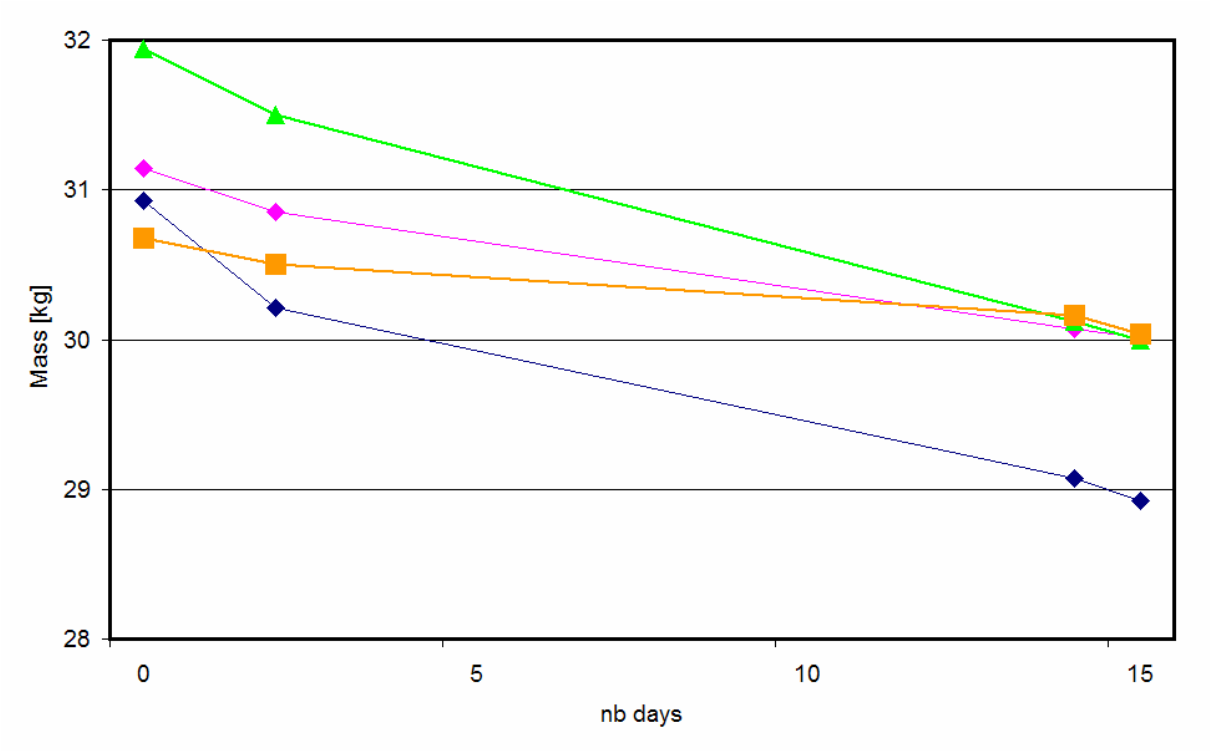

Figure 2-2: Sample mass time evolution

Figure 2-2 shows the time evolution for the 4 samples tested on the last day (which were weighed four times).
One can notice the loss of weight for each of the 4 samples.
The samples were stored inside a warehouse subjected to important temperature variations. Air moisture content was recorded but no correlation was found concerning weight loss which may be due to the natural drying of wood when kept in such storage conditions.

Special care was given to the mass and moisture content of each sample. The moisture content was recorded at 3 points along the wood sample before testing: at the level of either right and left support and at the centre of the beam.

Figure 2-3 Moisture content measurement

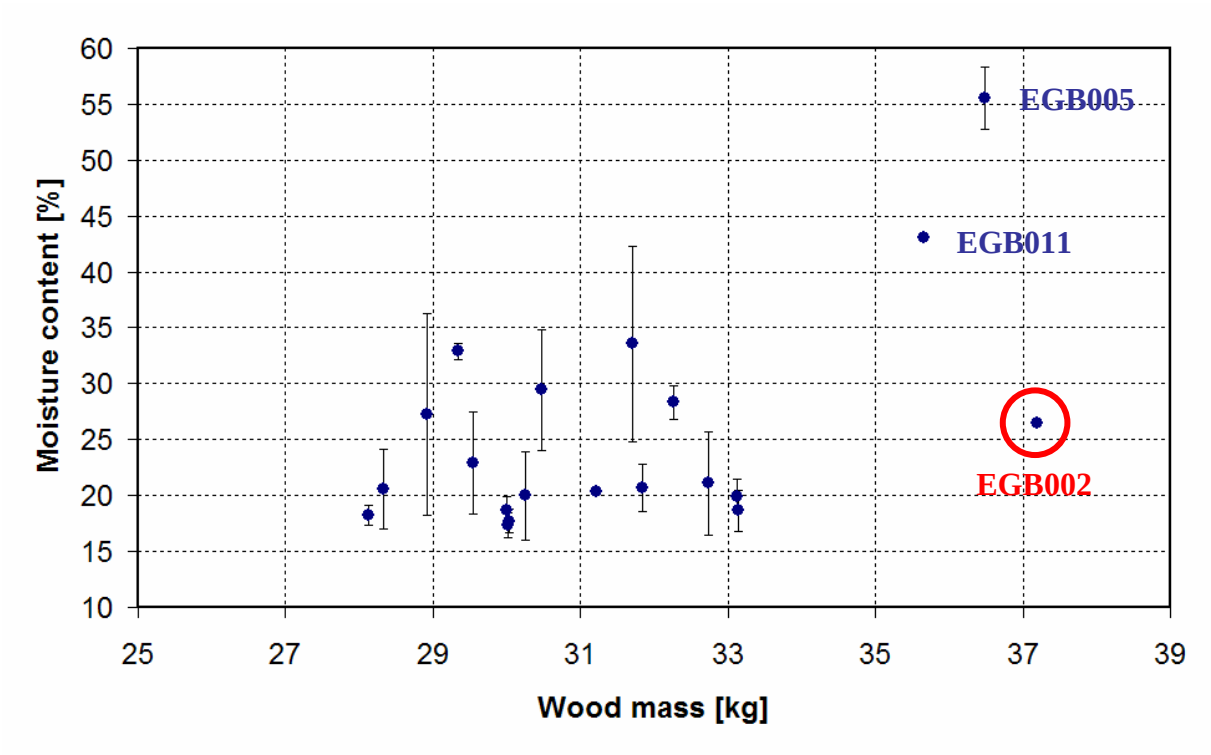

Figure 2-4 Wood samples moisture content versus mass

Figure 2-4 shows there is extensive spread of moisture content. Similarly, spread of wood sample mass is also large. Nevertheless, no correlation between these two parameters has been obtained. Therefore such results highlight the heterogeneity of wood on the one hand and other parameters must have an impact on the density of the material on the other hand (for instance growing conditions). This may explain the characteristics of the sample circled in red which has an important mass and a regular moisture content. This particular sample was used for test ID EGB002 and led to an unexpected behaviour which was removed from our analysis.

The two other samples out of the cloud were used for tests EGB005 and EGB011. Nevertheless, as regards these two samples, the relation between the mass and the moisture content seems to be logical and the behaviour observed in the experiment was in accordance with the other samples in the same configuration.

2.1.2. Tests protocol and matrix

2.1.2.a. Test equipment

Tests were performed at IFSTAR-Bron catapult with a 2 tons bogie vehicle.

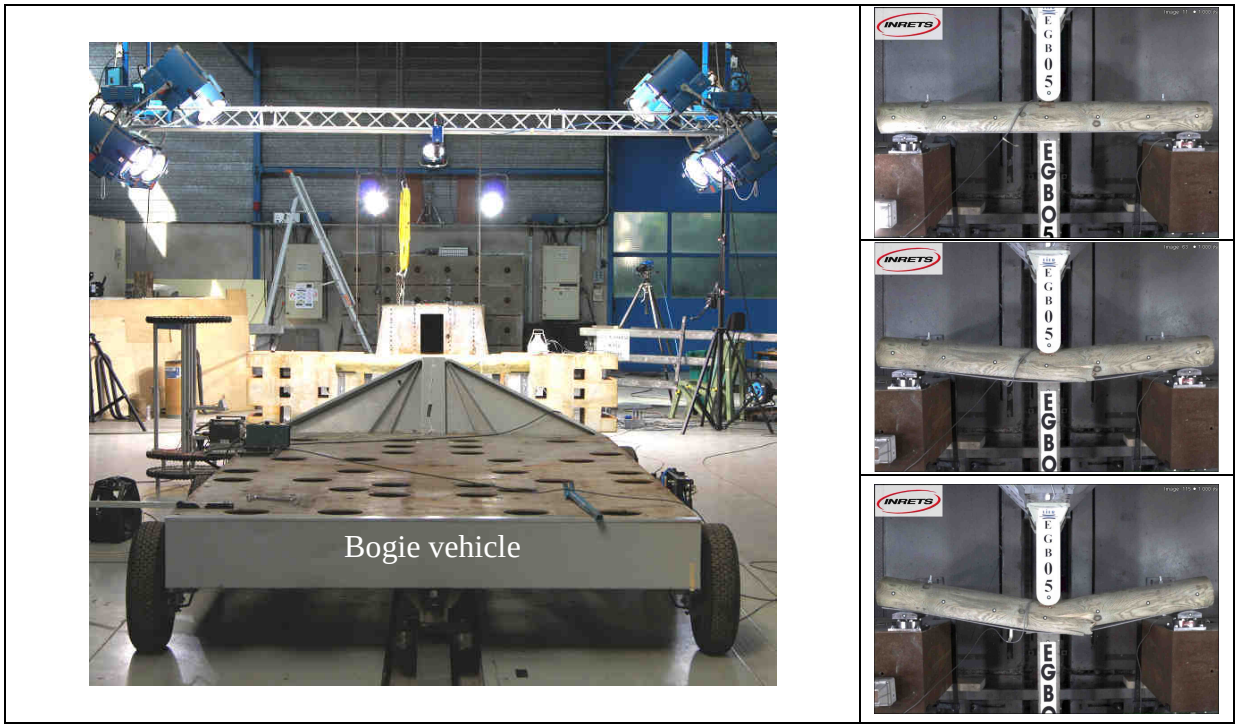

Figure 2-5 Test set-up

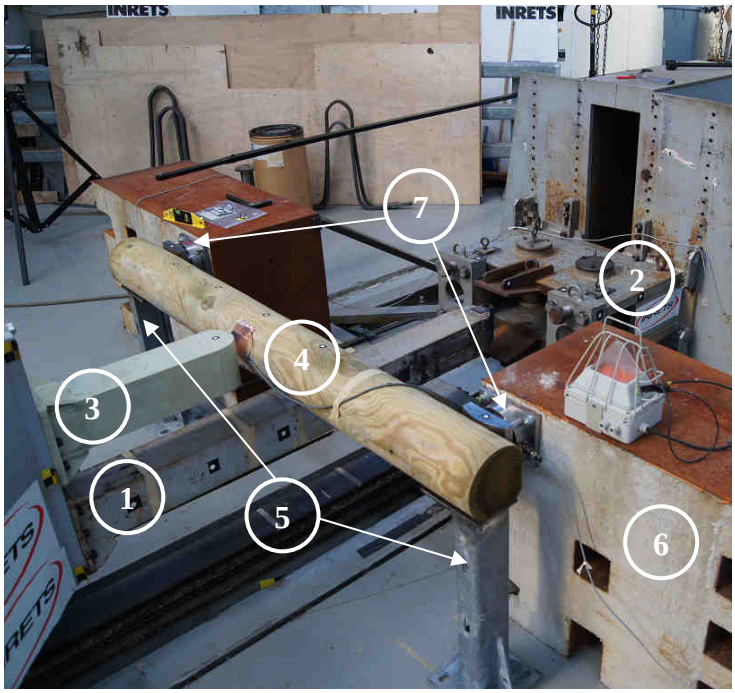

Figure 2-6 Test set-up - details

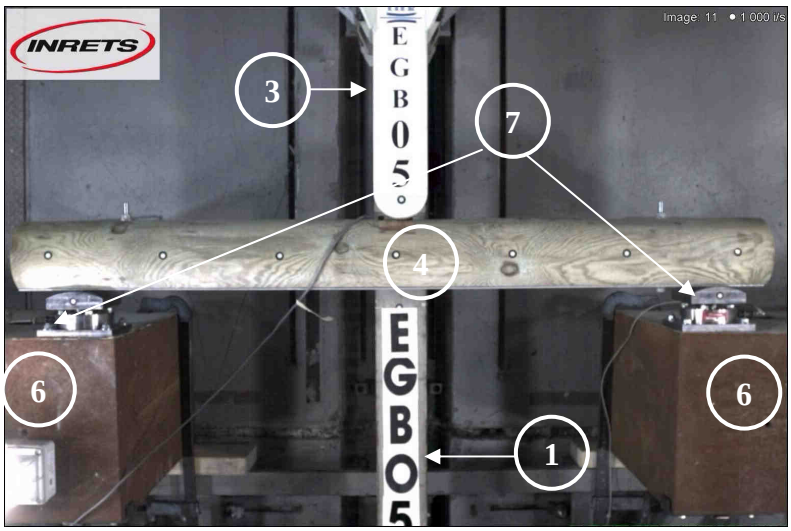

Figure 2-7 Test set-up top view

Two rigid structures were fixed at the front of the bogie:
The longer (1) one was used for the breaking (2) of the bogie and the shorter (3) one was used to impact the structures.
The two meter length samples (4) are simply supported (5) in front of two rigidly fixed concrete blocs (6) with a distance of 1.7m between supports (7).

2.1.2.b. Test matrix

Three levels of velocity were chosen and each configuration was tested three times to assess the repeatability of the process. Two configurations were repeated because of unexpected measurement problems.

A total of 20 tests were performed following the above Design of Experiment:

Test ID	Type of structure	Target impact speed
EGB 001	Wood	10 km/h
EGB 002	Wood	10 km/h
EGB 003	Wood	10 km/h
EGB 004	Wood+Steel	10 km/h
EGB 005	Wood+Steel	10 km/h
EGB 006	Wood+Steel	10 km/h
EGB 007	Wood	20 km/h
EGB 008	Wood	20 km/h
EGB 009	Wood	20 km/h
EGB 010	Wood	20 km/h
EGB 011	Wood+Steel	20 km/h
EGB 012	Wood+Steel	20 km/h
EGB 013	Wood+Steel	20 km/h
EGB 014	Wood	5 km/h
EGB 015	Wood	5 km/h
EGB 016	Wood	5 km/h
EGB 017	Wood+Steel	5 km/h
EGB 018	Wood+Steel	5 km/h
EGB 019	Wood+Steel	5 km/h
EGB 020	Wood	5 km/h

Table 2-1: Test matrix

Initially, it was planned to test at seed range between 10 km/h and 30km/h in order to reach a momentum of same magnitude as the one of a TB32 test.
During the test sessions, at 20 km/h, all the samples failed and the supporting structure appeared to suffer. It was decided for safety reasons but also to have some points without failure of the samples to carry on tests at 5km/hwhich could provide information in view of model calibration.

2.1.3. Measurement analyses

For each test, acceleration data is recorded on two distinct locations of the bogie.
Concerning data recording, time zero is detected by contact on the impacted structure. This contact also lights a flash visible by all the video cameras. All the measurements were filtered using a low pass band Butterworth filter (CFC180).

2.2. Results

2.2.1. Impact conditions

Several parameters were controlled during the test. Impact speed was measured thanks to an optical system just before the impact. Table 2-2 presents for each configuration the average value, the standard deviation and the coefficient of variation. The impact speed was very well controlled and the test configurations were highly repeatable. The highest variation is observed for the lowest impact speed due to the fact that this was the lowest speed admissible for the regulation system which works much better at higher speed (for which the variation is not higher than 1%).

target speed [km/h]		wood	steel-wood
5	μ	4.9	4.9
	σ	0.1	0.2
	σ/μ	2%	4%
10	μ	9.7	9.8
	σ	0.0	0.0
	σ/μ	0%	0%
20	μ	19.7	19.3
	σ	0.1	0.3
	σ/μ	1%	1%

Table 2-2: Impact speed [km/h]

Table 2-3 to Table 2-5 presents the average, standard deviation and coefficient of variation, by configuration, for the total mass of the tested samples (i.e. measurement included the steel reinforcement and bolt masses for steel-wood configurations), the Moisture Content and the room temperature.

The wood samples were taken in order of storage and no particular care was givben to the choice of a sample with respect to the configuration to be tested leading to an arbitrary repartition of the samples.

target speed [km/h]		wood	steel-wood
5	μ	32.0	39.2
	σ	1.3	0.5
	σ/μ	4%	1%
10	μ	33.4	43.2
	σ	2.7	1.8
	σ/μ	8%	4%
20	μ	28.6	41.3
	σ	0.5	2.7
	σ/μ	2%	7%

Table 2-3: Sample mass [kg]

Sample mass variation is always lower than 8%

target speed [km/h]		wood	steel-wood
5	μ	22.5	21.1
	σ	7.4	4.4
	σ/μ	33%	21%
10	μ	22.5	35.0
	σ	2.8	14.8
	σ/μ	13%	42%
20	μ	23.9	28.6
	σ	6.4	10.3
	σ/μ	27%	36%

Table 2-4: Moisture Content [%]

Moisture content variation is high and is supposed to be representative of the one that may be observed on the roadsides.
This parameter cannot be controlled easily. It is worth mentioning that, on average, moisture content varies between 20 and 30%.

target speed [km/h]		wood	steel-wood
5	μ	23.8	25.7
	σ	1.4	2.1
	σ/μ	6%	8%
10	μ	23.3	25.4
	σ	0.9	0.0
	σ/μ	4%	0%
20	μ	21.6	25.4
	σ	1.4	0.4
	σ/μ	6%	1%

Table 2-5: Temperature [°C]

The temperature was recorded just before each test, after the lights were turned on. The temperature varies between 20 and 25°C on average.

The biggest variation observed concerned Moisture content (27 %) while the other parameter variations were below 5%. The variation on deceleration peak remained under 10%, on average.
No correlation could be found between the input and the output variations.

2.2.2. Deceleration results at 5 km/h

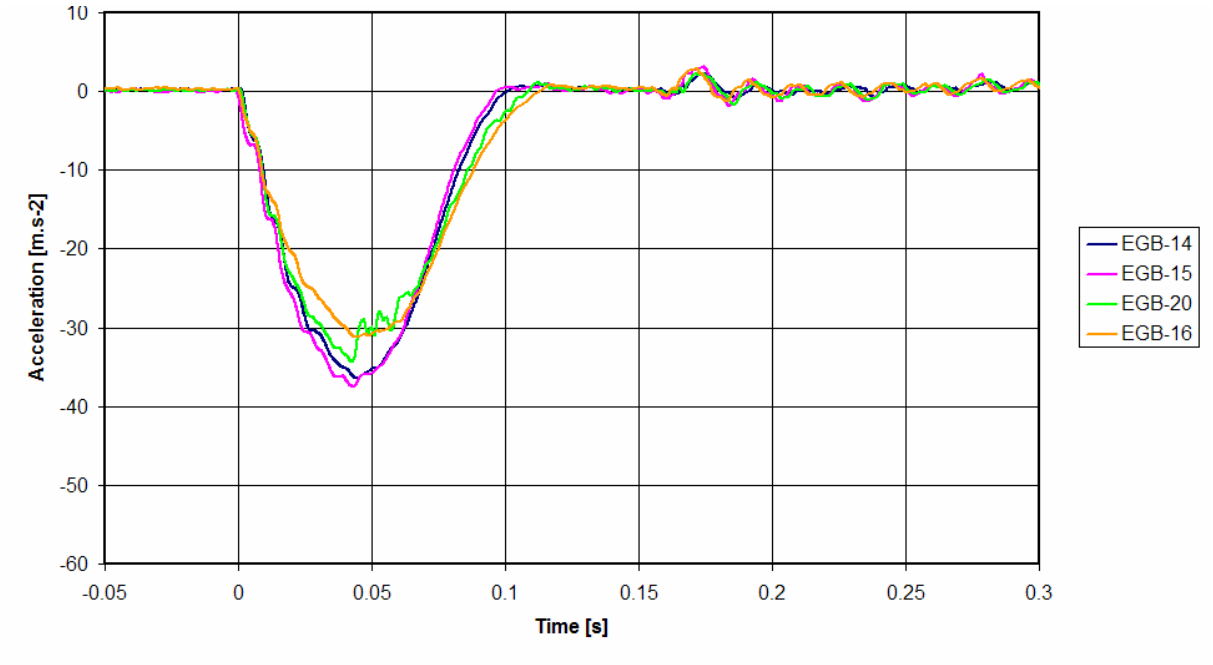

Figure 2-8: Deceleration results - wood samples - 5 km/h

Figure 2-8 shows the deceleration profiles obtained for the four tests performed at 5 km/h on the wood samples which are very close from one to the other. All the tests led to a rebound of the bogie without any failure of the samples.

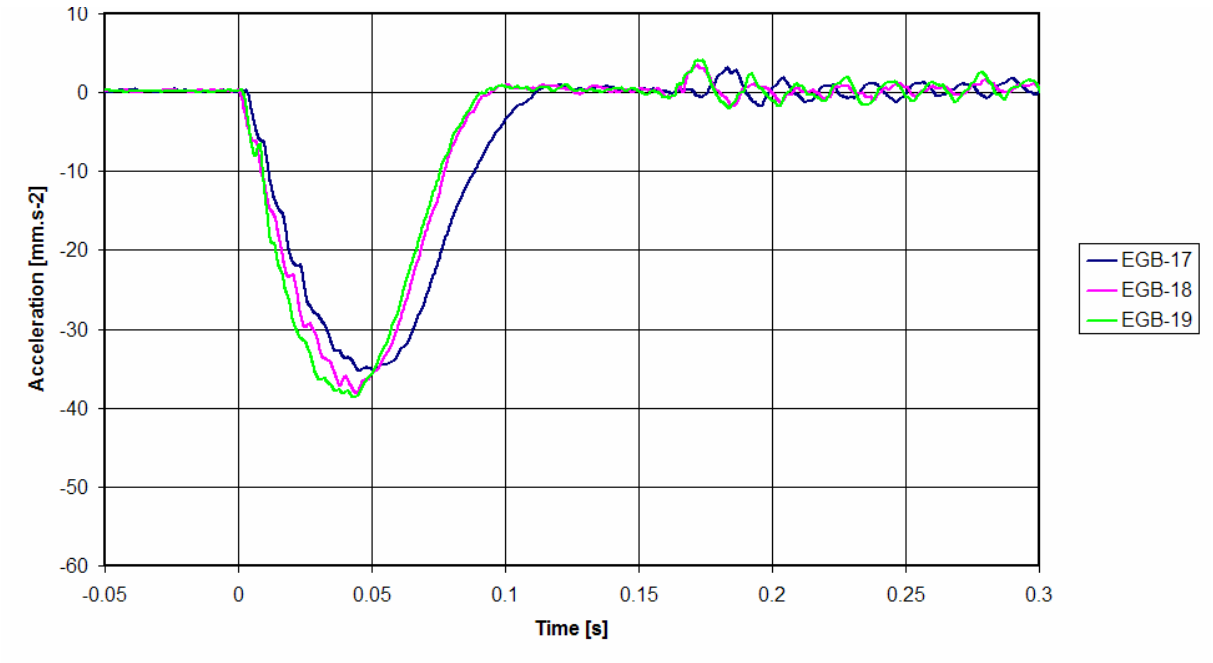

Figure 2-9: Deceleration results - steel-wood samples - 5 km/h

Figure 2-9 illustrates the deceleration profiles obtained at 5 km/h on the wood samples with a steel reinforcement. As for the samples without steel reinforcement, no failure was observed during three tests which are also very similar in results.

2.2.3. Deceleration results at 10 km/h

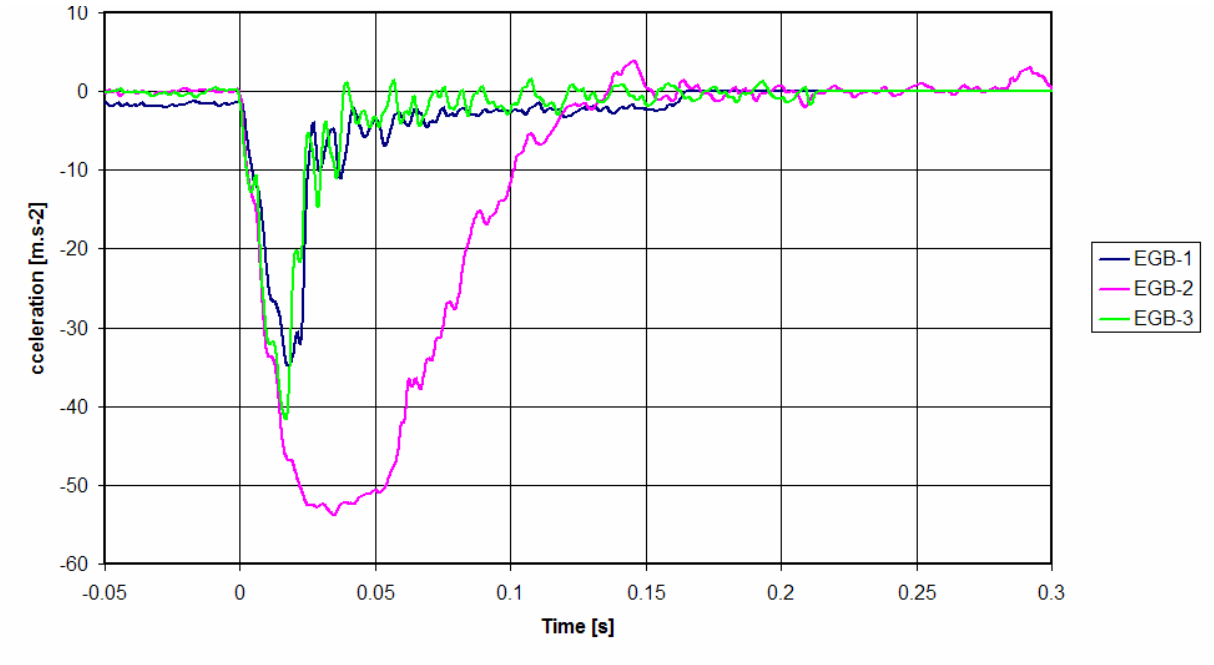

Figure 2-10: Deceleration results - wood samples - 10 km/h

Figure 2-10 presents the deceleration profiles obtained at 10 km/h for the wooden samples. Test EGB-002 did not fail and presented a deceleration profile very different from the other two where the wood sample failed. The sample used for that test was the one highlighted in the previous Figure 2-4. Its peak shape is comparable to those obtained at 5 km/h (peak width around 0.1s) with a peak value significantly higher.
On the other hand, for the two other tests, a brittle failure is observed, characterized by a shorter peak in both time and amplitude.

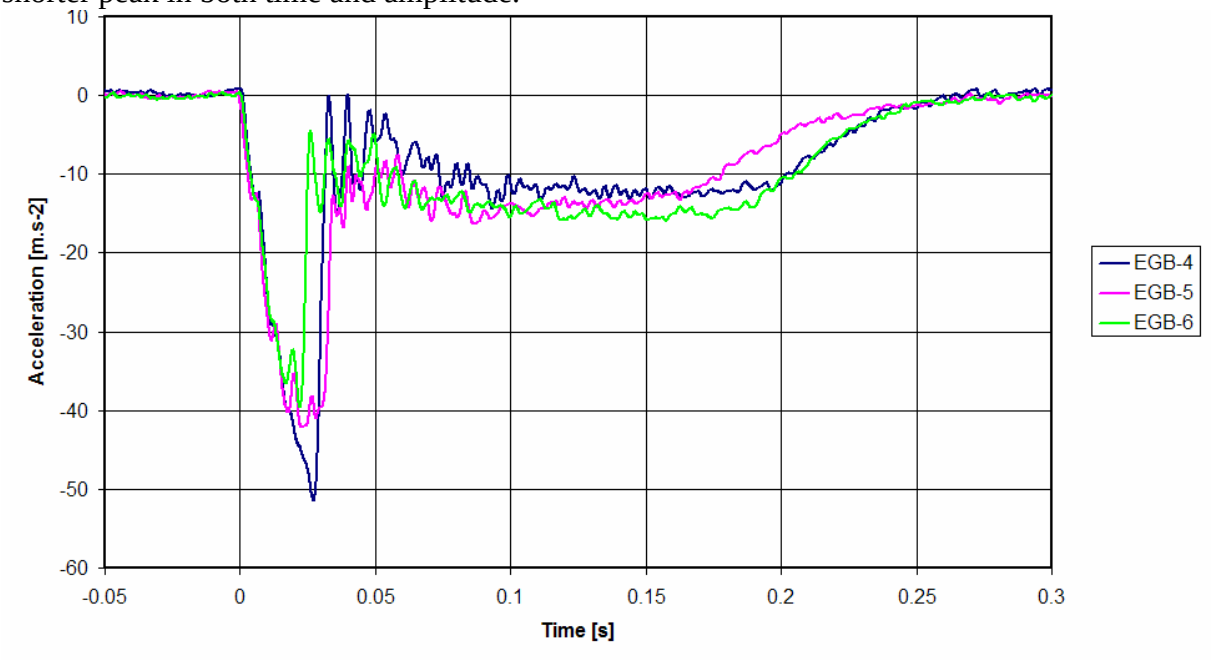

Figure 2-11: Deceleration results - steel-wood samples - 10 km/h

Figure 2-11 shows the deceleration profiles obtained for steel-wood samples at 10km/h. The peak values are close to those obtained for wood samples which failed. The main difference is observed after the peak: A deceleration plateau related to the yielding of the steel reinforcement after the wood failure.

Test EGB-004 is significantly different from the other two in term of deceleration peak value. Nevertheless, no distinction could be found either in the sample mass or in the moisture content.
Finally let us mention the reproducibility of the deceleration plateau for all samples.

2.2.4. Deceleration results at 20 km/h

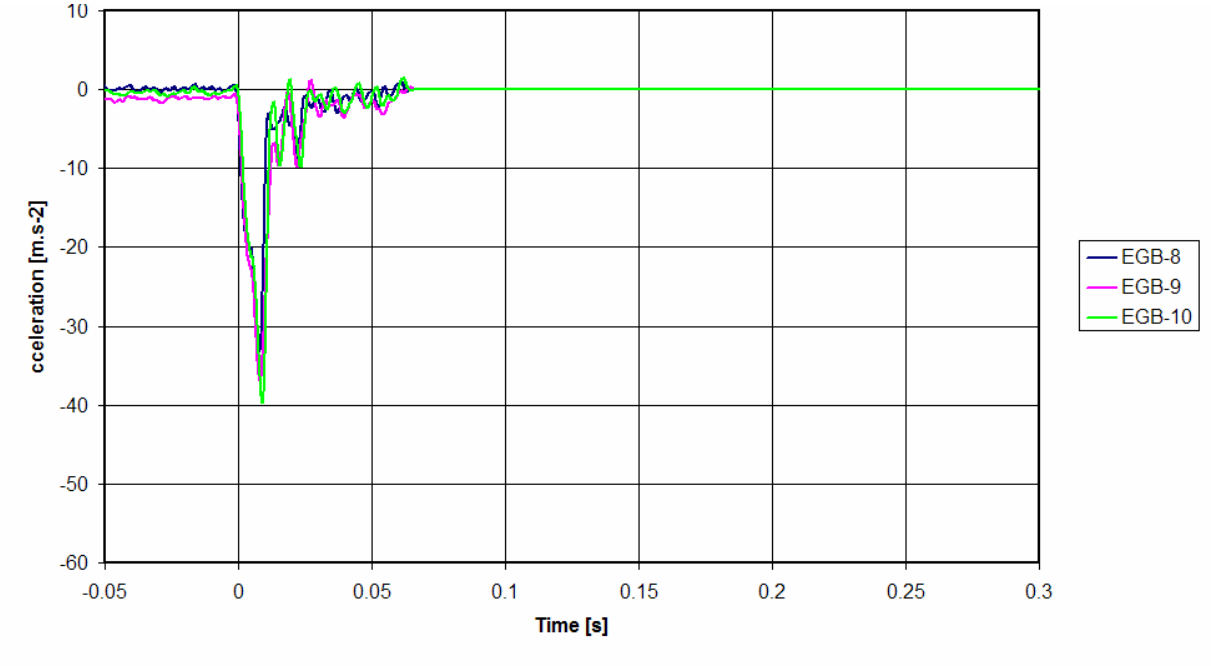

Figure 2-12: Deceleration results - wood samples - 20 km/h

In Figure 2-12 the curves have been set to zero around 0.055s because a second deceleration peak corresponding to the breaking of the bogie was recorded but out of interest.
The single peaks presented, characterized the wood failure (as observed at 10 km/h). One can notice the reproducibility of this test configuration.

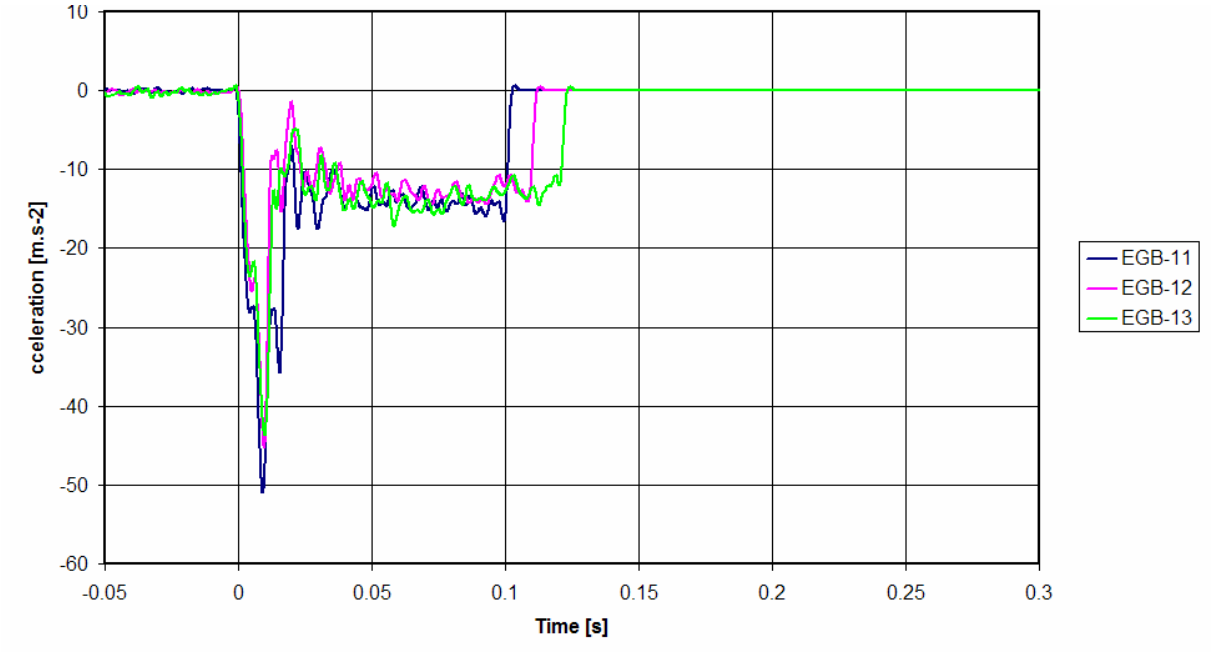

Figure 2-13: Deceleration results - steel-wood samples - 20 km/h

Figure 2-13 present the results at 20 km/h for steel-wood samples. As for wood samples, the curves where set to zero around 0.1s to avoid the peak resulting from the breaking of the bogie.
The pulses obtained are very comparable and the deceleration plateaux are really similar.

Synthesis

target speed [km/h]		wood	steel-wood
5	μ	-34.9	-37.4
	σ	2.4	1.5
	σ/μ	-7%	-4%
10	μ	-38.2	-44.4
	σ	3.4	5.1
	σ/μ	-9%	-12%
20	μ	-36.6	-46.7
	σ	2.7	3.1
	σ/μ	-7%	-7%

Table 2-6: Deceleration peak [mm/s²]

The analysis of Table 2-6 raises several issues:

- A significant difference is observed between wood and steel-wood structures at every target speed.
- No correlation is obtained between the test impact speed and the deceleration peak value
- No correlation can be obtained between the variability of the test conditions (reported in Table 2-2 to Table 2-5) and the variability of the deceleration.

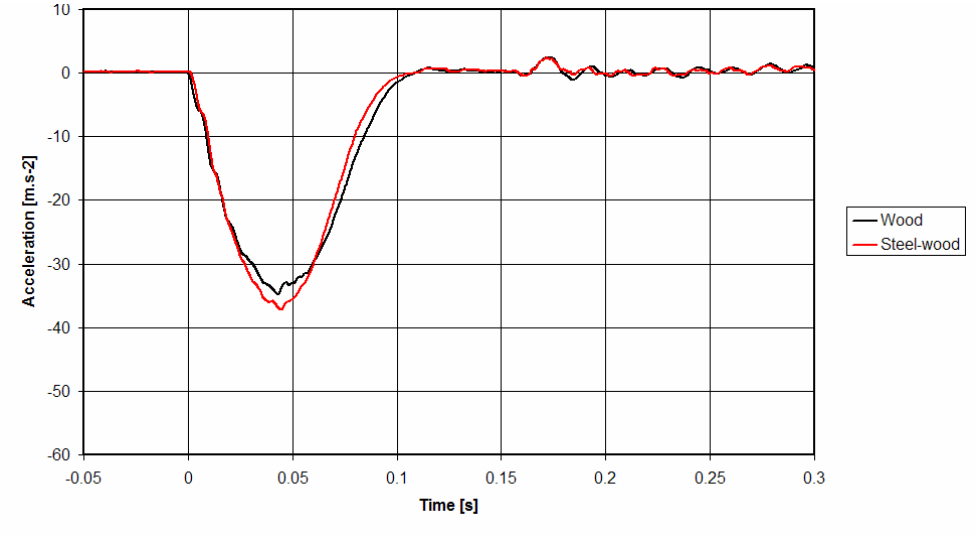

Figure 2-14: Average deceleration profiles at 5 km/h

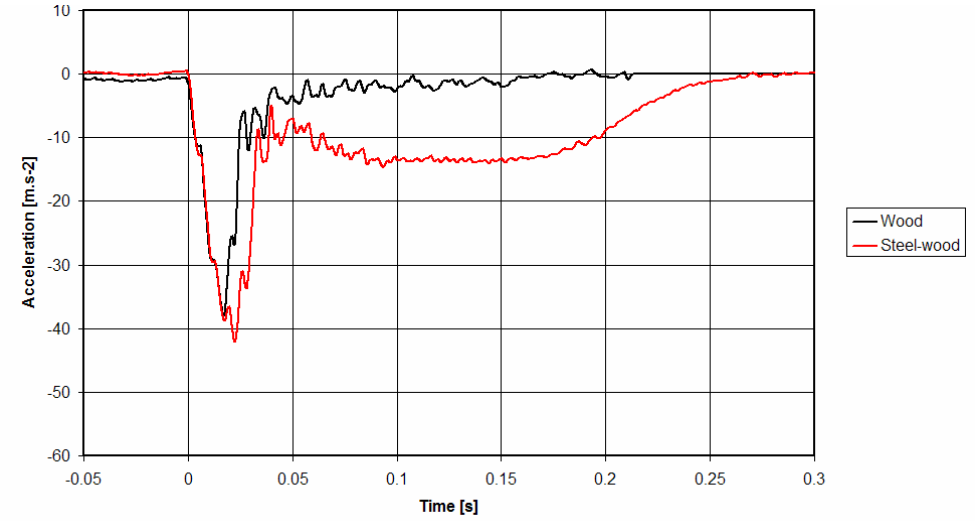

Figure 2-15: Average deceleration profiles at 10 km/h

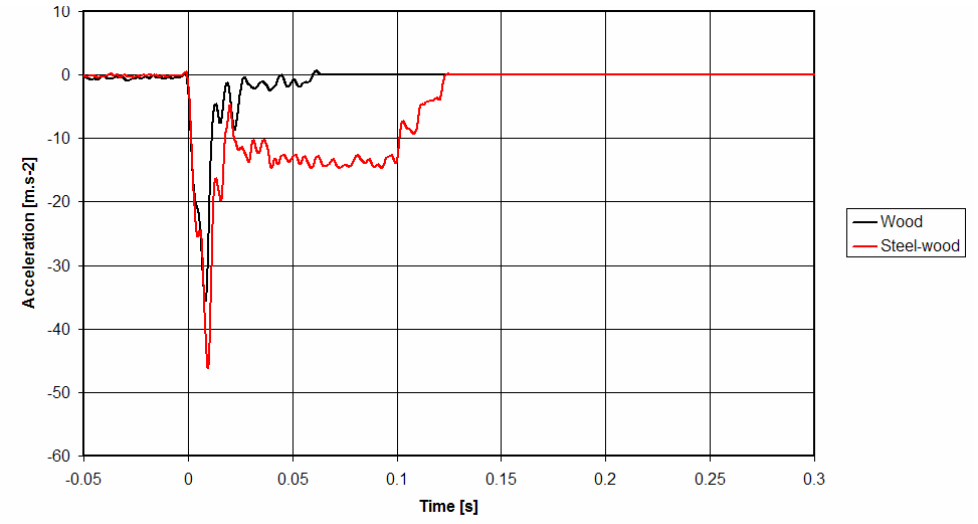

Figure 2-16: Average deceleration profiles at 20 km/h

Figure 2-14, Figure 2-15 and Figure 2-16 present, for each configuration (impact speed and sample type), the average of the test deceleration curves.

The configuration at 5 km/h, for which no failure of wood samples occurred, shows no significant difference between the two types of structures.
At higher impact speeds the wood beam failure allows the yielding of the steel reinforcement and a deceleration plateau is observed for all steel-wood samples. The deceleration peaks have a comparable value for the two impact speeds whereas the peak width is significantly narrow at 20 km/h.

2.3. Conclusion

Dynamic tests were performed on wood samples and steel-wood structures allowing to investigate the failure modes of these structures under impact loading. Acceleration curves were obtained which are necessary for the validation process of the wood material constitutive law.
While no discrepancies were found between the two types of structures at low velocity, differences were observed after wood failure which is systematically observed for the two other impact speeds.

Chapter 3 Dynamic three point bending tests simulations

3.1. Introduction

The aim of this chapter is to develop a model for multi-material beams tested and to validate it according to experimental results. The simple test configuration allows to explore a lot of numerical parameters.
First, the focus will be on the convergence of the numerical model.
After that, the wood material constitutive law available in Ls-Dyna will be evaluated in order to select a set of parameters which best fit to wood used in our experiment.

3.2. Models

3.2.1. Wood

Wood is one of the oldest construction materials used by human beings. As a consequence, current design rules are often based on experience and traditions. Furthermore, wood specialists are not mechanics experts, and experts in mechanics are not used to deal with a living, highly anisotropic and non homogeneous material which may explain the lack of data concerning this material. [GUI86]. Nevertheless some information can be found in the literature to understand the behaviour of the material.

3.2.1.a. Anatomy and mechanical properties

Wood is a complex living material. To understand its behaviour, one has to focus on its anatomy.
At a macroscopic scale, wood is commonly considered as cylindrical orthotropic.
In fact, after a cut perpendicular to the fibres axis of a trunk, one can see growing rings which are concentric (Figure 3-1). The mechanical properties associated to this anatomy are then related to a cylindrical reference frame Longitudinal (fibbers axis) Radial (radius of growing rings) and tangential (perpendicular to growing rings).

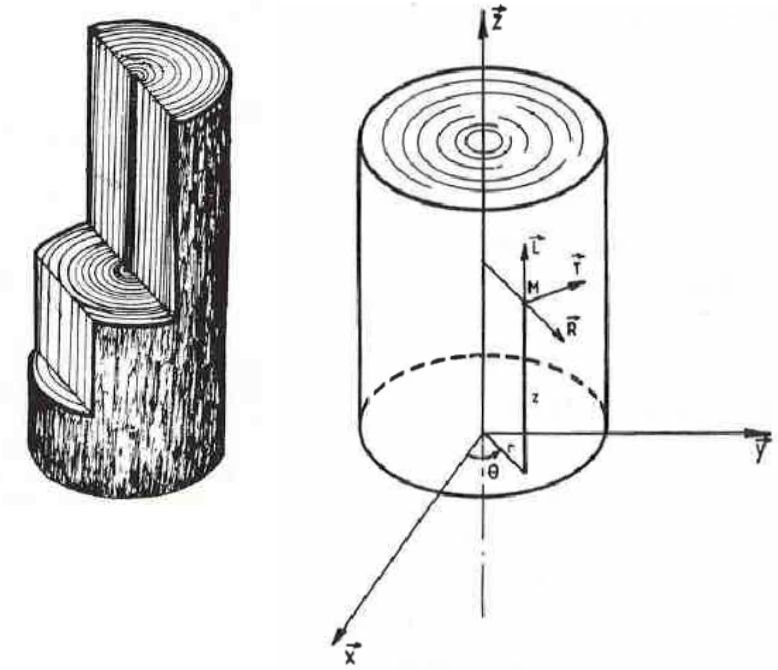

Figure 3-1: Cutting sections of wood and associated reference frame [GUI86]

Nevertheless, the mechanical properties differences between Radial and tangential directions are much lower than the one with the longitudinal direction (Table 3-1) which leads us to consider wood as a transverse isotropic material.

	EL/ER	EL/ET	ER/ET
hardwood	8	13.5	1.7
sofwood	13	21	1.6

Table 3-1: Young modulii order of magnitude in the three anatomical directions

Table 3-1 presents the average value for the two main families of wood:
Hardwood and softwood. Inside each of these families an important variation can be observed depending on the species and models have been proposed to determine the elastic properties depending on of wood nature (hard or soft) and its density at 12% of MC:

	Hardwood ρ_0=0.65 g/cm^3	Softwood ρ_0=0.45 g/cm^3
E_l	$14400\times\left(\frac{\rho}{\rho_0}\right)^{1.03}$	$13100+41700\times(\rho-\rho_0)$

Table 3-2: Predictive model of wood elastic properties

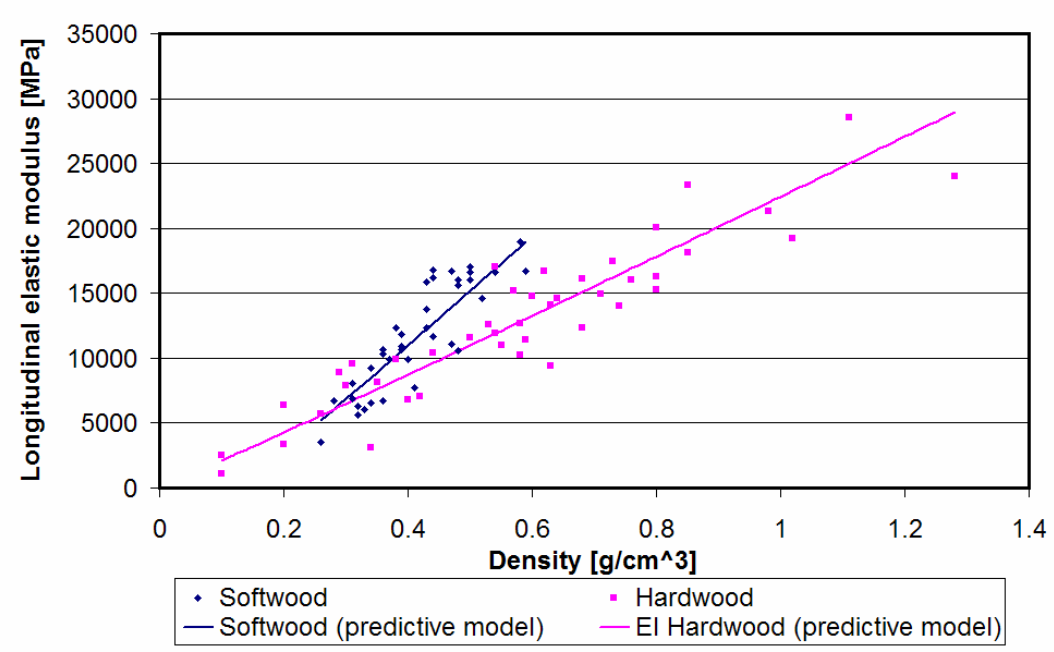

Figure 3-2: Wood elastic modulus as a function of density

3.2.1.b. Sensibility to temperature and moisture content

The hygroscopic nature of timber can be divided in two aspects:
"Free water", inside the wood at high moisture content, in liquid and vapour phases in the intra-cells spaces whose rate fluctuation does not affect mechanical properties.
"Absorbed water" requires a higher amount of energy for its extraction in order to break the related chemical bonds. Moisture content fluctuations below fibres saturation point go along dimensional changes, shrinkage or swelling.
Wood material can be considered as a complex natural composite consisting mainly of three bio polymers. The effect of moisture content toward vitreous transition of these constituents has been studied.

The transition from vitreous to rubbery state of polymer is characterized by temperature called vitreous transition temperature (Tg). This transition goes with a important decrease of elastic properties among other things.
As regards wood constitutive polymers, the transitions appear at relatively high temperatures (around 200°C). Nevertheless the increase of moisture content decreases the vitreous transition temperature.
For two out of the three main wood polymers, a sufficient amount of water absorbed (20%) decreases the transition temperature down to ambient temperature and, thus affects the mechanical properties of wood.

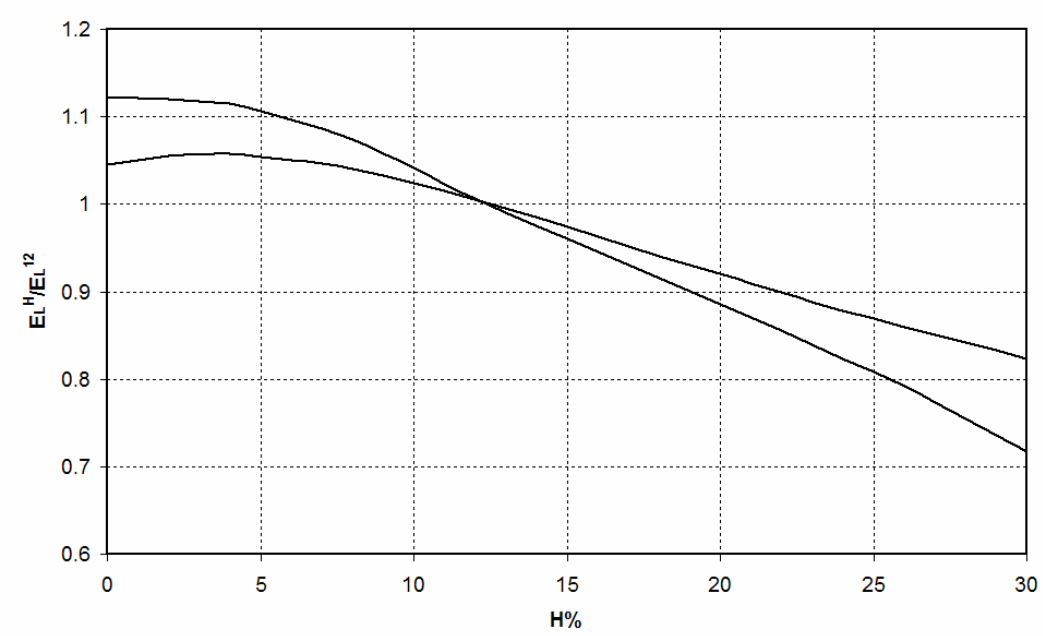

Figure 3-3: Relative variation of E_L as a function of moisture content for various wood species

On a practical way, [GER82] proposes a variation of elastic modulus as function of moisture content (Figure 3-3) and [GUI87] proposes the following correction of the mechanical properties advised for a 6 to 20% moisture content range of variation :

$$E_L^H = E_L^{12}[1-0.015(H-12)]$$

Equation 10

$$E_R^H = E_R^{12}[1-0.030(H-12)]$$

Equation 11

$$E_T^H = E_T^{12}[1-0.030(H-12)]$$

Equation 12

For wood modelling purpose, MAT_WOOD (type 143 available in Ls-Dyna) was used. This model, developed under contract from the FHWA [MUR05] and [MUR07], consists in a transversely isotropic material with damage and erosion.
Our interest is that default material properties for yellow pine are available and temperature and moisture content can be changed (0°C - 10°C - 20°C - 30°C and 0% - 10% - 20% -30% respectively) which makes the material law easy to use with respect to other constitutive laws which are directly available in the software and without default properties [TAB00_2]
Wood, as a natural material, is not homogeneous and presents some defects (nodes by example). Some authors tried to model explicitly the defects [CAS07]. The localization of a wood defect could obviously influence the global behaviour of a wood beam under impact loading but it is not possible, before a crash test to analyse one hundred meter of wood material to explicitly localise its defects and mesh all of them.

The mechanical properties of wood are obtained for clear wood samples (without defects). One common approach to take into account the existence of the defects is to apply quality factors to the clear wood mechanical properties in order to obtain homogeneous properties for a degraded material.
Empirical equations are implemented which are from quadratic fit of experimental data. Table 3-3 presents the related coefficient for Moisture Content effect towards mechanical properties and Figure 3-4 illustrate its behaviour in regards of literature.

Parameter	$P=A(MC)^2+B(MC)+C$		
P	A	B	C
Moduli			
EL Parallel Normal (MPa)	-8.50	-45.3	16774
ET Perpendicular Normal (MPa)	-2.06	17.2	944
mLT Parallel Poisson's Ratio	-0.00013	-0.00354	0.307
Strengths			
XT Tension Parallel (MPa)	-0.448	10.51	80.57
YT Tension Perpendicular (MPa)	-0.016	0.33	2.82
XC Compression Parallel (MPa)	0.011	-3.25	90.17
YC Compression Perpendicular (MPa)	0.000	-0.555	16.93

Table 3-3: Effect of Moisture Content

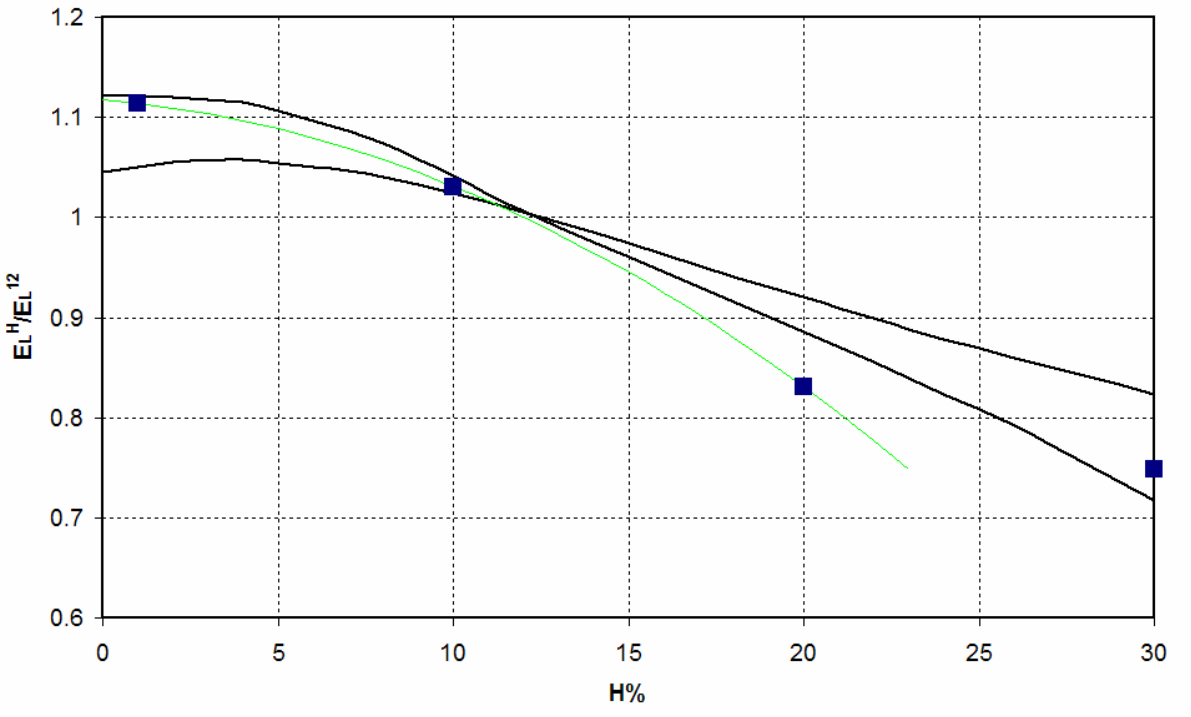

Figure 3-4: Moisture content effect

The proposed law seems to be in accordance with the literature for value of moisture content below 12%. For value above 12%MC the LS Dyna law appear to decrease significantly more than expected. For instance, at 20% of MC Ls Dyna applies ELH=0.83*EL12. In the literature, it appears that the module at 20% should not be less than 88% of the module at 12%MC.
In the LS-Dyna material law, all the material properties are held constant above 23% of moisture content. This is reported to be the fibre saturation point at which the cell walls are saturated with water but no water exists in the cell cavities.
As a result, at 30% of MC, the Ls-Dyna model returns back in the literature corridor.
Furthermore, the variations of Moisture Content and Temperature are not continuous but tabulated. The available parameters are materialized by the blue squares in Figure 3-4.

A factor is implemented to scale clear wood moduli as a function of input temperature. In conformity with chemical phenomenon described in paragraph "Sensibility to temperature and moisture content" the factor depends on temperature and on moisture content according to following equations:

$$F_M(T) = \bar{a}(T-20)^2 + \bar{b}(T-20) + 1$$

Equation 13

With

$$\bar{a} = a_1(MC)^2 + a_2(MC) + a_3$$

Equation 14

And

$$\bar{b} = b_1(MC)^2 + b_2(MC) + b_3$$

Equation 15

Where :

Coefficient	Value
a_1	-0.0000000377625
a_2	-0.000001416
a_3	-0.0000003125
b_1	-0.000004817
b_2	-0.000109895
b_3	-0.000875

Table 3-4 quadratic fit coefficient for temperature effect

Another factor is implemented to scale clear wood strength as a function of temperature as far as the experiment has shown that the effect of temperature is twice important for strength as for moduli:

$$F_S(T) = 2[F_M(T) - 1] + 1$$

Equation 16

Finally, reduction factors can be applied towards clear wood properties according to a wood grade which is a way to take into account wood defects.
The exact positions of defects are not known except in highly controlled laboratory tests. A practical approach for addressing defects is to modify the material properties globally as a function of visual grade.
For Pine option, 3 grades are available which apply reduction factors for the strength in tension (Qt) and in compression (Qc) according to following Table 3-5

Grade	Qt	Qc
Clear wood	1.00	1.00
Grade 1	0.80	0.93
Grade 0	0.47	0.63

Table 3-5: Strength reduction factors for grade modelling

		Temperature			
		1°C	10°C	20°C	30°C
M.C.	1%	17 024	16 883	16 720	16 552
	10%	16 091	15 823	15 471	15 063
	20%	13 456	13 037	12 468	11 790
	30%	12 740	12 105	11 236	10 194

Table 3-6: Parallel normal module as a function of MC and T from theory

Tensile tests on a single element were simulated and corresponding tensile module and strength were computed in order to check the adequacy between the theory and the model. The results are reported in Figure 3-5, Figure 3-6 and Table 3-7. The adequacy is quite good as far the error between theoretical and computed values is, on average less than 1%.

		Temperature			
		1°C	10°C	20°C	30°C
M.C.	1%	17 024	16 881	16 716	16 545
	10%	16 113	15 840	15 472	15 083
	20%	13 550	13 119	12 554	11 870
	30%	12 404	11 948	11 332	10 594

Table 3-7 Parallel normal module[MPa] as a function of MC and T from tensile test simulations

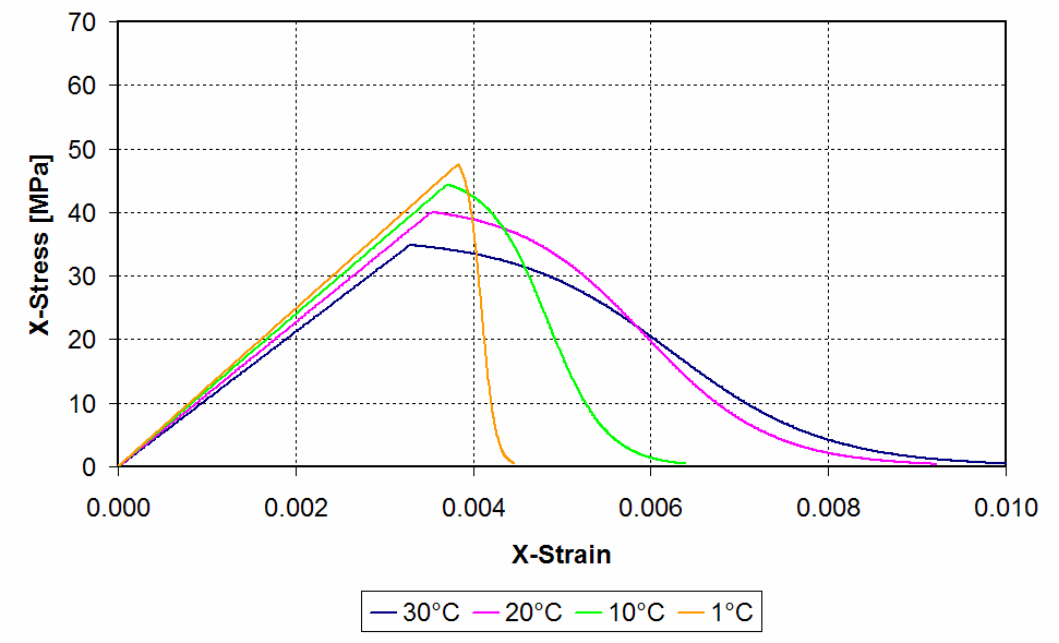

Figure 3-5: Temperature effect - Tensile test simulation results

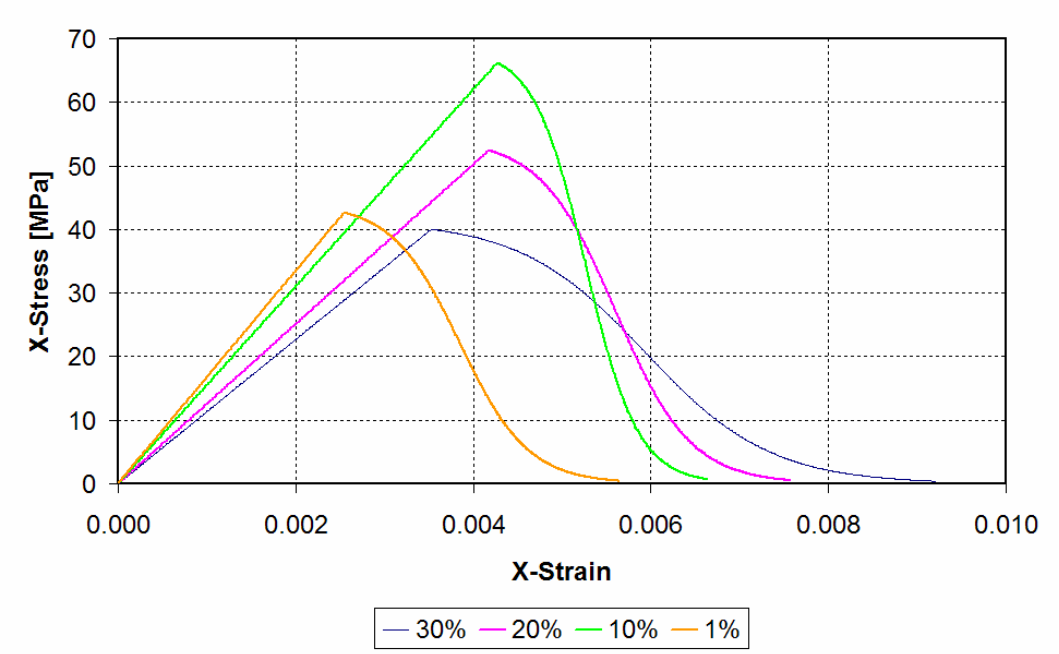

Figure 3-6: Moisture Content effect - Tensile test simulation results

3.2.2. Meshes

3.2.2.a. General information

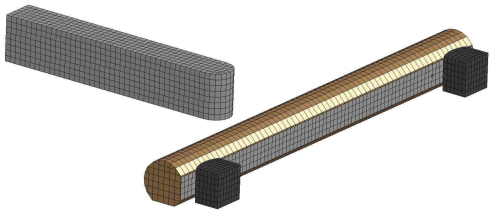

Figure 3-7 Mesh general view

The impactor is considered rigid and an initial velocity is applied depending on the test configuration to simulate.
The two supports are also modelled as rigid bodies and boundary conditions are applied to avoid any displacement.

The wood beam is modelled with brick elements and the material law detailed in the previous section is applied.
For under integrated elements, Ls-Dyna type 1 (Default) “Constant Stress Solid” is used.
For fully integrated simulations, element type 2, S/R solid full integrated formulation is used.

The steel reinforcement is modelled with Ls-Dyna type 2 Belytschko-Tsay shells in addition with an elasto-plastic law of MAT 24 (MAT_PIECEWISE_LINEAR_PLASTICITY).

3.2.2.b. Bolt modelling

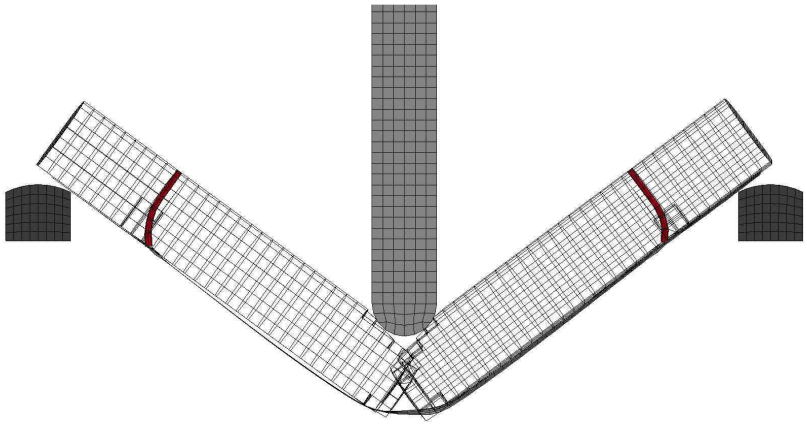

Figure 3-8: Bolt model deformation

Special care was applied to the modelling of the bolted connection between the wood beam and the steel reinforcement and a summary can be found in the appendix 1 of the document. The link between the wood beam and the steel reinforcement is done via M16 bolts.

The use of Hughes Liu type beams discretized along the beam length with a coupling interface (Lagrange in solid) with the wood component allows consistent deformation of the beams with respect to the experiment as illustrated in Figure 3-8. The Lagrange-in-solid coupling (used to model the steel reinforcement inside reinforced concrete) is a very convenient way to reduce the meshing effort (the beams are localized at their proper place and there is no need to represent the holes).
The non linear discretisation of the beam doesn't bring better results. Thus the solution with a regular discretisation homogeneous with the wood mesh size will be used for the next steps.

3.3. Model validation

3.3.1. Methods

Before exploring the material constitutive law, it seems necessary to validate numerical aspects of the modelling.

3.3.1.a. Mesh refinement

Two meshes were used and are represented in Figure 3-9 :

- A "coarse" mesh with a mesh size of 30mm which is the current size for most applications of road equipment modelling.
- A fine mesh for which the brick elements were split.

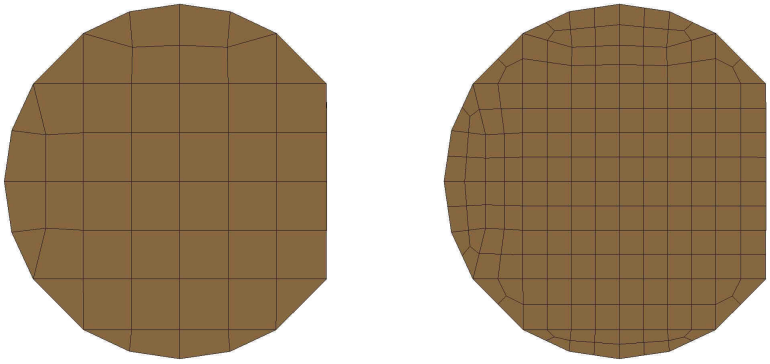

Figure 3-9: Mesh refinements

3.3.1.b. Hourglass control and reference model

In roadside equipment modelling, under-integrated elements (one-point integration for eight-nodded elements) are often used due to their low cost in term of CPU time.
The biggest disadvantage to one-point integration is the need to control the zero energy modes which arise, called hourglassing modes.

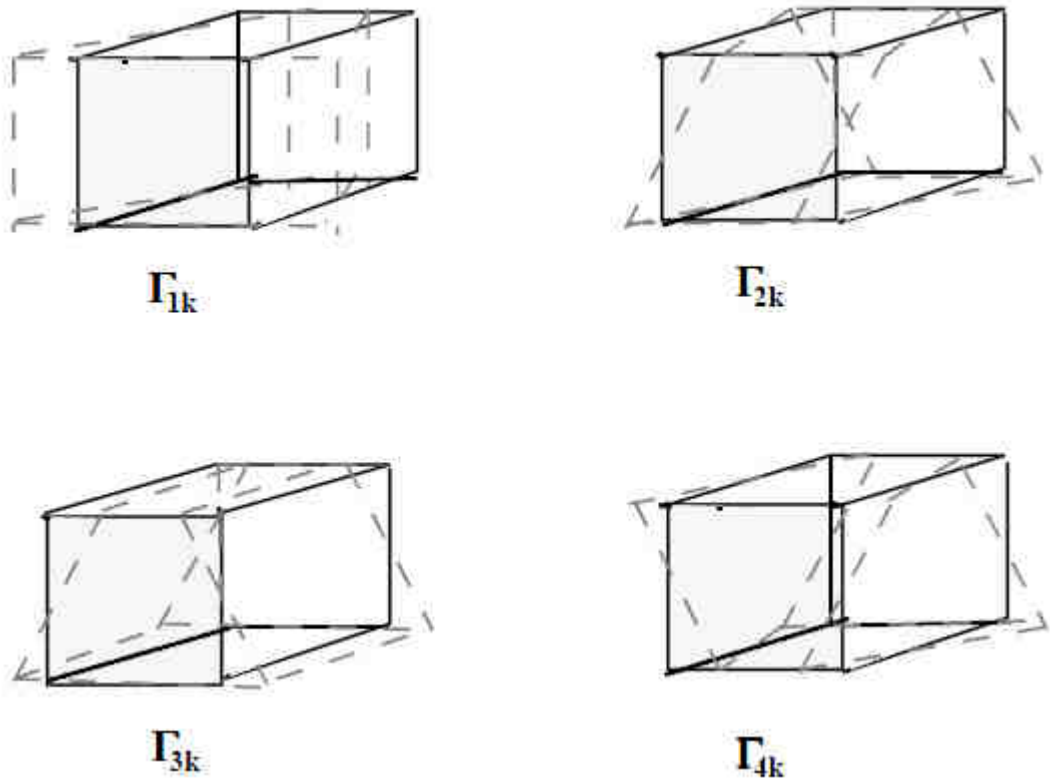

Figure 3-10; Hourglass modes from [HAL98]

One way to withstand undesirable “hourglassing” is to apply a small elastic stiffness capable of stopping the formation of the anomalous modes but having a negligible effect on the stable global modes.
It appeared during the work that Hourglass control may affect the results.

A reference set of results will be presented with fully integrated elements and four Hourglass stiffness controls will be compared (0.05, 0.005, 0.001 and without)

3.3.1.c. Time-step control

The time step is of main interest because it will (if not fixed) determine the duration of a simulation. Ls-Dyna, by default, takes the critical time step which is the smallest value obtained by the following equation computed for all the elements of the model:

$$\Delta t_e = \frac{L_e}{c}$$

Equation 17

where c is the adiabatic sound speed :

$$c = \left[\frac{4G}{3\rho_0} + \frac{\partial p}{\partial \rho} \right]^{\frac{1}{2}}$$

Equation 18

where ρ is the specific mass density

The analyst also has to check if the time step is compatible with the proper use of the contact interfaces. In fact, Ls-Dyna give a warning with the contact interface maximum time step but it is the responsibility of the analyst to check if the conditions are satisfactory.

By default, during a calculation the time step could change while elements deform. As a result, the total duration or simulation could be easily multiplied by two or worse, never end if a highly distorted element gives a very small time step.

Two ways exist and were explored to control the time step of the calculation:

3.3.1.d. Mass scaling

Often used for global models.
For a constant Δte, if L_e decreases due to element distortion, c has to decrease. A way is to increase ρ for the specified element.

3.3.1.e. Time step erosion

To avoid numerical problem during erosion of an element with an important density which causes local numerical instabilities, another way is to erode the element for which the time step is too low and drives the global time step of the simulation.
This method was tested but will not be reported here (see appendix n°2) because it didn't give more accurate results than the mass scaled solution on the one hand, and had a significant effect on the CPU time on the other hand. In fact, to be efficient, one has to allow the time step to decrease significantly before erosion (or most of the element would be eroded) and thus, the total CPU time needed could be severely affected.

In order not to jump to conclusions on the basis of one result only, a set of simulations was performed with "Pine" default properties at 2 temperatures (20°C & 30°C) and two moisture content levels (20% & 30%) which enclose the experimental values of these parameters. Thus, 4 shots were run with Ls-Dyna explicit solver [HAL97] for each parameter. This analysis was performed for the 20 km/h impact speed which is the closest to the orthogonal component of the velocity of an EN1317 TB32 test.

Parameter	Nb of value	Value
Time step control	2	Mass scaling and time step erosion
Element formulation	5	Fully integrated, Under integrated without Hourglass control and with hourglass control (0.001, 0.005, 0.05)
Mesh	2	Coarse and fine mesh
Structure	2	Wood and steel-wood

Table 3-8 Summary of tested parameters

3.3.2. Results

In the following figures, the results are presented for each element formulation by meshes and structure type. Four simulation results are averaged (corresponding to the four combinations of temperature and moisture content).

3.3.2.a. Quadratic error

For each simulation, the quadratic error between each simulation acceleration signal A(t) and its corresponding case (i.e. same structure and same wood properties) ran with fully integrated element B(t) is computed following Equation 19. The values obtained are normalized dividing the results by the maximum obtained by structure type (wood or steel-wood).

$$\sqrt{\frac{1}{n}\sum_{n}\left(A(t_n)-B(t_n)\right)^2}$$

Equation 19: Quadratic error

To facilitate the comparison, the results are normalized dividing the obtained value by the maximum value obtained between the eight cases (2 meshes x 4 element formulations)of each structure (wood or steel-wood).

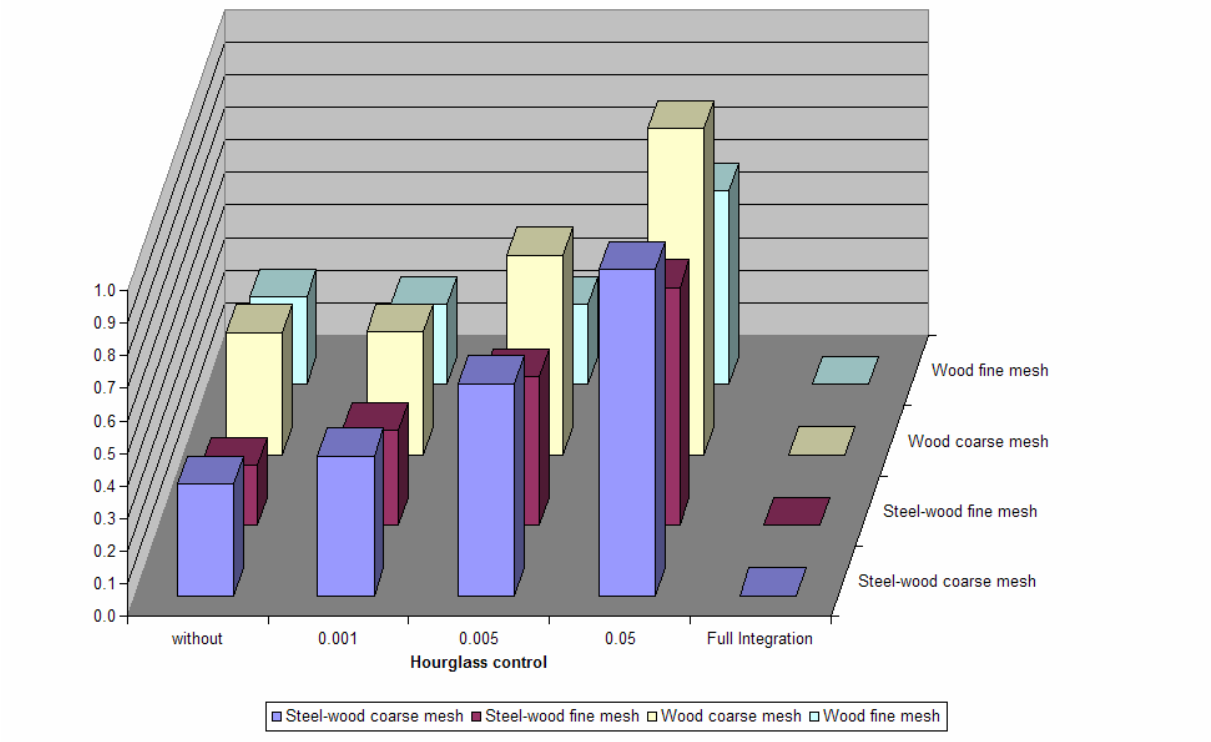

Figure 3-11 Squared Error (Fully Integrated run reference)

It is worth noticing that the stiffer the hourglass control is the bigger the quadratic error. The simulations run without hourglass control are the closest to the one performed with fully integrated elements.
One can notice that the mesh refinement has a poor effect on the numerical quality of the results either for Steel-wood or wood structures models. This shows that the mesh refinement is sufficient. Furthermore, in the simulations run with fine mesh, 20% failed for a numerical reason while all the simulations run with coarser mesh had a normal termination.

3.3.2.b. Energy ratio

To evaluate the numerical accuracy of a model using under integrated element, the energy ratio between hourglass energy and internal energy has to be checked. Common advice is to check that this ration may not exceed 10%. This ratio was computed for each simulation of the wood material. The normalized results are presented in Figure 3-12.

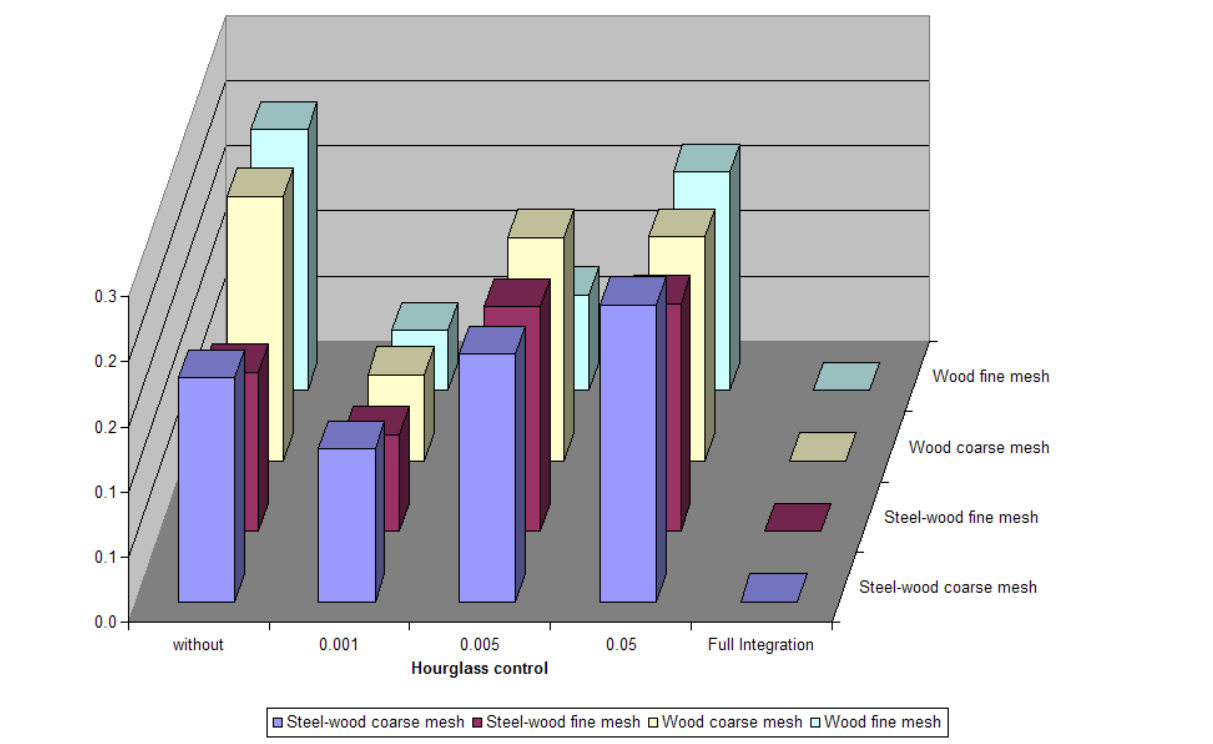

Figure 3-12: Energy ratio

As no hourglass mode can be activated with fully integrated elements, the ratio is always zero. The simulations with under integrated elements and no hourglass control which presented the best results in term of quadratic error are here disqualified by a poor numerical quality.

3.3.2.c. CPU time

In addition to numerical accuracy, the time needed to get the result of a simulation is a first order factor (at present time, for a global VRS impact simulation, the order of magnitude is about a day). The main idea is to have a model which allows the performance of parametric studies in a reasonable time. Figure 3-13 presents the normalized results in term of CPU time needed to complete a simulation. The normalization is performed dividing the average CPU

time of the four simulations of each case by the maximum value obtained for each structure type (wood or steel-wood).

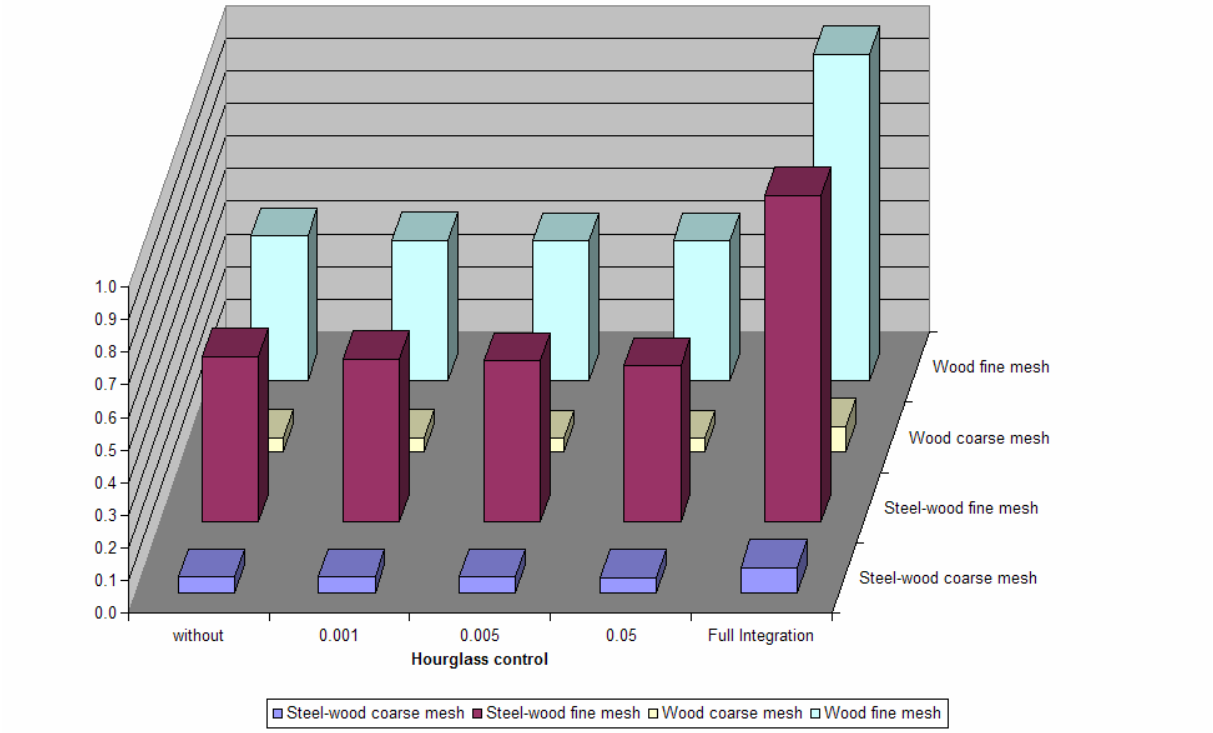

Figure 3-13: CPU time

For each configuration (Mesh size and structure type), the simulations carried out with under integrated elements took more or less the same time (no effect of the hourglass stiffness toward the CPU time). On the contrary, the use of fully integrated elements means a calculation time multiplied by nearly two.
The first order parameter affecting the CPU time is the mesh refinement. A brick element of the coarse mesh becomes eight brick elements in the fine mesh. As a result, the total CPU time is multiplied by an average factor of ten.

3.3.3. Discussion

For each of the above tables, it is worth noticing that Fully integrated simulations are on one hand characterized by the obvious numerical quality (no hourglass energy), but, on the other hand by unacceptable CPU time (total CPU time multiplied by two). The kind of CPU time obtained for fully integrated elements, may lead for full restraint system models to calculation time incompatible with the performance of parametric studies.
The fine mesh doesn't give much better results than the coarse one which means that the wood material constitutive law is either not too sensitive to mesh size or the mesh size used in the coarse mesh is sufficient (convergence of the mesh is obtained)
The simulations without hourglass control are surprisingly the best in terms of squared error with respect to fully integrated results but with a poor numerical quality represented by the poor results obtained for the energy ratio criteria.
The hourglass control with 0.001 stiffness appears to be the best compromise between numerical quality accuracy of results and CPU cost.
The first order difference between coarse mesh and fine mesh is situated at the level of CPU time.
Thus, in the following section a coarse mesh with under integrated element and a 0.1% hourglass stiffness will be used.

3.4. Wood material constitutive law evaluation

3.4.1. Methods

Previously an effort has been made in order to find out some numerical parameters. Thus results of simulations have been compared to other simulation carried out with fully integrated elements.

In this part, the aim is to check the capability of the Ls-Dyna wood material law to represent properly the results obtained in our three point bending experiment and to select the grade which best compares to experimental results.

Therefore, only the conditions which enclose the experimental conditions will be kept (20%-30% and 20°C – 30°C). For each velocity (three levels) and each structure (wood and steel-wood), the twelve combinations of T°, H% and grade were simulated and compared to the mean value of the related experiments.

Each simulation acceleration signal (B(t)) is compared to the corresponding experimental configuration acceleration signal (A(t)). The root mean quadratic error is computed and normalized as follow:

$$\frac{\sqrt{\frac{1}{n}\sum_{n}\left(A(t_n)-B(t_n)\right)^2}}{\left(\max(A(t))-\min(A(t))\right)}$$

Equation 20

3.4.2. Results

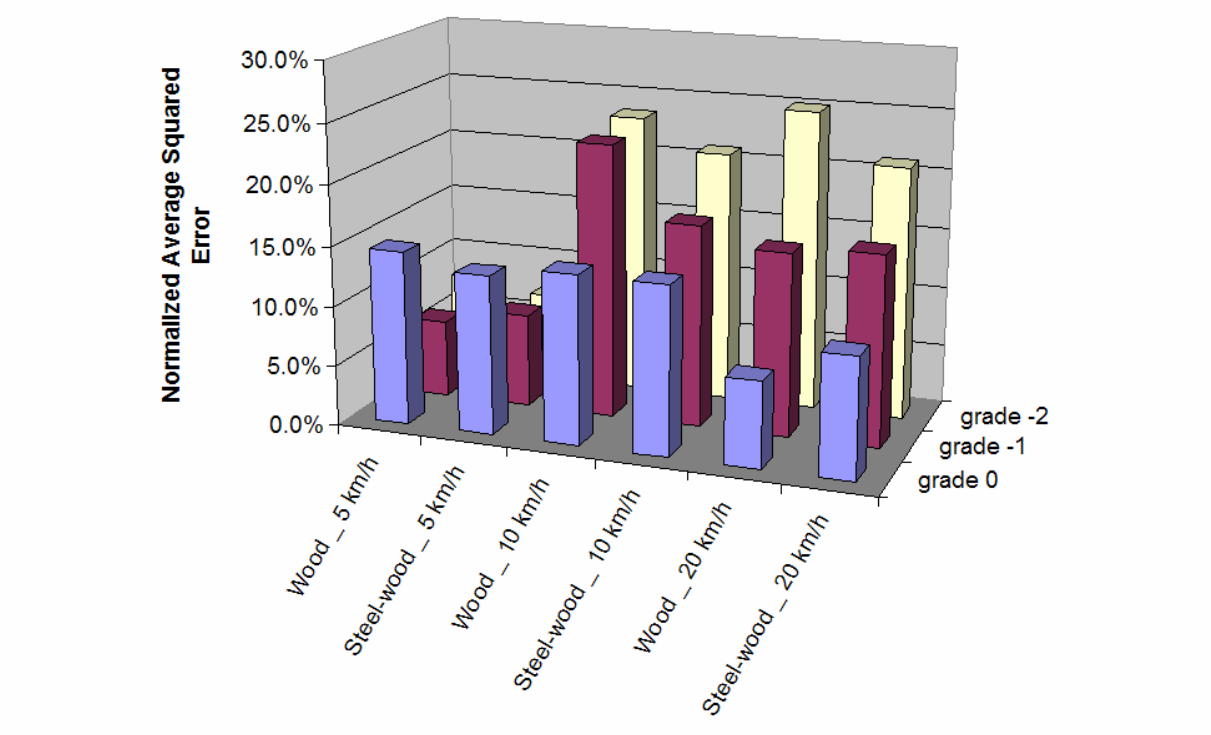

Figure 3-14: Normalized Squared error (experimental reference)

In Figure 3-14, grade -2 corresponds to clear wood mechanical properties. The results obtained with this grade are very good for both structures (wood and steel-wood) at 5 km/h. But, at higher impact speeds, the results are the worst in comparison with the experiment. Grade -1 which corresponds to a quality factor of 0.80 in tension and 0.93 in compression, the results are also very good at 5 km/h but far less for the two others impact speeds.

Finally, grade 0 which corresponds to a quality factor of 0.47 in tension and 0.63 in compression, presents the most stable results and the best ones for the higher impact speed.

3.4.3. Discussion

Considering 10 and 20 km/h results, the grade 0 is clearly the one which best fit the experimental data with respectively 14% and 8,6% of normalized root mean squared error.
For the lowest impact speed, all the grades fit quite correctly with the experiment. This may be explained by the fact that no failures were expected and that the elastic response of the wood or steel-wood beam is easier to capture. The relatively poor fit of the grade 0 for this impact speed could be due to a too weak behaviour in the contact area in compression.
It might have been possible and interesting to tune the quality factors in order to find out a best set of quality factors. Nevertheless the grade 0 results have been considered satisfactory mainly because the results were very close to the experiment for the highest impact speed (which is closer to the future application use).

3.5. Conclusion

In this chapter, some numerical factors have been explored in order to obtain a model which combines numerical quality and a reasonable CPU cost.
This section has illustrated that numerical parameters such as Hourglass control has an important influence on the results for the impact cases presented in this study where failure occurred and element distortion could drive the global dynamic of the impact sequence.
One important aspect was to check if the mesh was fine enough. A comparison with a model with eight times more elements has shown that a relative coarse mesh (30mm mesh size) was sufficient, as far as 15mm mesh size gives no better results but much higher CPU cost.

In a second step, with the optimized numerical model, the material constitutive law has been evaluated and the set of parameters which best fit the experimental results has been selected.

Chapter 4 Steel wood VRS modelling

4.1. Introduction

In previous chapter, an optimized model of the steel-wood assembly was found.
In this chapter, a numerical model of a steel-wood VRS using these conclusions will be presented and validated with respect to crash test results (EN1317-1&2 TB32 test).

Then, the validated model will be used to assess the effect of wood mechanical properties variations toward the VRS performances. The grade of wood (grade 0) which best corresponds to the wood used in the local experiment will be used and the performances of the VRS will be evaluated for all the combinations possible of environment variables (Temperature and moisture content)

4.2. VRS Device

4.2.1. Device details

A French steel-wood N2-device “solobois” from SOLOSAR Company has been modelled.

Figure 4-1: Steel-wood VRS

This device is made of a C profile post driven into the ground every two meters. Wood beams consisting of 180mm diameter cylinders by 2 meters long, are joined together by means of a spacer and 4 M16 4.6 bolts at the level of each post. For this purpose, a mechanism is performed at the rear face of the wood beam in order to obtain a plane face of 100mm height. A steel reinforcement (100x5mm), 4 meters long is situated in a slot in the middle of the wood beam. Each spacer is connected to the post by a M12 4.6 bolt.

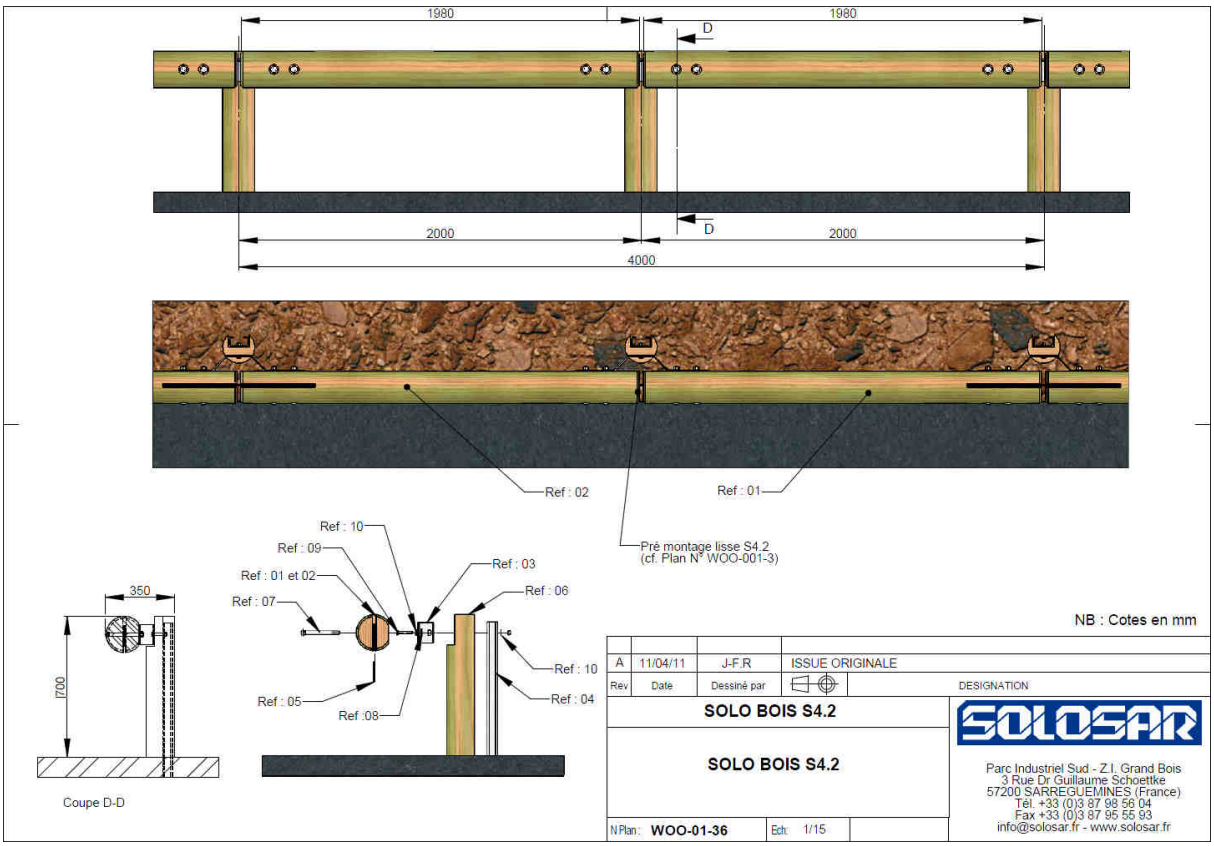

Figure 4-2: VRS drawings

4.2.2. Device performances

4.2.2.a. Test conditions

We focussed on the TB32 test whose theoretical impact conditions are:

- Impact speed:110 km/h $^{+7\%}$ / $_{-0\%}$
- Impact angle: 20° $^{+1.5°}$/$_{-1°}$
- Vehicle mass: 1500 kg ±75kg

The real test conditions of the TB32 performed on the Solobois device were:

- Impact speed:113.3 km/h
- Impact angle: 20.0°
- Vehicle mass: 1430 kg

4.2.2.b. Device results

Figure 4-3: Crash test results, damages to the device

- The impact creates a bow 24 meters long with a permanent deflexion of 0.56m at the level of post n°17.
- The wooden posts facing n°11 to 17 are disconnected from their posts.
- The steel wood beams n°9 to 19 are deformed
- Post n° 6 to 18 are bended.
- No element from the device penetrated the interior of the vehicle.
- The vehicle didn't break the device nor overpassed the device. It didn't roll over and remained inside the CEN box (exit angle 13°).

Figure 4-4: Crash test overview

4.2.2.c. Severity indices

- ASI 0.6
- THIV 21.8 km/h
- Which leads to A severity class.

4.2.2.d. Deflexion measurements

- Maximal dynamic deflexion : 1.5m
- Working with 1.7m
- Working with level : W5(≤1.7m)

4.3. Numerical model

4.3.1. VRS Mesh

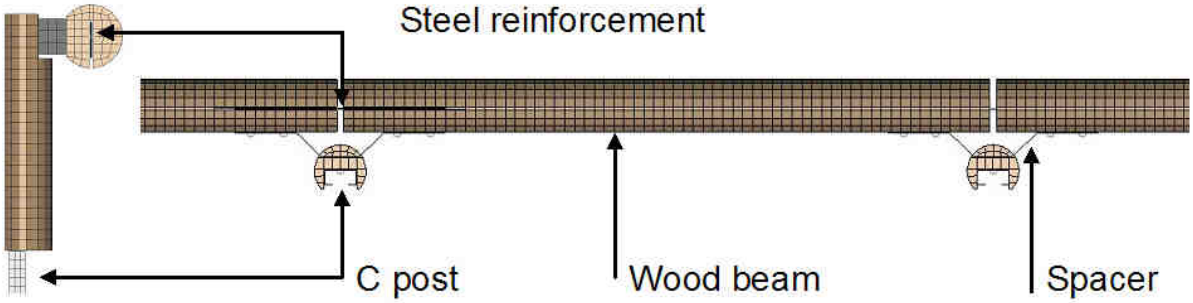

Figure 4-5: VRS FE model presentation

The device was modelled in accordance with the drawings provided in the test report for a total length of 64m with 135 795 finite elements.

The wood beam is modelled with brick elements and with the material law detailed in the previous section.
Under integrated elements, Ls-Dyna type 1 (Default) “Constant Stress Solid” are used.

The steel reinforcement is modelled with Ls-Dyna type 2 Belytschko-Tsay shells in addition with an elasto-plastic law of MAT 24 (MAT_PIECEWISE_LINEAR_PLASTICITY).

The posts are modelled thanks to Ls-Dyna type16 element (Full integrated shells) which allows to capture a proper plastic hinge deformation with a relative coarse mesh while a mesh refinement is needed for under integrated elements type 2.

The Bolts are modelled, as presented in the local model, using Hughes Liu type beams with a discretisation along the length of the beam which allows consistent deformation of the beams in regards of the experiment. The Lagrange-in-solid coupling (used to model the steel reinforcement inside reinforced concrete) is a very convenient way to reduce the meshing effort (the beams are localized at their proper place and there is no need to represent the holes).

4.3.2. Vehicle model description

The car model used in the simulations matches the guidelines of CEN TC226/WG1/TG5.

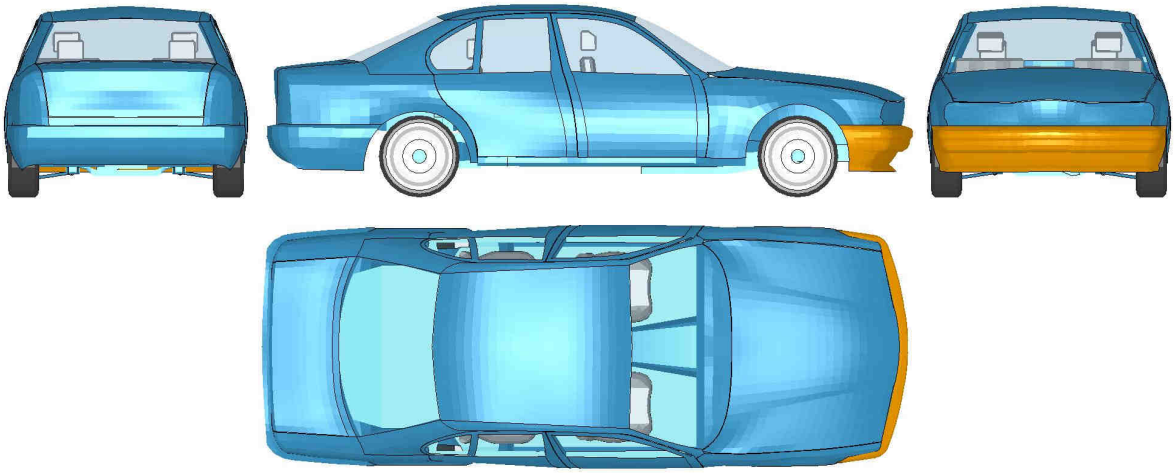

Figure 4-6: Vehicle model presentation

	Model	Spec. -	Spec +	
Type of vehicle	CAR			
Total mass [kg]	1 454	1 425	1 575	OK
Total length [m]	4.71			-
Total width [m]	1.77			-
Total height [m]	1.39			-
Front track [m]	1.49	1.28	1.73	OK
Rear track [m]	1.49	1.28	1.73	OK
Wheel radius [m]	0.30			
Wheel base [m]	2.76			
Number of axles	1S +1	1S + 1	1S + 1	OK
Ground clearance of the front bumper measured at the corner [m]	0.19			
Centre of gravity – longitudinal axis [m]	1.31	1.12	1.36	OK
Centre of gravity – transversal axis [m]	0.00	-0.08	0.08	OK
Centre of gravity – vertical axis [m]	0.55	0.44	0.54	OK
Total number of finite element	21 304			

Table 4-1: Vehicle model specifications

4.3.3. Boundary conditions

The soil is modelled by means of a rigid wall with a friction coefficient.
A boundary condition (all degrees of freedom constrained) is set for the nodes of the posts located 20cm below the ground level. All the post nodes situated below 10cm from the ground level are not taken into account by the rigid wall, allowing a deflexion of the post in accordance with the experience of stabilized soil.

4.3.4. Initial conditions

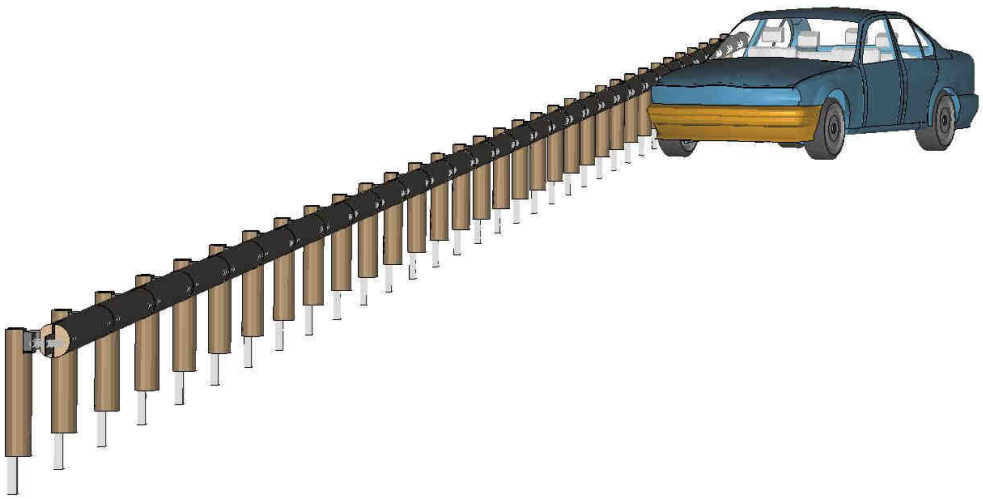

Figure 4-7: Global model general view

The vehicle model is aligned with post n°12 at an angle of 20° and an initial velocity of 113.3km/h is applied.

4.4. Model validation

In case of a crash of a vehicle against a VRS, a lot of parameters may have an effect on the global behaviour and, thus, on the severity indices and W results.
As the structures are highly solicited (for some component until failure point) the use of standardized data for parameters such as steel yield point may lead to poor correlation or poor predictions. Furthermore, even if the components are checked after crash, uncertainties concerning the real component mechanical properties remain.
In the field of roadside safety, as reported in chapter 1, when talking about correlation between a simulation and a real test, it is frequent to draw up on the comparison between one crash configuration (mainly due to the crash test cost) and one simulation.
This point-to-point comparison is unfortunately very poor, as the variation of mechanical properties is quite important and can affect significantly the device performances.
One important issue in this section is to build up a procedure for assessing the intrinsic variability of a VRS and then to compare an experimental result to a cloud of numerical simulations.

4.4.1. Failure mode analysis

The procedure is based on the failure modes analysis. The main idea is to identify, for each failure mode, the physical parameter which could drive its apparition (will it appear or not, and if it appears, at what time?).

Table 4-2 shows a TB32 simulation carried out with SOLOBOIS model. The redirection of the vehicle is obtained thanks to several mechanisms:
The vehicle contact force is transferred via the steel-wood beam to the neighbouring posts.
The posts bend allowing an articulation between two consecutives beams
The post to beam bolt fails, ensuring a proper height for the beam/vehicle interaction
The sequence is repeated until the total force offered by the device is sufficient to obtain the redirection of the vehicle.

This sequence of event can easily be illustrated thanks to numerical tool. In Table 4-3, four snap shots taken from a simulation illustrate the repartition of the Von Misses resultant stress in the main steel components of the device, the wood being in transparency.

t=0.0 s	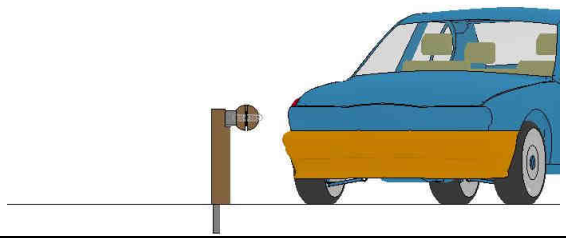	
t=0.2 s	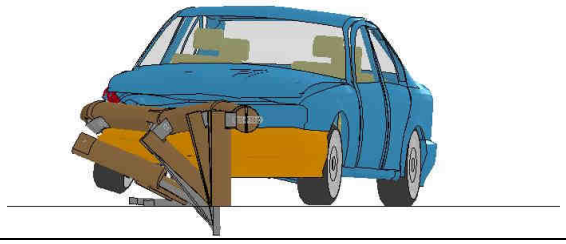	
t=0.4 s	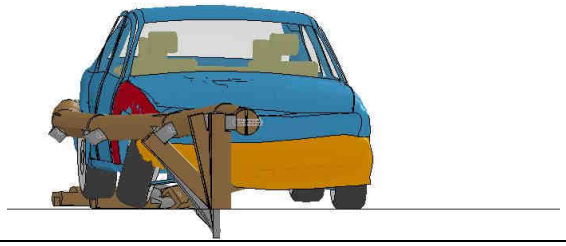	
t=0.6 s	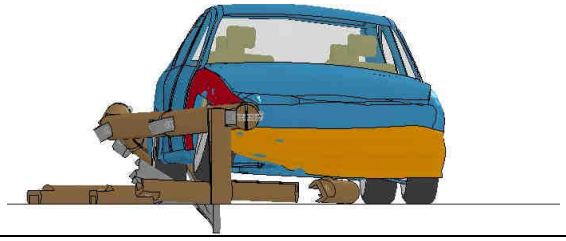	
t=0.8 s	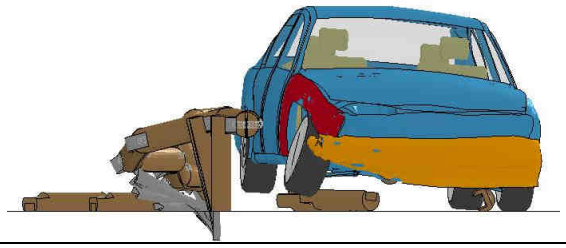	

Table 4-2: TB32 crash sequence

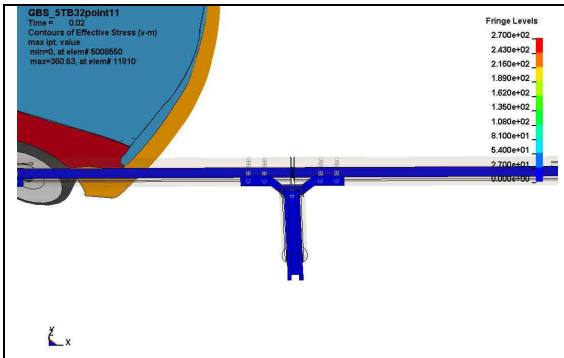	Initial state
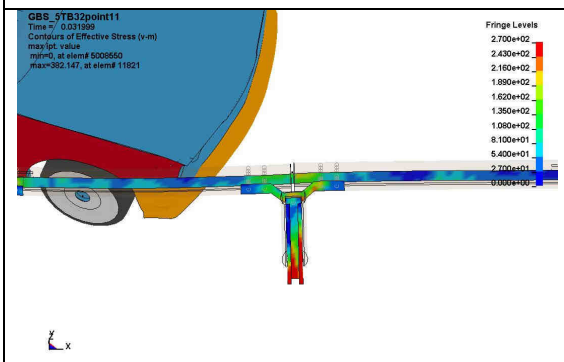	Plastic hinge formation at the post base
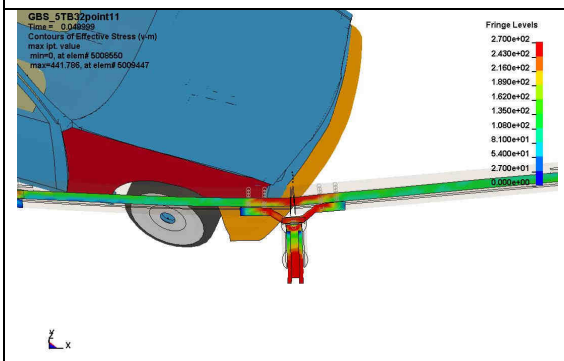	Plastic hinge formation at the beam articulation
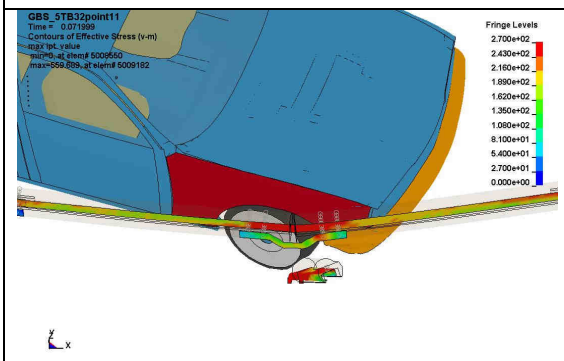	Post/beam bolt failure

Table 4-3: Failure modes analysis

The repartition of stress clearly confirms the sequence of events.
The vehicle/device interaction, and therefore the acceleration signals, may be affected by a lot of parameters. The performance of parametric studies, in order to catch what happens in a crash test or in order to explore the robustness of a device before testing, is obvious but requires the identification of relevant parameters and ranges of variation.
Among all the available parameters, those which can be linked to the failure modes of the device are of first order interest. In fact, the mechanisms activated during a crash are those for which the analyst has to play with in order to reach a good correlation or to check the robustness before going to crash test.
By example, as far as the last failure mode was identified in Table 4-3, the force needed to break the bolt (and thus the time at which the bolt will fail) could affect a lot the interaction between the car and the device. Depending on the time at which the disconnection appears the vehicle wheel could impact the post before or after the disconnection which will not have the same consequence on the decelerations signals and thus on the redirection of the vehicle.
In a predictive work, the analyst has to check if the expected failure mode is robust enough to appear in the whole range of possible mechanical properties.

For the first two failure modes identified, the mechanism consists of a plastic hinge formation. This phenomenon appears when the stress level in the component is above yield stress. Therefore, the physical parameter which will drive the apparition of the plastic hinge is the yield stress of component material.

The last failure mode identified is the disconnection of the post/beam link which is obtained in this device with a bolt failure.
Thus the physical parameter which will drive the apparition of the bolt failure is the ultimate stress of the material which is linked to the total force at failure point via the resistant section.

One can notice that wood is not included in this failure modes analysis. Nevertheless wood beam is responsible for the force transfer and for the localization of the plastic hinges. In this specific design, the wood beam size raises the assumption that this force transfer and plastic hinge localization should not be affected by a reasonable variation of wood mechanical properties.

4.4.2. Design of experiment

Once the failure modes and related physical parameters are identified, one can select a range of variations for each of these parameters.

Based on LIER experience in the field, the following range will be used:

Failure mode	Physical parameter	Values
Post plastic hinge	Steel yield stress	240 – 270 – 300 MPa
Articulation plastic hinge	Steel yield stress	240 -270 -300 MPa
Bolt failure	Force at failure	33700 - 37950 – 42200 N

Table 4-4: Failure modes and range of variation

Each parameter can get 3 values leading to 3^3=27 simulations in a complete factorial Design of Experiment (DOE).
In the following section, the results of the project which gives the best results are presented. The same approach (27 simulations DOE) has been used to evaluate several numerical parameters (friction coefficient, element formulation …). Detailed results can be found in the appendix n°3 to the document.

4.4.3. Results

	Post yield	Spacer and reinforcement yield	Bolt failure force	ASI	THIV	W	CM-E requirements
	[Mpa]	[Mpa]	[N]	[N.U.]	[km/h]	[m]	
point1	300	300	42 200	0.60	25.78	1.49	No
point2	300	300	37 950	0.60	25.49	1.56	No
point3	300	300	33 700	0.68	24.72	1.52	No
point4	300	270	42 200	0.57	25.14	1.62	No
point5	300	270	37 950	0.60	25.47	1.59	No
point6	300	270	33 700	0.54	24.48	1.56	Yes
point7	300	240	42 200	0.56	24.71	1.72	Yes
point8	300	240	37 950	0.59	24.91	1.69	Yes
point9	300	240	33 700	0.53	24.18	1.63	Yes
point10	270	300	42 200	0.59	25.45	1.52	No
point11	270	300	37 950	0.65	25.00	1.61	No
point12	270	300	33 700	0.83	24.15	1.56	No
point13	270	270	42 200	0.59	25.16	1.57	No
point14	270	270	37 950	0.58	24.80	1.66	Yes
point15	270	270	33 700	0.53	24.08	n.c.	No
point16	270	240	42 200	0.55	25.12	1.67	No
point17	270	240	37 950	0.56	24.58	1.7	Yes
point18	270	240	33 700	0.51	23.89	1.66	Yes
point19	240	300	42 200	0.58	24.93	1.55	No
point20	240	300	37 950	0.56	24.60	1.65	Yes
point21	240	300	33 700	0.52	23.67	n.c.	No
point22	240	270	42 200	0.56	24.66	1.61	Yes
point23	240	270	37 950	0.54	24.34	1.69	Yes
point24	240	270	33 700	0.51	23.65	1.64	Yes
point25	240	240	42 200	0.54	23.82	1.77	Yes
point26	240	240	37 950	0.54	24.01	1.77	Yes
point27	240	240	33 700	0.49	23.19	1.7	Yes
μ	270	270	37 950	0.57	24.59	1.63	
σ	24	24	3 470	0.06	0.64	0.07	
σ/μ	9%	9%	9%	11%	3%	5%	
Real test	unknown	unknown	unknown	0.57	21.75	1.70	

Table 4-5: EN1317 results

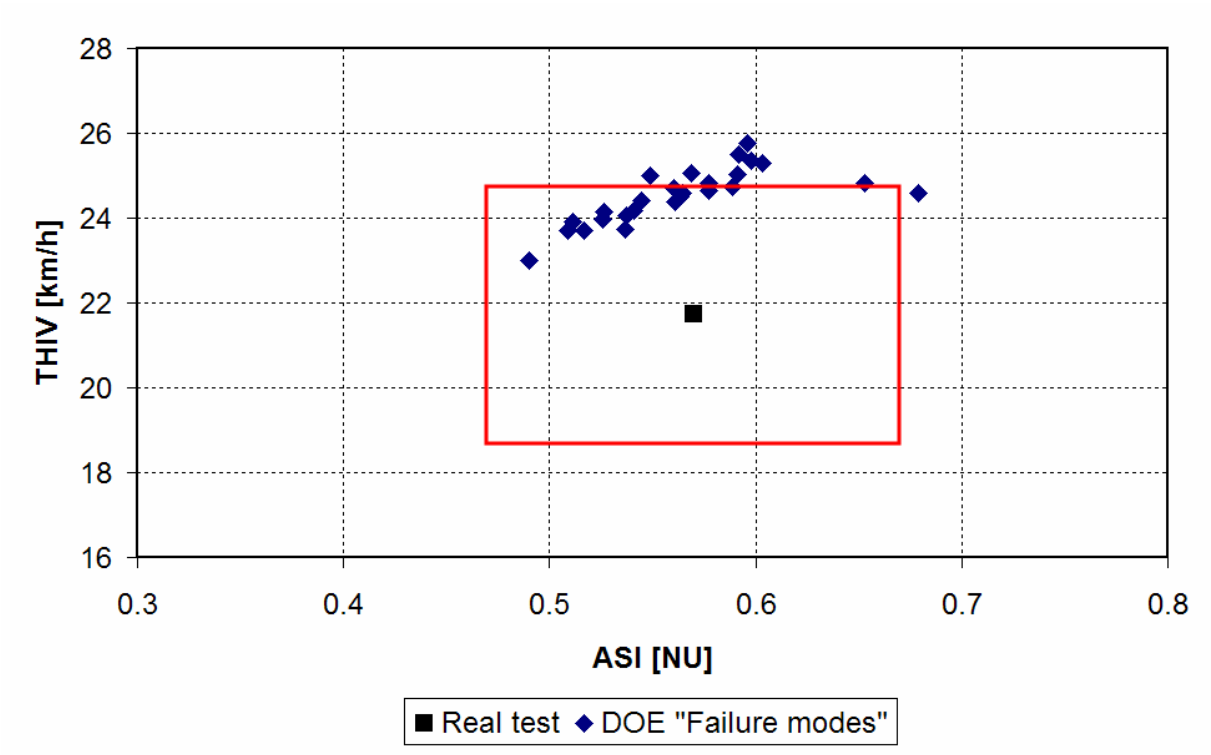

Figure 4-8: EN1317 Severity indices

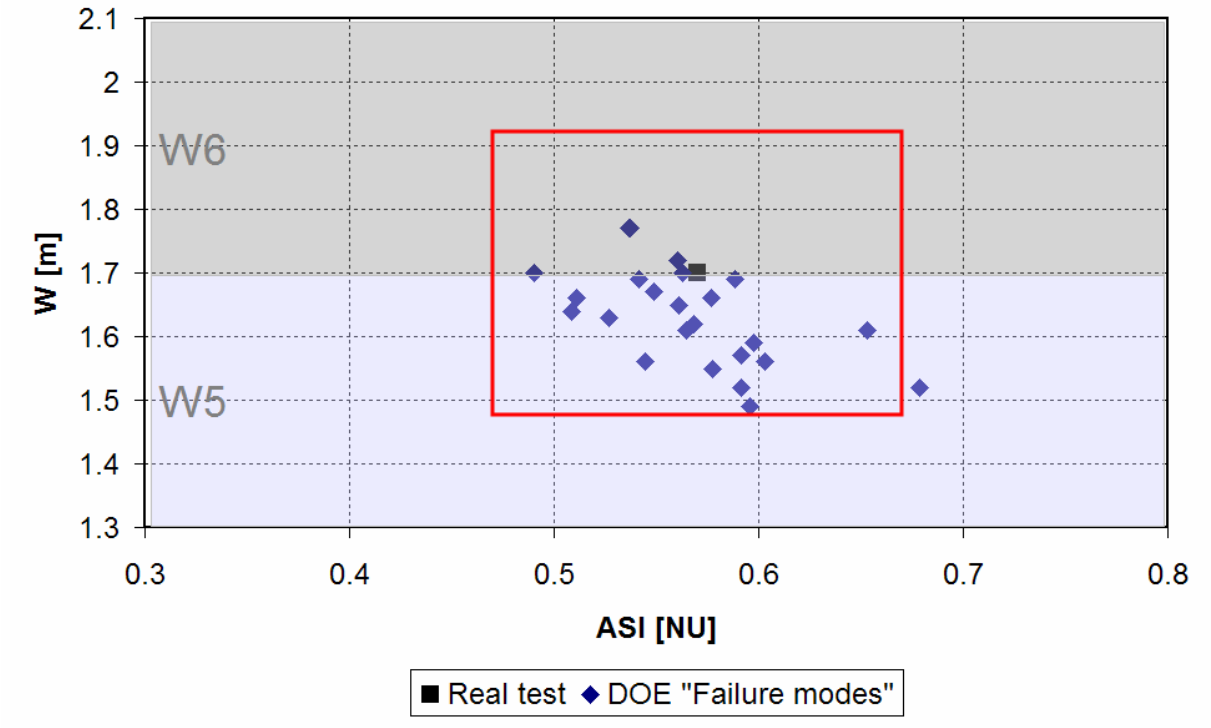

Figure 4-9: EN1317 Criteria

The tolerances proposed by the TG5 (identified by the red rectangles in the above figures) result in the exclusion of 13 out of the 27 simulations (most are excluded due to THIV criteria). Nevertheless, all the simulations are in accordance with EN1317 criteria remaining in severity class A (ASI≤1.0 and THIV≤33km/h). The results obtained vary between two working width class (W5 and W6, real test standing at the border of W5 class) but with a 5%

variation which is reasonable compared to +/- 10% of variation of the design variables of the DOE. These results highlight the robustness of the device.
Furthermore, it's worth noticing that the chosen DOE enclose very well the experimental result in terms of ASI and W.

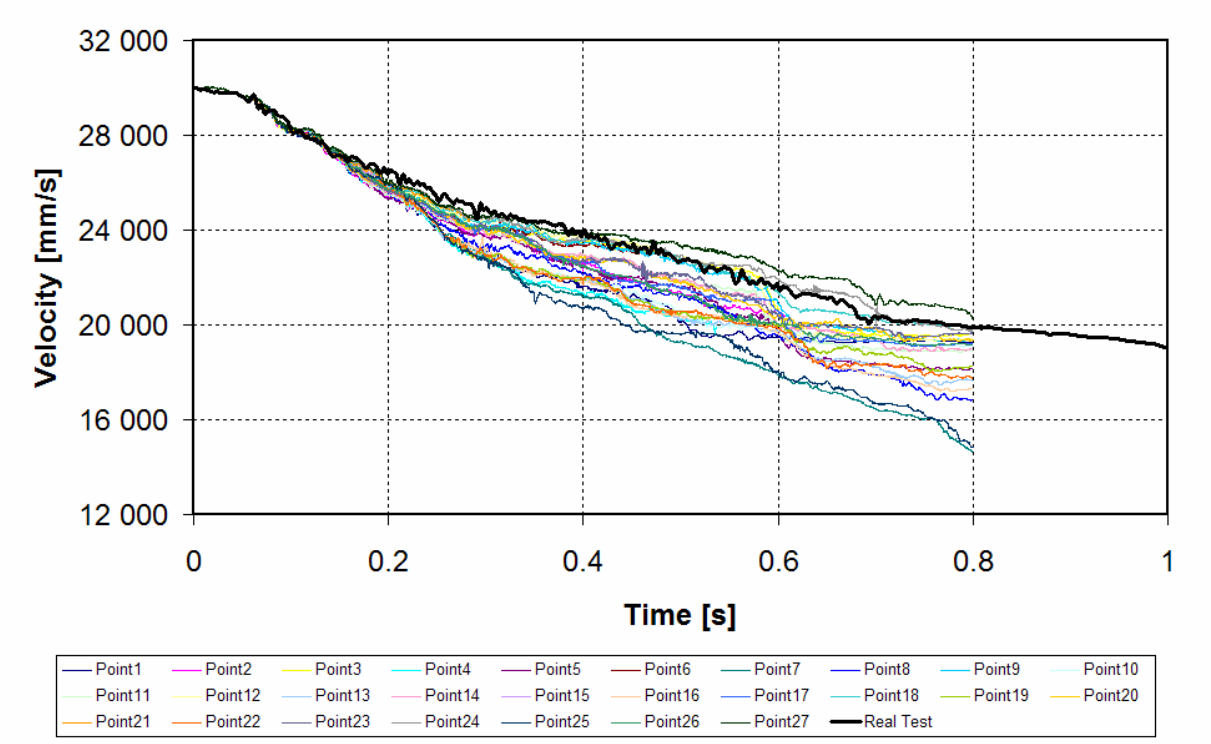

Figure 4-10: X velocities

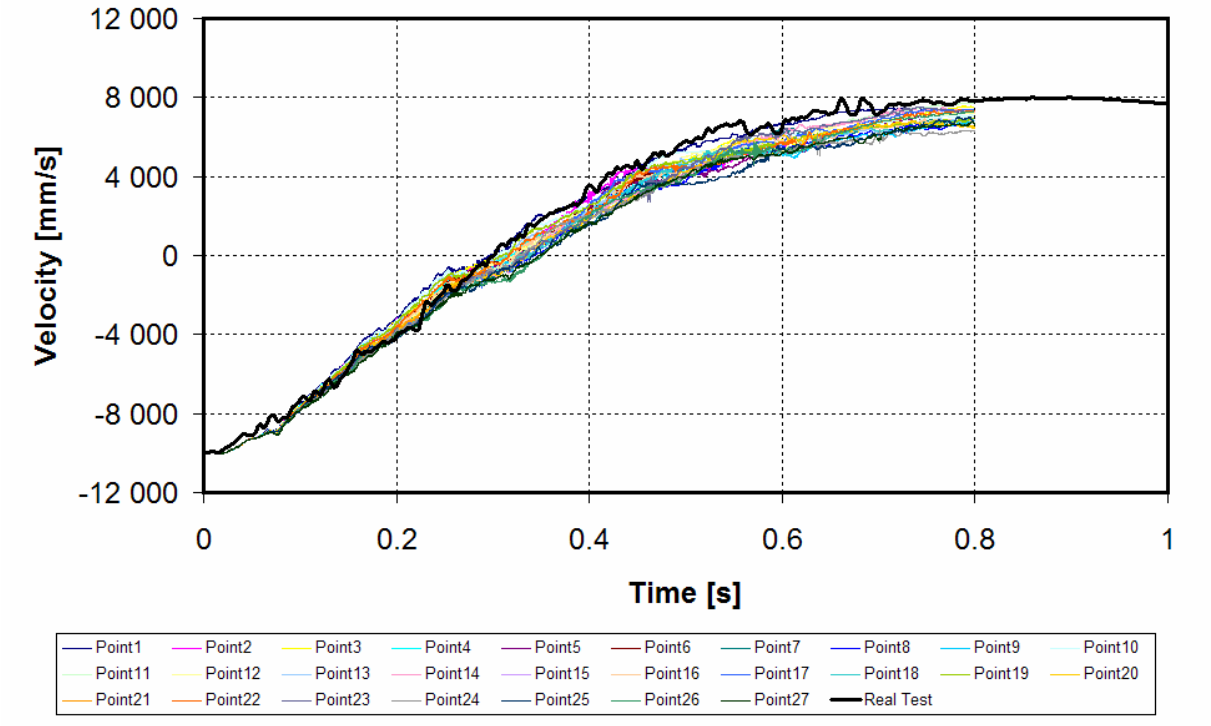

Figure 4-11: Y velocities

Figure 4-10 & Figure 4-11 show the computation of the velocity components of the vehicle's centre of gravity in the global fixed reference framework.
For both components, the simulations define a corridor which encloses the experimental velocity components.

For each simulation, the total quadratic error with respect to the real test curve is computed. The following Figure 4-12 and Figure 4-13 illustrate the velocity components with the lowest quadratic error. This simulation (Shot 18) is well correlated with the experiment and all the results obtained for this set of parameters meet the requirements for the model validation (see Table 4-5).

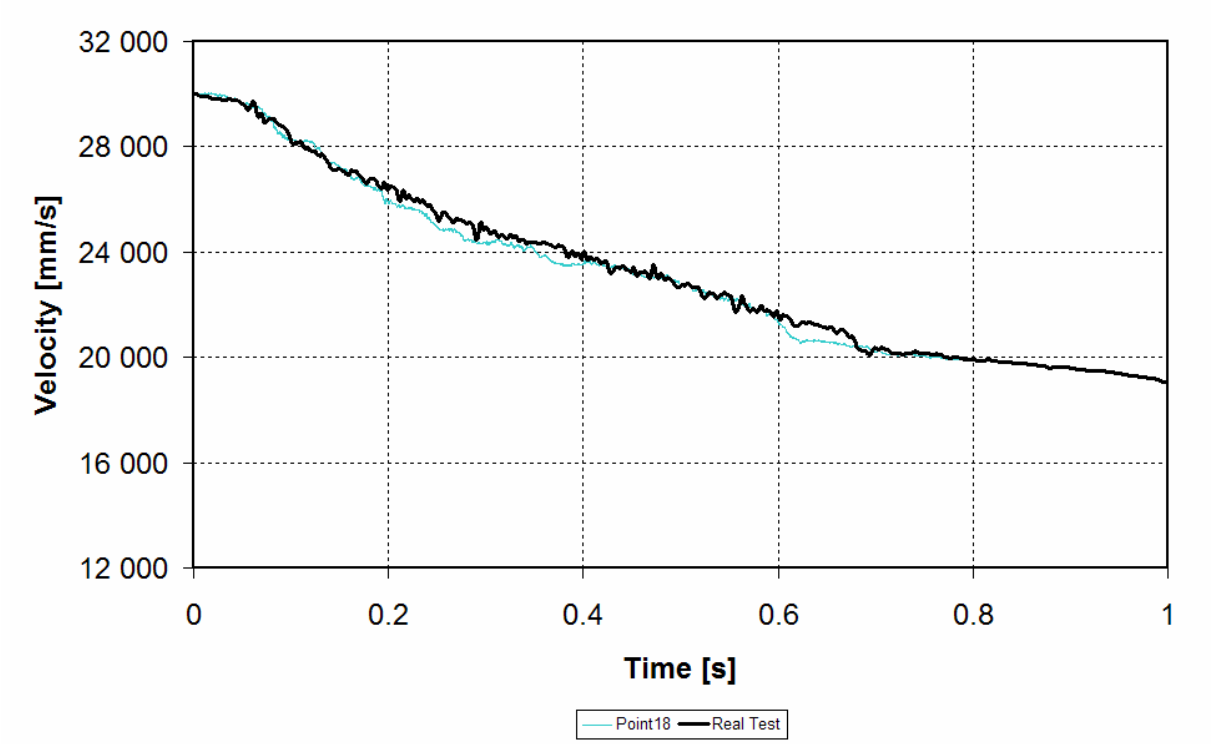

Figure 4-12: X velocity component - Best fit

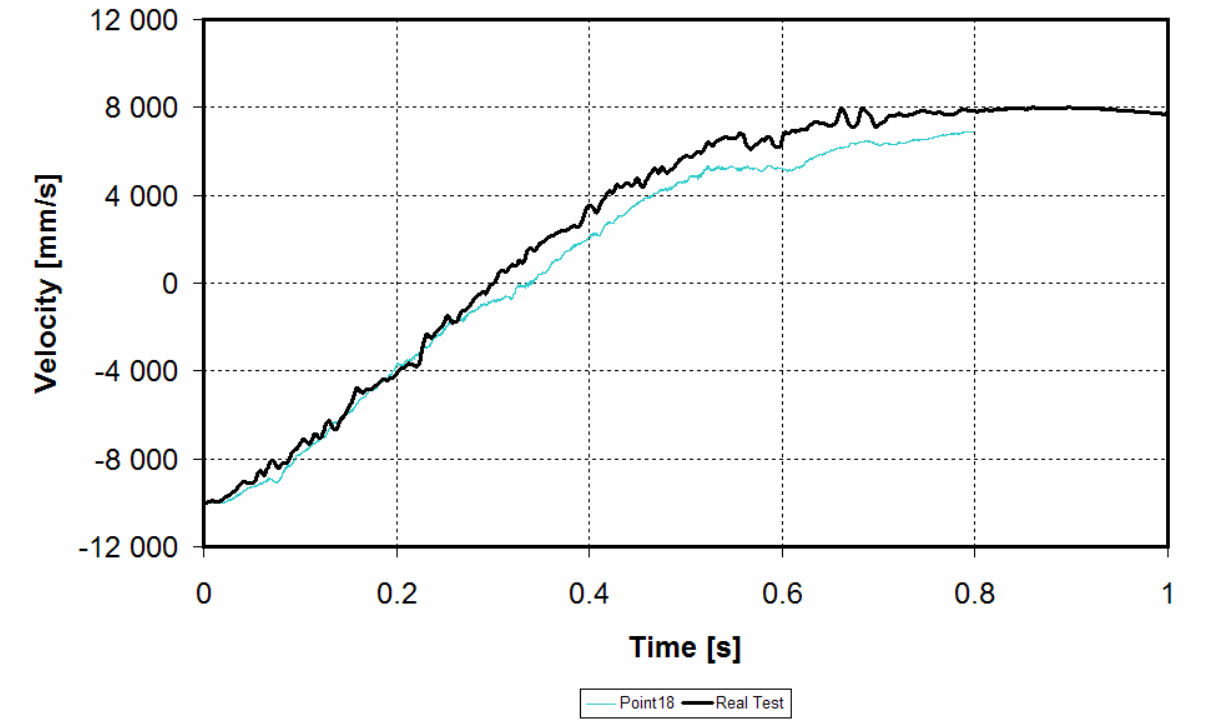

Figure 4-13: Y velocity component - Best fit

4.4.4. Discussion

The proposed parametric approach, based on structure failure modes analysis, allows the obtainment of a good correlated model and can be easily applied to every kind of structure.
This approach needs the identification of the failure modes and an assessment of a range of variations for the physical parameter which drive the apparition of the mechanism.

This approach could be used not only in a correlation process but also for development purpose before real crash testing, in order to assess the robustness of a design.
One common alternative to this approach is too often to perform “only” the worst case.
In most cases, the worst case does not exist. First of all, considering EN1317 crash tests, one will have to select its worst case! Is the worst case related to deflection or to severity? These worst cases are usually contradictory.
In traditional design, the goal is to remain in the domain of elasticity. Therefore, safety coefficients can be applied and loading worst cases can be identified.
This approach becomes meaningless if one wants to be predictive or if one intends to reach a good correlation.

4.5. Evaluation of wood mechanical properties variation

Since the numerical model is validated following CEN/TC226/WG1/TG1/CM-E recommendations, a new parametric study is defined to assess the effect of wood mechanical properties variations.

4.5.1. Design of Experiment

A complete factorial DOE was defined to assess the effect of wood mechanical properties variation using the 16 combinations of room temperature and moisture content offered by the material law.

4.5.2. Results

	MC	T	ASI	THIV	W
	[%]	[°C]	[N.U.]	[km/h]	[m]
point1	30	30	0.50	23.66	1.65
point2	30	20	0.51	23.89	1.65
point3	30	10	0.51	22.87	1.80
point4	30	1	0.51	21.94	n.c.
point5	20	30	0.52	23.86	1.66
point6	20	20	0.51	23.91	1.66
point7	20	10	0.49	23.03	1.87
point8	20	1	0.49	22.34	2.19
point9	10	30	0.51	24.17	1.67
point10	10	20	0.52	23.46	1.77
point11	10	10	0.51	22.63	1.82
point12	10	1	0.54	22.28	1.85
point13	1	30	0.52	22.24	1.86
point14	1	20	0.52	22.04	1.81
point15	1	10	0.49	22.10	2.29
point16	1	1	0.48	22.52	2.28
μ			0.51	22.93	1.86
σ			0.01	0.75	0.21
σ/μ			2%	3%	12%

Table 4-6: Wood DOE - EN1317 results

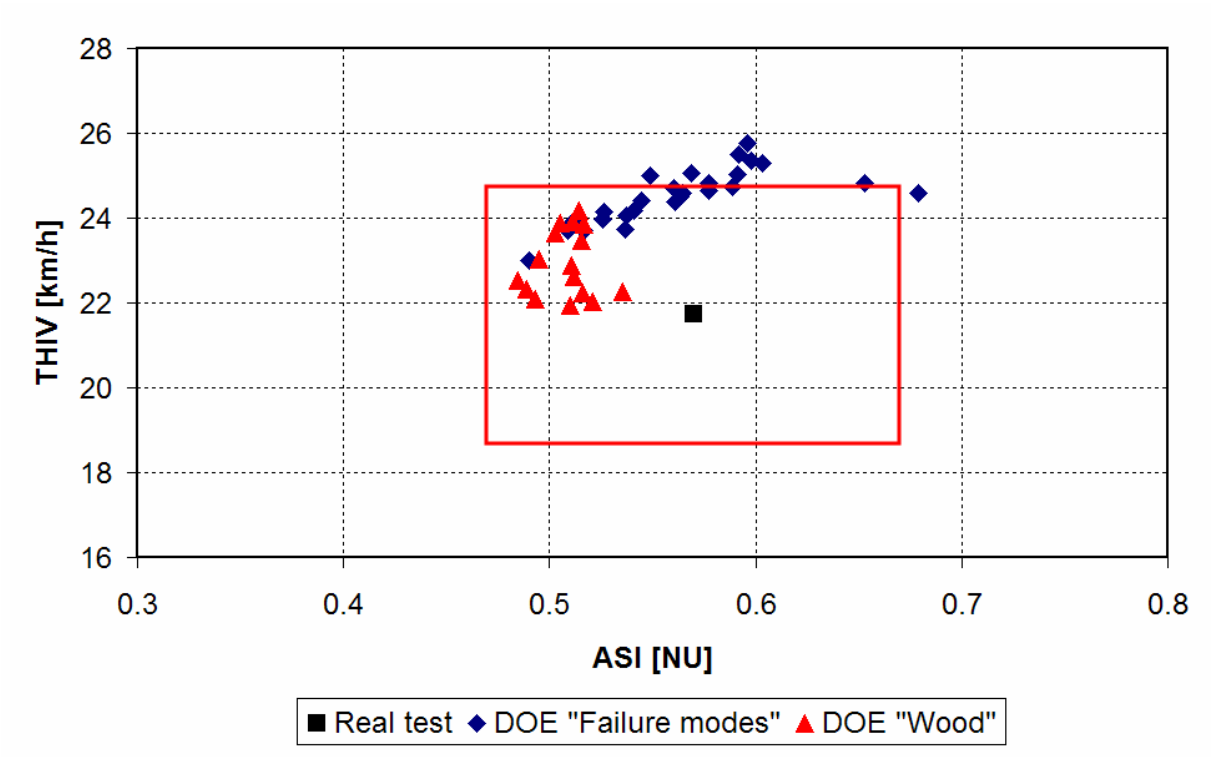

Figure 4-14: Wood DOE - Severity indices

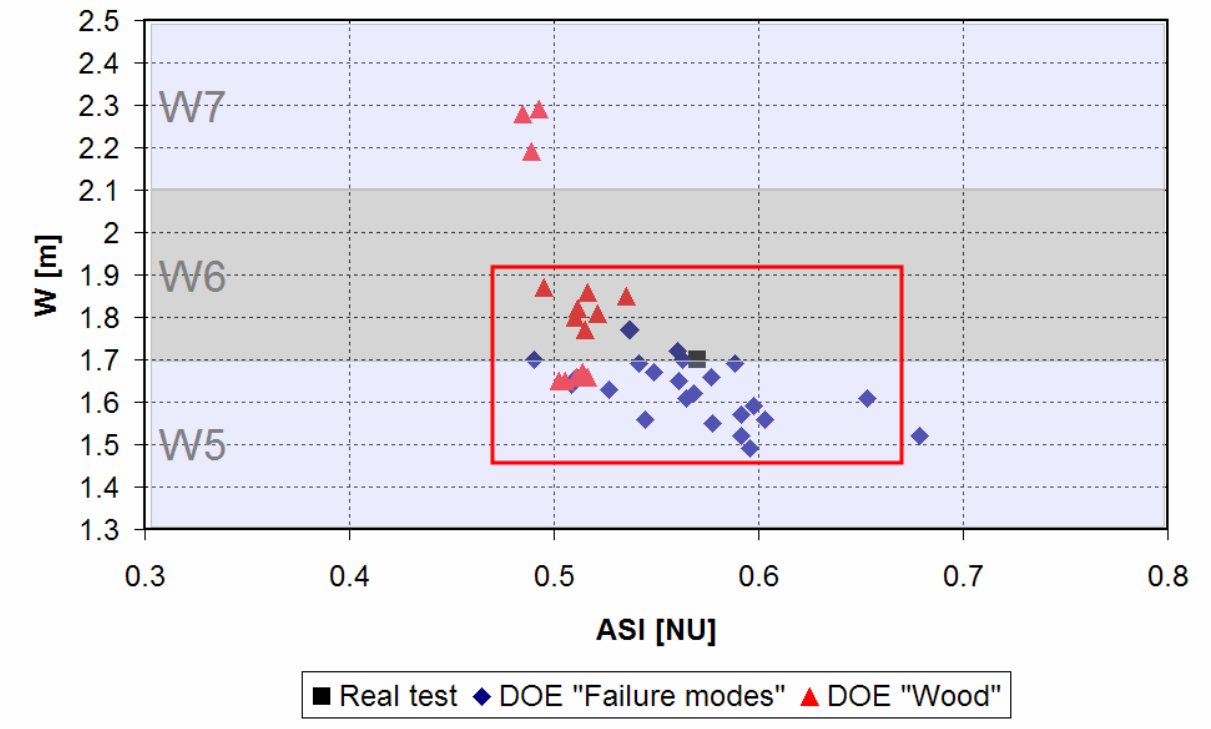

Figure 4-15: Wood DOE - EN1317 Criteria

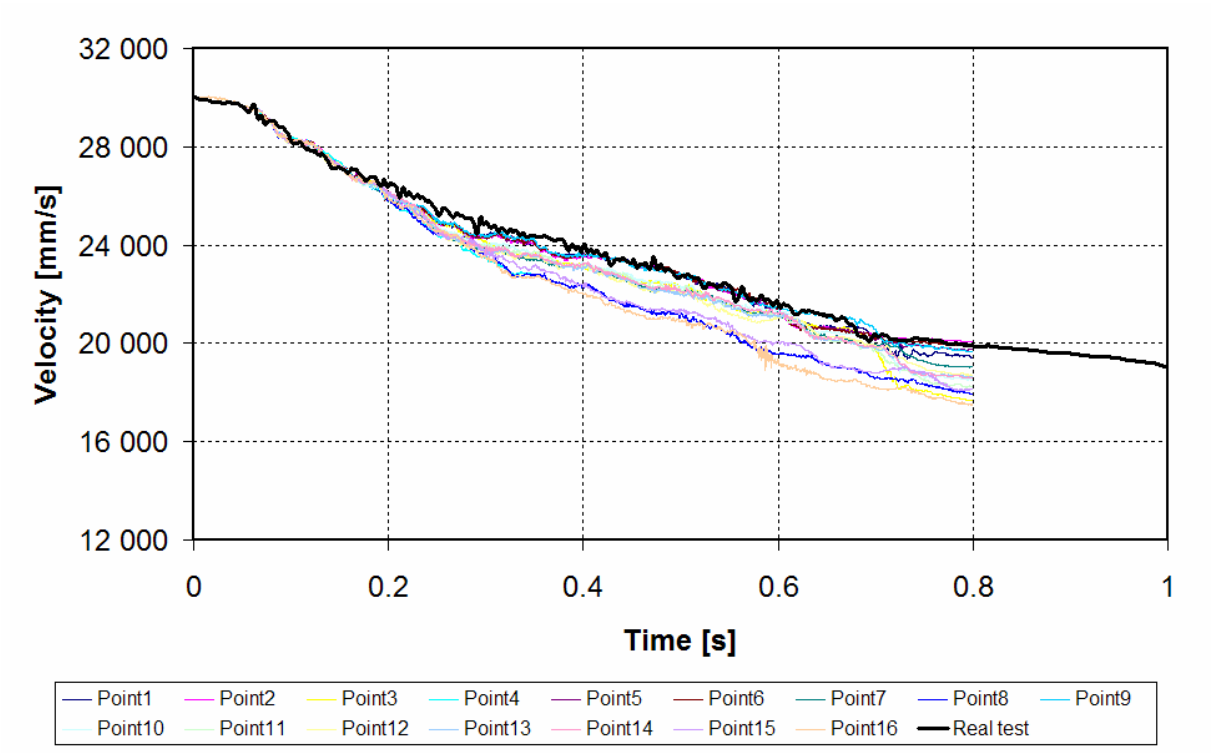

Figure 4-16: Wood DOE: X Velocity components

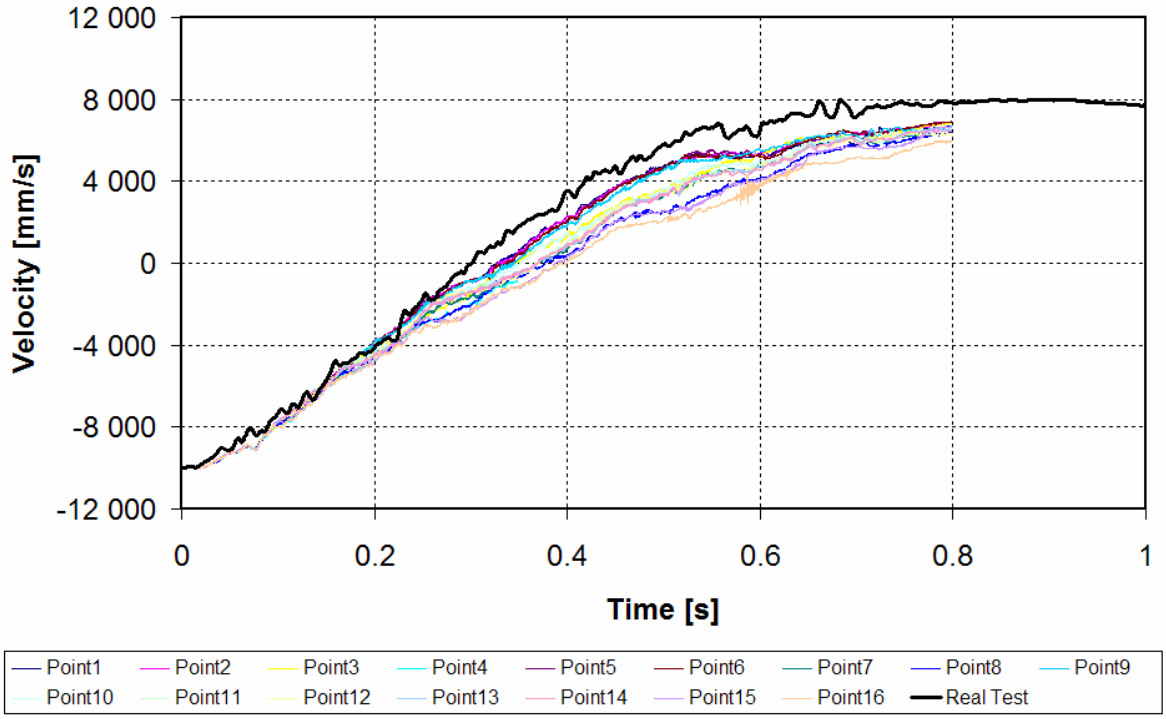

Figure 4-17: Wood DOE: Y Velocity components

Although the mechanical properties variation due to Moisture Content and Temperature variation affect noticeably the modules and the strengths (respectively 15% and 20% of standard deviation), Table 4-6 shows that the variation of EN1317 severity indices (ASI and THIV) remains around 3%.

The main effect of wood mechanical properties variation is on W results because of wood beams failure that occurs in almost all simulations performed below 10°C and below 10% of MC.

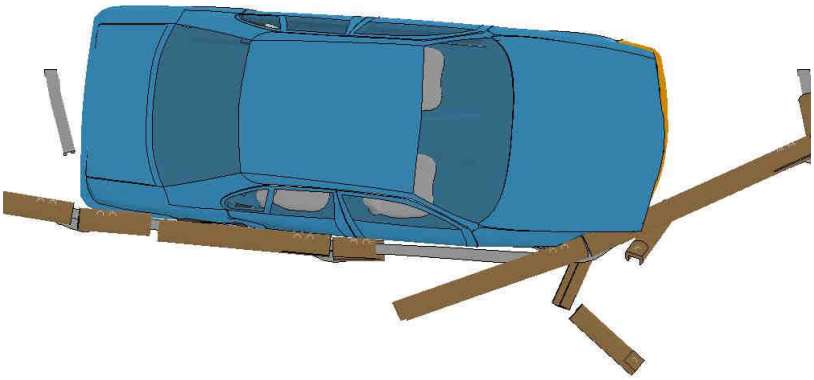

Figure 4-18: Wood failure at low T° and MC

This failure is clearly due to a more brittle behaviour of the wood material under these test condition parameters.
In terms of velocity components, Figure 4-16 and Figure 4-17 show the corridors obtained in the global reference framework which are narrower than those obtained in the Failure modes DOE.

4.5.3. Discussion

The parametric study performed with wood mechanical properties variation due to environment variables (Temperature and Moisture content) within a large spectrum (respectively from 1°C to 30 °C and 1% to 30%) show little effect toward VRS performances.
The variation obtained for VRS performances remains low (2.5% for severity indices and 12% for W) in relation to the variation of wood strengths (20%).
This fact leads to the conclusion that the wood, in this specific design, does not enter in the failure modes of the structure.
The brittle behaviour leading to the highest W values is observed for temperatures below 10°C and for Moisture content below 10%. Our experiments were performed with temperatures between 20°C and 30°C and Moisture content between 20% and 30%. Thus, no validation of material law has been provided for the lowest values.

4.6. Conclusion

In a vehicle crash test against a VRS, a sequence of physical phenomena occurs leading to the redirection of the vehicle. These phenomena, called failure modes, can be easily identified with high speed films. This identification can be facilitated by a numerical analysis.
Unfortunately, the activation of a failure mode is often linked to a physical property which varies a lot. The tolerances of the material used for roadside purpose are usually very large.
This explains why correlation performed with standardized data present a poor agreement as regards real test results or behaviour.
The parametric approach presented in this chapter defines a method to identify a set of parameters which best represent what occurs in a real test.
Furthermore, this approach emphasises an important evaluation of the device robustness which cannot be assessed by real crash testing firstly on ground of economical purpose and secondly because it is almost impossible to control all the test characteristics.
This approach could be used after a crash test in order to evaluate what might be the real life condition performances of a device.
As an example, the approach has been applied to wood mechanical properties variation.
The environment (mainly temperature and moisture content) affects wood mechanical properties. On the road side, those parameters vary and cannot be controlled. One benefit of a numerical model is to take into account these variations in order to obtain a corridor of responses and, thus, to assess their effect to the Vehicle Restraint System performances.
The variation of this environment variables proposed in the material law has been applied to a VRS numerical model in a parametric study. The effect of this variation is very limited towards the device performances in terms of severity. For lowest value of Moisture Content and Temperature, the resulting brittle behaviour of wood leads to failure of some wood beams which affect deflexion measurements.

General conclusion

Context

The use of Computational Mechanics in the field of roadside safety has increased in the last decade and its use in the certification process is under discussion at European level.
In the meantime, expectations on model outputs are more and more precise and, nowadays, one expects the model to be predictive.
This predictability cannot be achieved without a parametric approach which takes into accounts most of the parameters which are known to present stochastic variations such as mechanical properties and impact conditions.
The accuracy of a parametric approach is based on the knowledge of a reasonable spectrum of variation for each parameter.
This work focussed on steel-wood products. Steel-wood VRS present an aesthetic interest and suffer of the wood reputation to be inhomogeneous, highly sensitive to environment variables and thus, non reliable.
The main issue for us lay in the development of a reliable model including modelling of wood as an anisotropic material, its coupling with the steel and the assessment of wood mechanical properties variation due to its heterogeneity and its sensibility to environment variables.

In Situ testing

A literature analysis relating to the knowledge of wood mechanical properties brought me to the conclusion that some data was needed concerning mechanical properties of wood under impact loading.

Hence, dynamic tests, consisting of three-point bending experiment were set-up at three distinct velocity levels, then performed on isolated pieces of wood and steel-wood structures received from a French roadside safety devices producer. No special care was required for the samples' preparation and they were in conditions of use for road equipment.
During these tests, special care was given to physical parameters such as wood moisture content and room temperature which are known to affect the wood mechanical properties.
At the lowest energy level (2 tonnes bogie at 5 km/h) none of the samples failed. In that configuration, no significant differences were observed between the two kinds of structures tested (wood and steel wood).
At the other two energy levels, failures occurred in both kinds of structures and differences clearly appeared: Steel-wood structures are then characterized by higher peak levels and with a plastic deformation phase of the steel reinforcement illustrated by a deceleration plate after the wood beam failure.

These tests permitted the building of deceleration experimental corridors which are necessary for the validation of numerical models. The spread concerning deceleration peak observed during these experiments (10%) has been compared to the controlled parameters (impact speed, sample mass, room temperature, moisture content). The first three parameters were well controlled and a reasonable spread has been reported (around 5%). For the last (MC), the spread recorded was about 30% and maximum values have been linked to the maximum spread of deceleration peak values. Nevertheless as far as no correlation was found between mass sample and moisture content, other parameters such as wood growing conditions may have affected the results.

Each configuration was repeated three times to allow the creation of corridors. This number is already quite low and, moreover, due to heterogeneity of wood material, unexpected behaviour were observed and had to be removed from the analysis.

A larger amount of samples would allow to build better corridors.
The room temperature was recorded during the experiment but was not controlled. Thus, the variation observed (from 20°C to 30°C) is not the only tested parameter. An installation allowing the control of the room's temperature would allow to test only this parameter and to test the other configurations allowed by the constitutive law (0°C and 10°C) which have not been validated.

Numerical approach

The in situ tests configuration was modelled and allowed, due to its relative small size, to explore several fields:

Numerical parameters:

- Mesh size: Two kinds of meshes coarse and fine, were evaluated in order to check the convergence of the model. A compromise between accuracy of results and computational time was found
- Element formulation: Two kinds of element formulation were tested (reduced and fully integrated elements)
- Hourglass control: For under-integrated elements, several hourglass control were tested
- A compromise was found combining the two parameters (under integrated element and Hourglass control).
- Mass scaling: Mass scaled solution is used for time step control and an optimal solution was found to avoid numerical problems.

Modelling techniques for steel-wood coupling:
It appears that for steel-wood samples the way of representing the steel-wood bolted joint affected greatly the global output of the model. A solution using an Eulerian/Lagrangian coupling (used to model reinforced concrete) allowed to better represent the deformations of the bolts and the local deformation of the wood samples.

Wood material constitutive law:
The transverse isotropic law available in LS-Dyna for wood modelling presents three main parameters: Wood grade, moisture content and room temperature. These parameters, which affect the mechanical properties of wood, were included in a factorial design of experiment in order to find out which set of parameters best fits the experimental results.
First, a wood grade was selected as being more accurate. Secondly, the variability of environment parameters (room temperature and moisture content) was achieved in the numerical model with a variation of physical parameters in accordance with the range observed during the experiment which definitively validated the constitutive law.

VRS model

The influence of mechanical properties of VRS components on the whole device's performances has rarely been assessed. In the literature, while dealing with correlation, authors often limit their presentation to the correlated case without deeply explain the iterative process which has led us to the correlation. In this work, a parametric approach, based on the structure failure modes analysis is presented and allows to take into account the above mentioned stochastic variations either in a predictive process or in a correlation research after crash testing.
This approach was used in a first step to reach a good agreement between the model and the real test results following the requirements under discussion in the TG5.
Once the model has been validated, a second parametric study was performed with the wood parameters in order to assess the effect of wood variability on the device performances.

A large number of iterations were performed with the aim of reducing the modelling hypothesis, avoiding numerical instabilities and getting a perfect correlation. Some solutions were found and could be applied directly to further applications.
A similar approach with other steel wood devices would allow to draw up some general conclusions on the utilisation of wood and to propose some optimisation techniques.

At the beginning of this research, one objective was to study the aim of wood in the steel wood VRS. Unfortunately, only one VRS has been studied and it seems difficult to come to a conclusion from only one case. Since the numerical tool is now available, a study dedicated to other devices will allow a better analysis.
For the VRS design subject of this study the use of wood can be characterized as:

- "Safe" as very little influence of wood mechanical properties can be observed on VRS performances. A variation of plus-minus ten percent of the mechanical parameters which drive the structure failure modes is much more effective than a variation of plus-minus 15% of wood mechanical properties.
- "Not optimized". In fact, the use of wood, according to most of steel-wood VRS manufacturers, is an aesthetic choice. Nevertheless, the wood beams act as plastic hinges localizers, and may be responsible for (too) high working width. Moreover, as illustrated during the failure modes analysis, the steel reinforcement is supposed to work mainly after wood failure which is not often the case due to the actual structure design.

Synthesis

The framework of this thesis is the use of numerical simulation within the certification process. The validation of numerical models has to be performed with a single experiment.
From a scientific point of view, the parametric approach which takes into account the stochastic variation of the parameters identified by a structural analysis presents a real interest for the field of roadside research and is a way to evaluate the robustness of a design. Furthermore, this approach, repeated for several numerical parameters, gives the opportunity to observe tendencies while comparing clouds of results.
From an industrial point of view, the method could be used as a complement of real testing. In fact, as previously highlighted, the number of parameters which can affect VRS performances is really high and it is not imaginable to repeat the crashes mainly for economical reasons. A numerical approach performed after a successful crash test series could allow to assess the robustness of a design (sensibility to impact point, permissible impact speed/angle/mass ranges …) and one can imagine a special rating (such as EuroNCAP stars) related to this numerical evaluation.

Concerning steel-wood structures, the scientific benefit of this work remains in the model improvements made possible by the local experiment inputs. An original method to model steel-wood bolted connection is proposed and gives very good results. Furthermore, the improvements tested in the local configurations have been developed with the care of applicability to full VRS models and performance of parametric studies.
This last point is a real interest from the industrial point of view because a tool is now available for the development of optimized steel-wood products.

Perspectives

The integration of the approach proposed in this thesis within the certification process of modified products by computational mechanics represents a first perspective. Indeed parametric studies allow comparison of clouds of results (between initial design and modified design) and the definition of new acceptance criteria for the modifications.

In view of continuing this work a second hypothesis is to try to characterize the link between working width criterion and wood beam dimensions with the final aim of reducing the wood inertial properties, without any change in the aesthetic aspect. This approach in addition with a study of steel reinforcement position could allow the optimization of steel-wood VRS performances.

Bibliography

[ANG09] Marco Anghileri, Luigi-Maria Leonardo Castelletti & Gabriele Borsani (2009): Preliminary investigation of driver head dynamics during impact of a small car with a high-containment safety barrier, International Journal of Crashworthiness, 14:2, 189-195

[ANG12] M. Anghileri "Validation methods for numerical certification of road restraint systems" minutes of International Crashworthiness Conference, July 18-20, 2012 - Milan

[BLO11] J. Bloch, « Développement, optimisation et certification des équipements routiers de sécurité », RGRA | N° 891 • février 2011

[CAS07] S. Casciati, M. Domaneschi « Random imperfection fileds to model the size effect in laboratory wood specimens » - Strictural safety 29 (2007) 308 321

[CEN12-1] CEN/TR 16303-1:2012: "Road restraint systems – Guidelines for computational mechanics of crash testing against vehicle restraint system" – Part 1: Common reference information and reporting

[CEN12-2] CEN/TR 16303-2:2012: "Road restraint systems – Guidelines for computational mechanics of crash testing against vehicle restraint system" – Part 2: Vehicle Modeling and verification

[CEN12-3] CEN/TR 16303-3:2012: "Road restraint systems – Guidelines for computational mechanics of crash testing against vehicle restraint system" – Part 3: Test item Modeling And Verification

[CEN12-4] CEN/TR 16303-4:2012: "Road restraint systems – Guidelines for computational mechanics of crash testing against vehicle restraint system" – Part 4: validation procedures

[CHA01] F. Charpentier « modélisation d'ouvrages de retenue en bois – thèse présentée à l'université de Bordeaux I –Ecole doctorale de physique soutenue le 03/04/01 n° d'ordre 2348

[CIRC 88] Circulaire n°88-49 du 09/05/1988

[GUI87] D. Guitard - Mécanique du matériau bois et composites – CEPADUES EDITIONS - 1987

[HAL97] J. O. Hallquist, "LS-Dyna Keyword User's Manual. Version 971", Livermore Software Technology Corporation, Livermore 2007 [MAR97] J.L. Martin, R. Huet, G. Boissier, P. Bloch, I. Vergnes, B. Laumon, "Evaluation of the consequences of systematically equipping the highway hard shoulder with safety barriers" – AAAM's 41st annual conference in Orlando, November 10-11, 1997

[HAL98] J. O. Hallquist, "LS-Dyna Theoretical Manual", Livermore Software Technology Corporation, Livermore 1998

[HUB12] J. Hubbel « Can EN1317 and NCHRP 350/Mash be used Interchangeably?" – Minutes of 2012 European workshop of AFB20 (2) Roadside Safety Design International Research Activities Subcommittee. July 17, 20123 Milan

[MAR07] D. Marzougui, P. Mohan, C. Kan, "Effect of Shoulder Drop-Off on W-Beam Guardrail Performance", National Crash Analysis Center, The George Washington University, working paper NCAC 2007-T-002, October 2007

[MUR05] Y.D. Murray, J.D. Reid, R.K. Faller, B.W. Bielenberg and T.J. Paulsen – Evaluation of LS-DYNA Wood Material Model 143, Report No. FHWAHRT- 04-096, Federal Highway Administration, 2005.

[MUR07] Y.D. Murray, Manual for LS-DYNA Wood Material Model 143, Report No. FHWAHRT- 04-097, Federal Highway Administration, 2007.

[NCA07-1] NCAC 2007-T-003 Evaluating W-Beam Guardrail Height Tolerances,

[NCA07-2] NCAC 2007-T-004 Development of a Finite Element Model for W-Beam Guardrails

[NCA07-3] NCAC 2007-W-002 Evaluation of Rail Height Effect of the safety Performance of W-Beam Barriers

[NCA09] NCAC 2009-W-006 Development of a New End Treatment for steel-Backed Timber Guardrail: Phase I Conceptual design

[NCA10-1] NCAC 2010-R-002 Development of a New End Treatment for steel-Backed Timber Guardrail: Phase IIA: Design of TL 2 SBT End treatment

[NCA10-2] NCAC 2010-R-003 Development of a New End Treatment for steel-Backed Timber Guardrail: Phase IIB: Test level 2 crash testing results.

[NFE10-1] NF EN1317 Road restraint systems - part 1: Terminology and general criteria for test methods – AFNOR , September 2010 ISSN 0335-3931

[NFE10-2] NF EN1317 Road restraint systems - part 2: Performance classes, impact test acceptance criteria and test methods for safety barriers including vehicle parapets – AFNOR, September 2010, ISSN 335-3931

[NCH93] H.E. Ross, D. Sicking, and R.A. Zimmer, “Recommended Procedures for the Safety Performance Evaluation of Highway Features”, NCHRP Report 350, Transportation Researsh Board, Washington D.C., 1993

[ONI01] La sécurité routière en France ; Bilan de l’année 2000 – Observatoire national interministériel de sécurité routière

[ONI09] La sécurité routière en France ; Bilan de l’année 2008 – Observatoire national interministériel de sécurité routière

[ONI10] La sécurité routière en France ; Bilan de l’année 2009 – Observatoire national interministériel de sécurité routière

[ONI11] La sécurité routière en France ; Bilan de l’année 2010 – Observatoire national interministériel de sécurité routière

[PER09] M. Pernetti, “Effect on elastic walls due to the collision of articulated trucks”, 88th TRB Annual Meeting, 2009

[PLA03] C A Plaxico, F Mozzarelli & M H Ray (2003): Tests and simulation of a w-beam rail-to-post connection, International Journal of Crashworthiness, 8:6, 543-551

[ROB06-1] Road Barrier Update of standards – ROBUST European project - deliverable 4.1.1 Full scale test results analysis – GRD-2002-70021 – March 2006

[ROB06-2] Road Barrier Update of standards – ROBUST European project - deliverable 5.3.1 Computational Mechanics Summary Report – GRD-2002-70021 – April 2006

[RAY96] M. H. Ray "Repeatability of Full-Scale Crash Tests and a criteria for Validating Finite Element Simulations", Transportation Research Record, Vol. 1528, pp. 155-160, (1996)

[RAY97] M. H. Ray "The use of finite element analysis in roadside hardware design", International Journal of Crashworthiness, 2:4, 333-348 (1997)

[REI98] J D Reid (1998): Tracking the energy in an energy absorbing guardrail terminal, International Journal of Crashworthiness, 3:2, 135-146

[REI00] J D Reid (2000): Designing for the critical impact point on a new bullnose guardrail system, International Journal of Crashworthiness, 5:2, 141-152

[SEC05] N R Seckinger, P N Roschke, A Abu-Odeh & R P Bligh (2005): Numerical simulation of mow strip subcomponents used with strong post guardrail systems, International Journal of Crashworthiness, 10:4, 419-427

[TAB00_1] Ala Tabiei & Jin Wu (2000): Validated crash simulation of the most common guardrail system in the USA, International Journal of Crashworthiness, 5:2, 153-168

[TAB00_2] Ala Tabiei & Jin Wu – "Three-dimensional nonlinear orthotropic finite element material model for wood" Composite structures 50 (2000) 143-149

[UDD99] W. Uddin & R.M. Hackett (1999): Three-dimensional finite element modelling of vehicle crashes against roadside safety barriers, International Journal of Crashworthiness, 4:4, 407-418

[WHI04] H A Whitworth, R Bendidi, D Marzougui & R Reiss (2004): Finite element modeling of the crash performance of roadside barriers, International Journal of Crashworthiness, 9:1, 35-43

[WU04] W Wu & R Thomson (2004): Compatibility between passenger vehicles and road barriers during oblique collisions, International Journal of Crashworthiness, 9:3, 245-253

[YON05] K Yonten, Majid T Manzari, D Marzougui & A Eskandarian (2005): An assessment of constitutive models of concrete in the crashworthiness simulation of roadside safety structures, International Journal of Crashworthiness, 10:1, 5-19

Appendix 1: Steel-wood bolted connection modelling

During the modelling phase of the three point bending experiments, several modelling techniques were evaluated concerning the steel wood bolted connection.
The simulations presented here after are carried out at 20km/h with 30% of wood Moisture content and 30°C for room temperature.
In the following tables, each configuration is compared to the initial model and a conclusion is drawn with regard to experimental behaviour.

Connection model	Initial model : Beam spotweld + spotweld interface
Connection details	2 beam elements are defined at each extremity and located between the neutral fibre of the steel reinforcement and rear face of the wood beam. A spotweld interface ensures the connection.
Final state	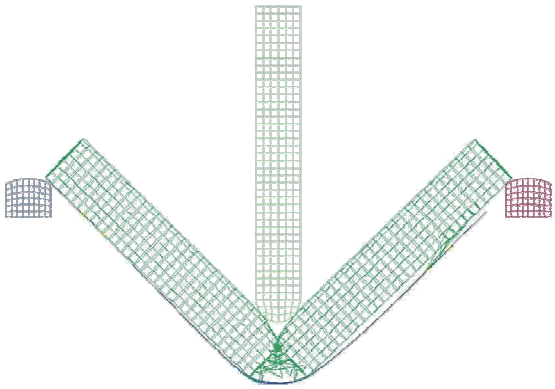
Steel reinforcement stress level	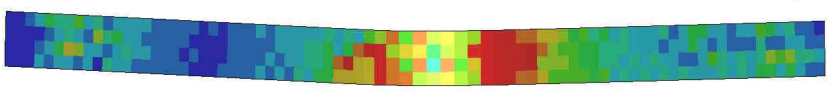
Deceleration time history	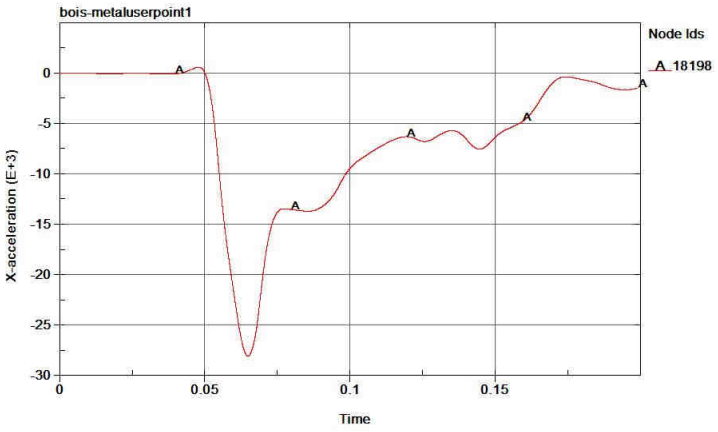
Conclusion	The small beam elements suffer of a brittle behaviour and no deformation of the bolts can be represented. The global behaviour is not in accordance with the experiment. In particular an important displacement of the steel reinforcement is observed and the deceleration plateau seems too short.

Table A - 1 Initial model

Connection model	Beam spotweld + spotweld interface and constrained nodal rigid body
Connection details	In order to better represent the connection behaviour, the spotweld beams are set longer and the spotweld interface (wood side) is replaced by a constrained nodal rigid body with several nodes of the wood beam surrounding the beam extremity.
Final state	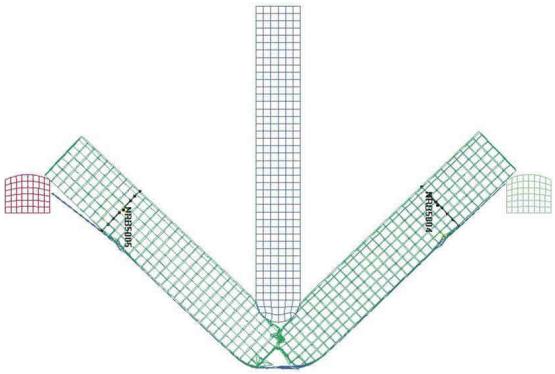
Steel reinforcement stress level	
Deceleration time history	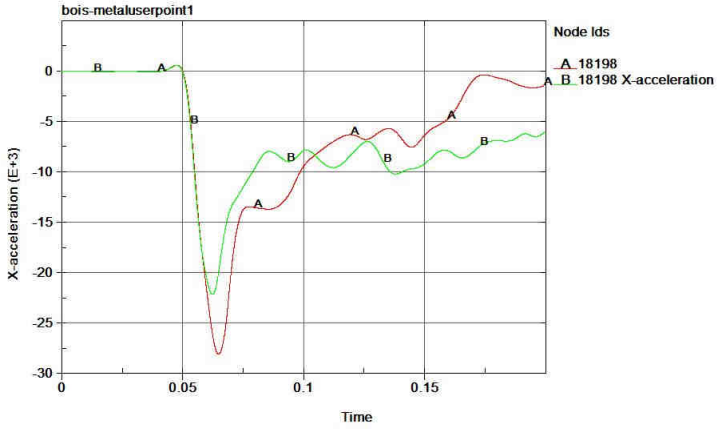
Conclusion	This model brings a rotation of the beam inside the wood due to nodal rotation. The displacement of steel reinforcement is limited and the deceleration plateau is better.

Table A - 2 Model modification #1

Connection model	Beam spotweld + spotweld interface + Lagrange in solid coupling
Connection details	The constrained nodal rigid body of the previous model is replaced by a constrained Lagrange in solid
Final state	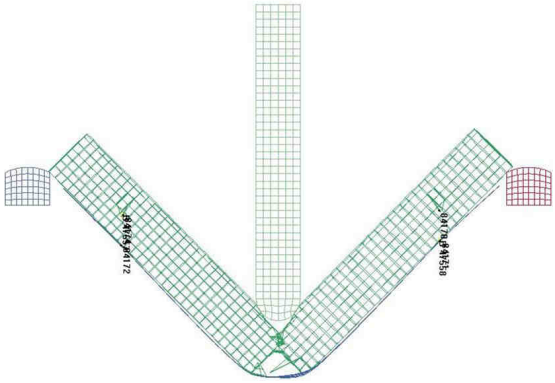
Steel reinforcement stress level	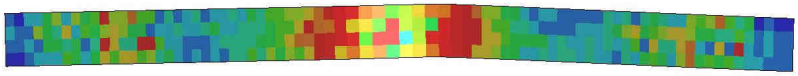
Deceleration time history	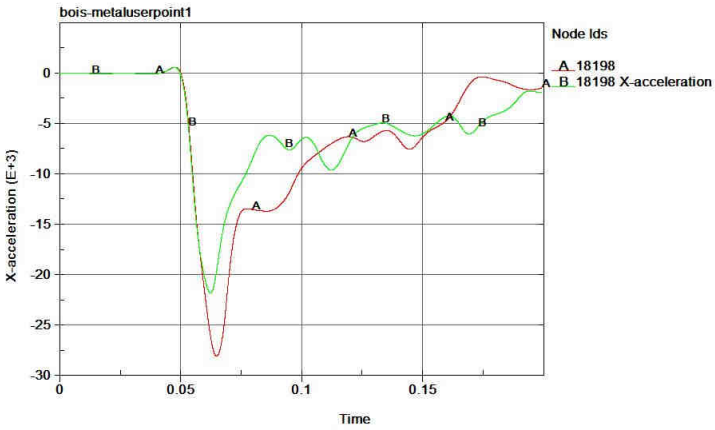
Conclusion	The displacement of the beam's nodes inside the wood is not realistic. This may be due to the limitation of the coupling techniques with a single node.

Table A - 3 Model modification #2

Connection model	Discretized spotweld beam + spotweld interface + Lagrange in solid coupling
Connection details	Each bolt is now modelled with several beams along the length
Final state	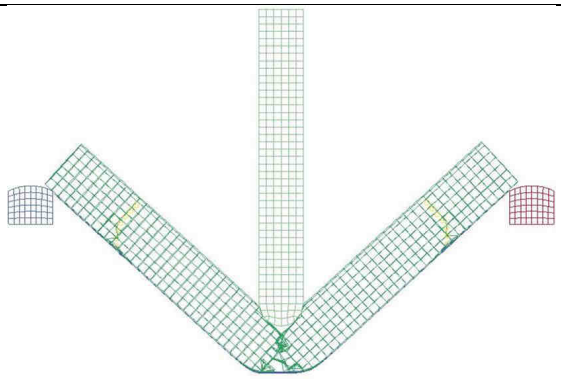
Steel reinforcement stress level	
Deceleration time history	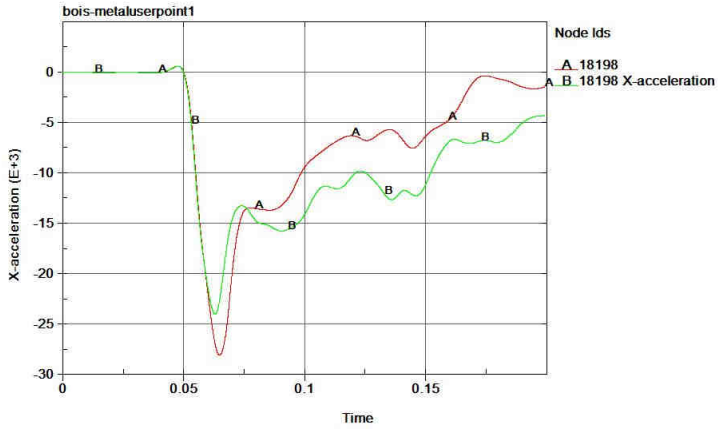
Conclusion	The deformations of the bolts obtained are much more realistic with the experiment.

Table A - 4 Model modification #3

Connection model	Discretized type1 beam + Lagrange in solid coupling + node-to-node connection
Connection details	Each bolt is now modelled with a Hughes Liu beams with a common node at the steel reinforcement and with a Lagrange in solid coupling with wood.
Final state	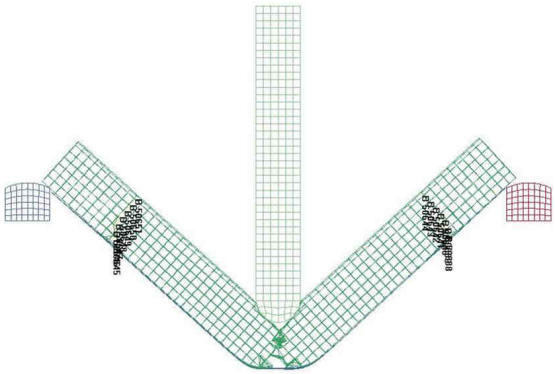
Steel reinforcement stress level	
Deceleration time history	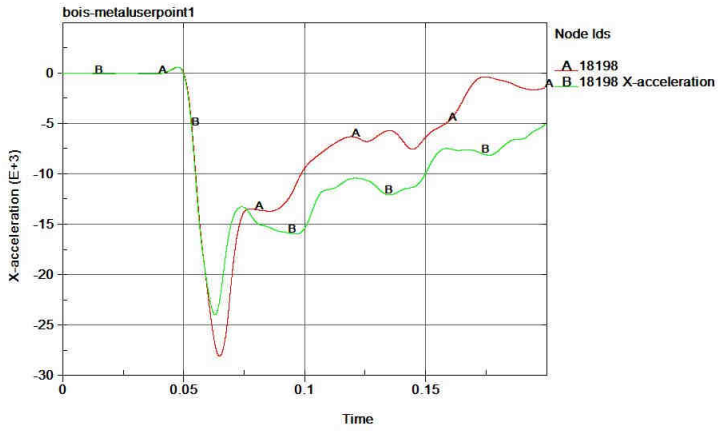
Conclusion	The behaviour obtained with this model present the best accordance with the experiment..

Table A - 5 Model modification #4

Connection model	Non linear discretization
Connection details	A refinement is applied on the beam mesh on steel reinforcement side (where displacement are localized)
Final state	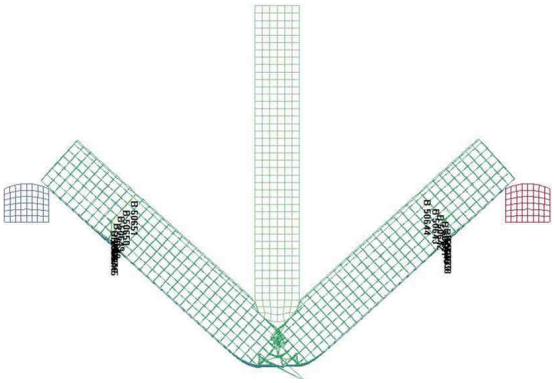
Steel reinforcement stress level	
Deceleration time history	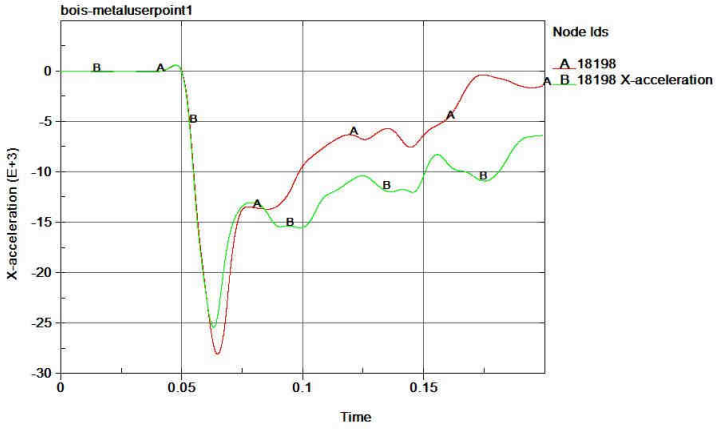
Conclusion	No significant difference appears as regards previous model

Table A - 6 Model modification #5

Appendix 2: Dynamic three point bending test simulations – detailed results

Mass scaled solutions - coarse mesh

Wood structures

Hourglass control	Squared Error Experimental reference	Squared error Fully integrated reference	Energy ratio	CPU time
without	2.58	3.02	0.20	308.75
0.001	2.68	3.04	0.07	305.50
0.005	4.57	4.94	0.17	297.75
0.05	7.69	8.07	0.17	296.00
Full Integration	1.53	0.00	0.00	563.75

Table A - 7 Wood structure results

Hourglass control	Squared Error Experimental reference	Squared error Fully integrated reference	Energy ratio	CPU time
without	0.34	0.37	1.00	0.04
0.001	0.35	0.38	0.33	0.04
0.005	0.59	0.61	0.84	0.04
0.05	1.00	1.00	0.85	0.04
Full Integration	0.20	0.00	0.00	0.08

Table A - 8 Wood structure normalized results

Steel-wood structures

Hourglass control	Squared Error Experimental reference	Squared error Fully integrated reference	Energy ratio	CPU time
without	3.89	5.49	0.17	414.50
0.001	4.52	6.89	0.12	410.50
0.005	7.40	10.46	0.19	407.25
0.05	13.01	16.08	0.23	395.00
Full Integration	5.27	0.00	0.00	664.00

Table A - 9 Steel-wood structure results

Hourglass control	Squared Error Experimental reference	Squared error Fully integrated reference	Energy ratio	CPU time
without	0.30	0.34	0.76	0.05
0.001	0.35	0.43	0.52	0.05
0.005	0.57	0.65	0.83	0.05
0.05	1.00	1.00	1.00	0.05
Full Integration	0.41	0.00	0.00	0.08

Table A - 10 Steel-wood structure normalized results

Mass scaled solutions - fine mesh

Wood structures

Hourglass control	Squared Error Experimental reference	Squared error Fully integrated reference	Energy ratio	CPU time
without	1.81	2.17	0.20	3221.67
0.001	1.77	1.98	0.05	3126.00
0.005	1.30	1.99	0.07	3110.00
0.05	4.24	4.78	0.17	3111.67
Full Integration	1.88	0.00	0.00	7260.50

Table A - 11 Wood structure results

Hourglass control	Squared Error Experimental reference	Squared error Fully integrated reference	Energy ratio	CPU time
without	0.23	0.27	0.99	0.44
0.001	0.23	0.24	0.23	0.43
0.005	0.17	0.25	0.36	0.43
0.05	0.55	0.59	0.83	0.43
Full Integration	0.24	0.00	0.00	1.00

Table A - 12 Wood structure normalized results

Steel-wood structures

Hourglass control	Squared Error Experimental reference	Squared error Fully integrated reference	Energy ratio	CPU time
without	4.57	2.95	0.12	4434.00
0.001	5.15	4.67	0.07	4376.50
0.005	4.77	7.30	0.17	4318.75
0.05	8.10	11.72	0.17	4195.00
Full Integration	5.50	0.00	0.00	8769.50

Table A - 13 Steel-wood structure results

Hourglass control	Squared Error Experimental reference	Squared error Fully integrated reference	Energy ratio	CPU time
without	0.35	0.18	0.54	0.51
0.001	0.40	0.29	0.33	0.50
0.005	0.37	0.45	0.76	0.49
0.05	0.62	0.73	0.77	0.48
Full Integration	0.42	0.00	0.00	1.00

Table A - 14 Steel-wood structure normalized results

Time step erosion solutions – coarse mesh

Wood structures

Hourglass control	Squared Error Experimental reference	Squared error Fully integrated reference	Energy ratio	CPU time
without	1.27	1.46	0.19	530.00
0.001	1.22	1.53	0.08	438.00
0.005	1.50	1.79	0.16	355.75
0.05	4.47	4.95	0.18	341.50
Full Integration	1.92	0.00	0.00	687.75

Table A - 15 Wood structure results

Hourglass control	Squared Error Experimental reference	Squared error Fully integrated reference	Energy ratio	CPU time
without	0.28	0.30	0.32	0.05
0.001	0.27	0.31	0.13	0.04
0.005	0.34	0.36	0.28	0.03
0.05	1.00	1.00	0.29	0.03
Full Integration	0.43	0.00	0.00	0.06

Table A - 16 Wood structure normalized results

Steel-wood structures

Hourglass control	Squared Error Experimental reference	Squared error Fully integrated reference	Energy ratio	CPU time
without	3.88	5.27	0.18	914.50
0.001	4.88	6.94	0.11	684.00
0.005	6.95	9.84	0.20	544.50
0.05	10.63	13.61	0.17	478.33
Full Integration	5.11	0.00	0.00	991.00

Table A - 17 Steel-wood structure results

Hourglass control	Squared Error Experimental reference	Squared error Fully integrated reference	Energy ratio	CPU time
without	0.37	0.39	0.89	0.06
0.001	0.46	0.51	0.56	0.05
0.005	0.65	0.72	0.98	0.04
0.05	1.00	1.00	0.85	0.03
Full Integration	0.48	0.00	0.00	0.07

Table A - 18 Steel-wood structure normalized results

Time step erosion solutions – fine mesh

Wood structures

Hourglass control	Squared Error Experimental reference	Squared error Fully integrated reference	Energy ratio	CPU time
without	1.27	1.46	0.60	5667.50
0.001	1.22	1.53	0.07	4163.25
0.005	1.50	1.79	0.08	3747.50
0.05	4.47	4.95	0.18	3325.50
Full Integration	1.92	0.00	0.00	11594.25

Table A - 19 Wood structure results

Hourglass control	Squared Error Experimental reference	Squared error Fully integrated reference	Energy ratio	CPU time
without	0.28	0.30	1.00	0.49
0.001	0.27	0.31	0.12	0.36
0.005	0.34	0.36	0.14	0.32
0.05	1.00	1.00	0.29	0.29
Full Integration	0.43	0.00	0.00	1.00

Table A - 20 Wood structure normalized results

Steel-wood structures

Hourglass control	Squared Error Experimental reference	Squared error Fully integrated reference	Energy ratio	CPU time
without	3.84	2.84	0.20	11781.67
0.001	3.50	4.60	0.12	7070.50
0.005	4.46	6.84	0.15	6382.00
0.05	9.85	12.60	0.20	4660.75
Full Integration	5.25	0.00	0.00	14837.25

Table A - 21 Steel-wood structure results

Hourglass control	Squared Error Experimental reference	Squared error Fully integrated reference	Energy ratio	CPU time
without	0.36	0.21	1.00	0.79
0.001	0.33	0.34	0.59	0.48
0.005	0.42	0.50	0.72	0.43
0.05	0.93	0.93	0.99	0.31
Full Integration	0.49	0.00	0.00	1.00

Table A - 22 Steel-wood structure normalized results

Appendix 3: Steel-wood VRS simulations – detailed results

The Design Of Experiment (DOE) defined in Chapter 4 has been used to assess the effect of several parameters of the numerical model:

- The formulation of post shell elements (Type 2: under integrated or Type 16 fully integrated)
- The friction coefficient for the contact interface between the vehicle and the barrier (from 0.3 to 0.5)
- The friction coefficient between the vehicle and the rigidwall (0.6 and 0.8)
- The wheel (front right) cinematic joints failure

In the following pages, the corresponding DOE are identified with all parameters delimited by an underscore character, example: T16_04_06 concerns the results obtained for the DOE with Type 16 shell elements for the post, a friction of 0.4 between the vehicle and the device, 0.6 between vehicle and the ground and without failure of the front right wheel).
The calculations performed with a wheel failure are identified by "_WF".

These parametric studies are performed with the aim of finding the best correlation with the real crash test results according to TG5 criteria on the one end. On the other hand the best correlation is defined as the simulation presenting the lowest total quadratic error obtained while comparing the simulation time histories to those from the real test for the two velocity components and the yaw angle. The sum of these three quadratic errors is normalized with the average obtained in each project and presented in the following tables as TOTAL NSE.
Finally all the non-failed simulations of all the projects are grouped and a new normalisation is computed with the global average value for a global comparison.

T2-03-06

	ASI	THIV	W	CM-E criteria	Total NSE
Shot 1	0.56	22.53	1.61	True	2.9
Shot 2	0.49	20.90	1.65	True	3.3
Shot 3	0.48	20.95	1.68	True	3.8
Shot 4	0.54	22.35	1.69	True	2.6
Shot 5	0.57	21.03	1.74	True	3.1
Shot 6	0.49	21.07		False	0.7
Shot 7	0.52	22.13	1.73	True	2.9
Shot 8	0.47	21.63	1.78	True	3.1
Shot 9	0.48	21.44	1.78	True	3.5
Shot 10	0.54	22.08	1.65	True	2.8
Shot 11	0.51	21.22	1.71	True	3.4
Shot 12	0.48	20.87	1.73	True	3.8
Shot 13	0.53	22.14	1.69	True	3.0
Shot 14	0.48	21.33	1.76	True	2.9
Shot 15	0.47	21.00	1.76	False	3.9
Shot 16	0.55	21.73	1.76	True	2.9
Shot 17	0.32			False	0.6
Shot 18	0.54	21.44	1.83	True	3.3
Shot 19	0.53	21.81	1.69	True	3.0
Shot 20	0.47	21.07	1.71	True	3.3
Shot 21	0.47	20.68	1.75	False	3.7
Shot 22	0.51	21.56	1.75	True	2.4
Shot 23	0.47	21.11	1.78	True	3.1
Shot 24	0.45	20.72	1.81	False	3.9
Shot 25	0.52	21.02	1.93	False	2.9
Shot 26	0.49	20.73	1.85	True	3.2
Shot 27	0.44	20.34	1.88	False	3.2

Table A - 23 - DOE T2-03-06 detailled results

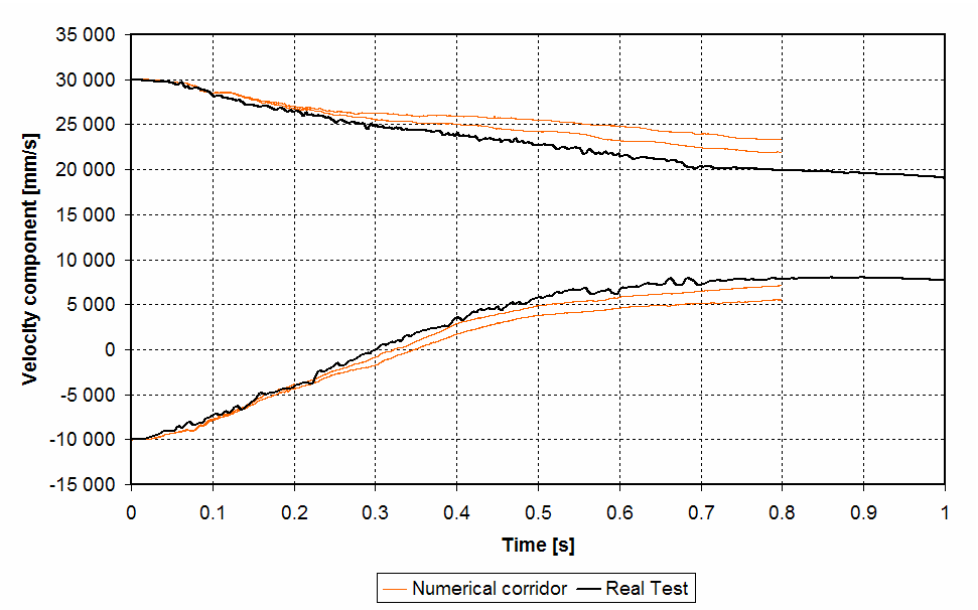

Figure A - 1 DOE T2-03-06 Velocity components

T16-03-06

	ASI	THIV	W	CM-E criteria	Total NSE
Shot 1	0.59	23.48	1.56	True	2.6
Shot 2	0.60	23.62		False	2.0
Shot 3	0.55	21.98	1.51	True	2.5
Shot 4	0.57	23.26	1.75	True	2.6
Shot 5	0.59	23.26	1.56	True	3.1
Shot 6	0.54	21.79	1.56	True	3.6
Shot 7	0.55	23.09	1.77	True	2.3
Shot 8	0.58	22.75	1.70	True	2.6
Shot 9	0.53	21.79		False	1.9
Shot 10	0.59	23.45	1.51	True	2.7
Shot 11	0.58	22.68	1.60	True	3.1
Shot 12	0.53	21.70	1.55	True	2.5
Shot 13	0.57	23.40	1.56	True	2.7
Shot 14	0.57	22.22	1.66	True	3.0
Shot 15	0.53	21.46	1.59	True	3.5
Shot 16	0.54	22.84	1.86	True	3.0
Shot 17	0.55	21.81	1.71	True	3.4
Shot 18	0.51	21.31	1.65	True	3.8
Shot 19	0.58	23.14	1.54	True	3.0
Shot 20	0.55	22.19	1.65	True	3.8
Shot 21	0.51	21.34	1.58	True	2.6
Shot 22	0.56	22.94	1.59	True	2.7
Shot 23	0.53	21.74	1.68	True	3.7
Shot 24	0.50	21.08	1.63	True	4.0
Shot 25	0.53	22.52	1.75	True	2.6
Shot 26	0.54	21.27	1.77	True	3.7
Shot 27	0.50	21.11	1.69	True	4.1

Table A - 24 - DOE T16-03-06 detailled results

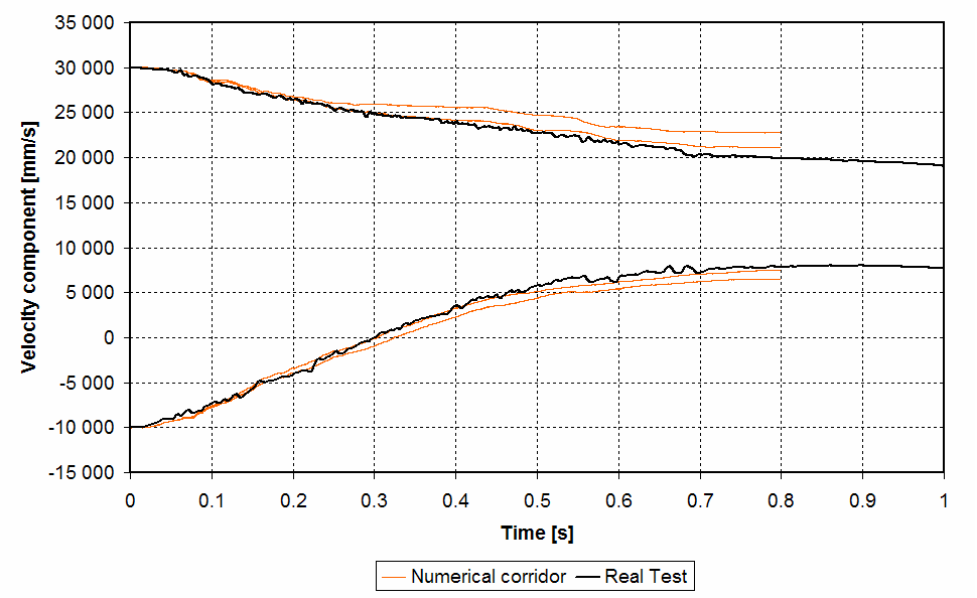

Figure A - 2 DOE T16-03-06 Velocity components

T16-03-06_WF

	ASI	THIV	W	CM-E criteria	Total NSE
Shot 1	0.62	23.93		False	2.2
Shot 2	0.59	22.75	1.47	False	3.7
Shot 3	0.55	22.55		False	2.5
Shot 4	0.60	23.71		False	1.7
Shot 5	0.59	22.69	1.53	True	3.6
Shot 6	0.55	22.42	1.54	True	3.0
Shot 7	0.60	23.75		False	1.4
Shot 8	0.57	22.80	1.56	True	3.3
Shot 9	0.54	22.20	1.61	True	3.0
Shot 10	0.61	23.62		False	2.0
Shot 11	0.56	22.56	1.64	True	3.2
Shot 12	0.54	22.30	1.53	True	4.9
Shot 13	0.61	23.58	1.49	True	3.0
Shot 14	0.55	22.84	1.56	True	4.0
Shot 15	0.52	21.75		False	2.5
Shot 16	0.59	23.71	1.55	True	3.0
Shot 17	0.54	22.60	1.62	True	4.0
Shot 18	0.51	21.76	1.66	True	3.2
Shot 19	0.61	23.50		False	1.6
Shot 20	0.68	22.62	1.55	False	2.9
Shot 21	0.52	21.59	1.58	True	5.1
Shot 22	0.60	23.46		False	1.4
Shot 23	0.57	22.62	1.60	True	4.0
Shot 24	0.51	21.68	1.64	True	4.8
Shot 25	0.58	23.45		False	1.2
Shot 26	0.52	21.36		False	1.4
Shot 27	0.50	21.51	1.70	True	4.3

Table A - 25 - DOE T16-03-06_WF detailled results

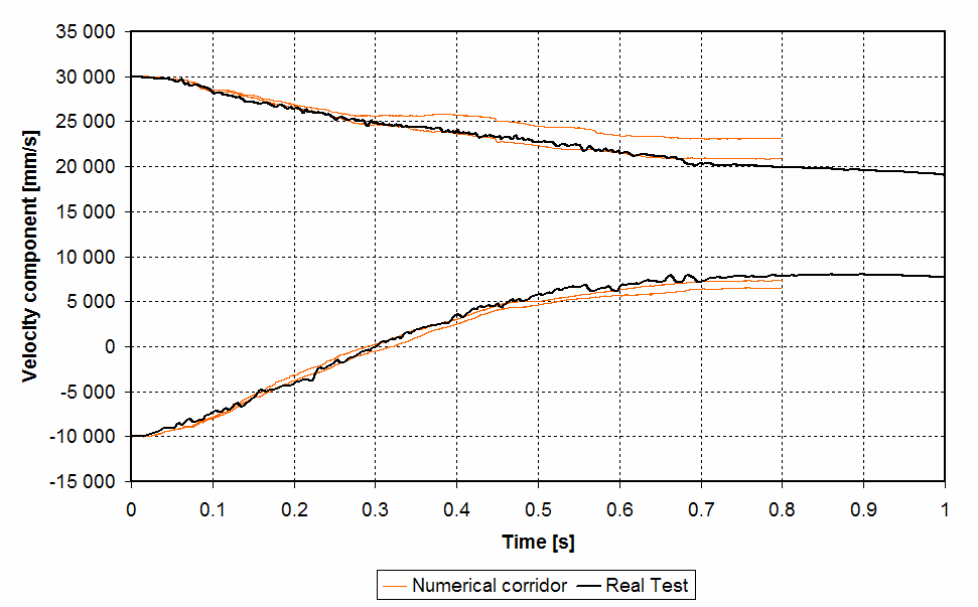

Figure A - 3 DOE T16-03-06 Velocity components

T16-04-06

	ASI	THIV	W	CM-E criteria	Total NSE
Shot 1	0.60	25.75	1.49	False	3.3
Shot 2	0.60	25.31	1.56	False	2.8
Shot 3	0.68	24.60	1.52	False	2.6
Shot 4	0.57	25.07	1.62	False	3.3
Shot 5	0.60	25.34	1.59	False	3.2
Shot 6	0.54	24.41	1.56	True	2.1
Shot 7	0.56	24.72	1.72	True	4.3
Shot 8	0.59	24.74	1.69	True	3.7
Shot 9	0.53	24.16	1.63	True	2.7
Shot 10	0.59	25.49	1.52	False	3.4
Shot 11	0.65	24.84	1.61	False	2.8
Shot 12	0.83	24.16	1.56	False	2.7
Shot 13	0.59	25.03	1.57	False	3.7
Shot 14	0.58	24.63	1.66	True	2.9
Shot 15	0.53	23.97		False	1.0
Shot 16	0.55	25.01	1.67	False	3.8
Shot 17	0.56	24.50	1.70	True	3.1
Shot 18	0.51	23.91	1.66	True	2.5
Shot 19	0.58	24.82	1.55	False	3.6
Shot 20	0.56	24.40	1.65	True	2.8
Shot 21	0.52	23.71		False	1.0
Shot 22	0.56	24.60	1.61	True	3.6
Shot 23	0.54	24.17	1.69	True	2.8
Shot 24	0.51	23.72	1.64	True	2.8
Shot 25	0.54	23.74	1.77	True	4.4
Shot 26	0.54	24.07	1.77	True	3.2
Shot 27	0.49	23.01	1.70	True	3.0

Table A - 26 - DOE T16-04-06 detailled results

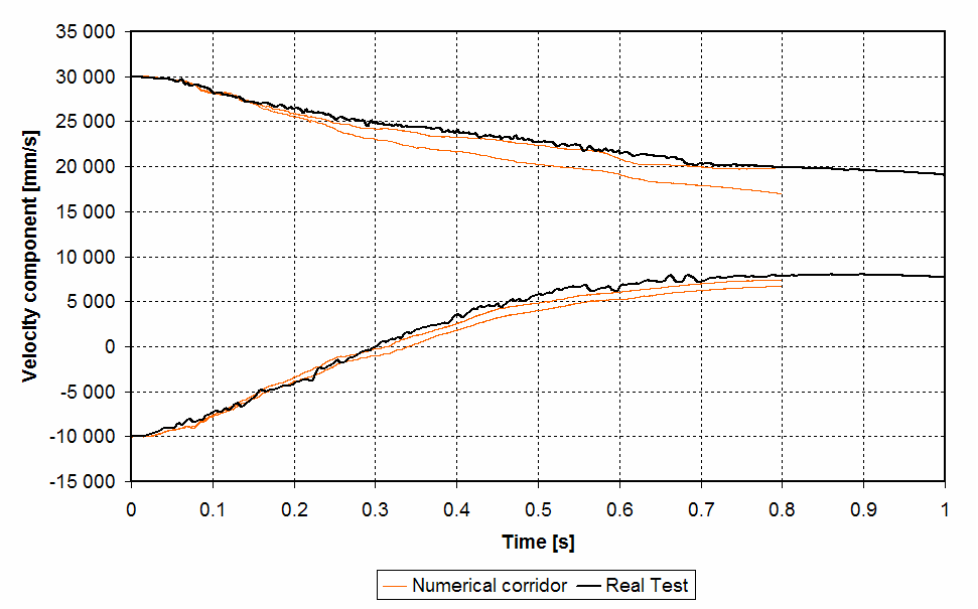

Figure A - 4 DOE T16-04-06 Velocity components

T16-04-06_WF

	ASI	THIV	W	CM-E criteria	Total NSE
Shot 1	0.60	25.87	1.53	False	3.1
Shot 2	0.59	25.53	1.57	False	3.2
Shot 3	0.56	24.97	1.56	False	2.5
Shot 4	0.59	25.14	1.60	False	3.0
Shot 5	0.59	25.52	1.63	False	3.0
Shot 6	0.55	24.79	1.59	False	2.7
Shot 7	0.58	25.45	1.54	False	3.0
Shot 8	0.57	25.32	1.70	False	3.8
Shot 9	0.54	24.38	1.65	True	3.0
Shot 10	0.60	25.81	1.48	False	3.8
Shot 11	0.58	25.27	1.57	False	2.7
Shot 12	0.55	24.64	1.56	True	2.5
Shot 13	0.58	25.51	1.57	False	3.1
Shot 14	0.58	25.38	1.62	False	2.8
Shot 15	0.54	24.10	1.63	True	2.7
Shot 16	0.58	25.10	1.57	False	3.0
Shot 17	0.54	24.40	1.69	True	3.2
Shot 18	0.53	23.87	1.69	True	2.7
Shot 19	0.60	25.88	1.52	False	4.3
Shot 20	0.57	24.90	1.60	False	2.7
Shot 21	0.52	23.95	1.62	True	2.7
Shot 22	0.58	25.33	1.64	False	4.8
Shot 23	0.56	24.77	1.67	False	2.7
Shot 24	0.51	23.87	1.66	True	2.4
Shot 25	0.57	25.06		False	2.2
Shot 26	0.55	23.85	1.71	True	2.9
Shot 27	0.51	23.75	1.73	True	2.5

Table A - 27 - DOE T16-04-06_WF detailled results

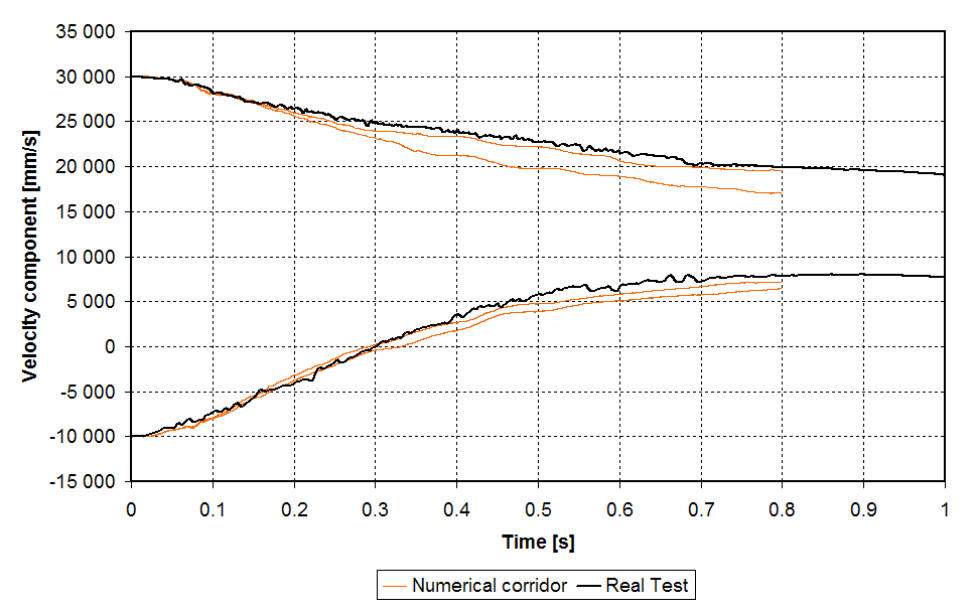

Figure A - 5 DOE T16-04-06_WF Velocity components

T16-04-08

	ASI	THIV	W	CM-E criteria	Total NSE
Shot 1	0.60	25.68	1.53	False	3.6
Shot 2	0.60	25.35	1.57	False	2.9
Shot 3	0.56	24.62	1.53	True	2.7
Shot 4	0.57	25.17	1.64	False	4.2
Shot 5	0.60	25.46	1.59	False	2.6
Shot 6	0.81	24.78	1.56	False	2.7
Shot 7	0.55	25.11	1.70	False	4.6
Shot 8	0.59	25.14	1.65	False	3.2
Shot 9	0.54	24.42	1.63	True	2.8
Shot 10	0.59	25.24	1.51	False	3.4
Shot 11	0.58	25.14	1.63	False	2.8
Shot 12	0.54	24.57	1.56	True	2.4
Shot 13	0.59	25.03	1.57	False	3.5
Shot 14	0.56	24.44	1.67	True	2.9
Shot 15	0.53	23.99		False	1.1
Shot 16	0.55	24.56	1.77	True	5.2
Shot 17	0.55	24.17	1.70	True	2.9
Shot 18	0.51	24.15		False	1.2
Shot 19	0.57	25.05	1.56	False	3.5
Shot 20	0.56	24.18	1.67	True	2.9
Shot 21	0.53	23.61	1.60	True	2.7
Shot 22	0.60	24.78	1.61	False	2.7
Shot 23	0.55	24.25	1.71	True	2.6
Shot 24	0.50	23.64	1.65	True	2.5
Shot 25	0.56	25.03	1.65	False	3.6
Shot 26	0.53	23.86	1.77	True	3.2
Shot 27	0.49	23.05	1.71	True	2.7

Table A - 28 - DOE T16-04-08 detailled results

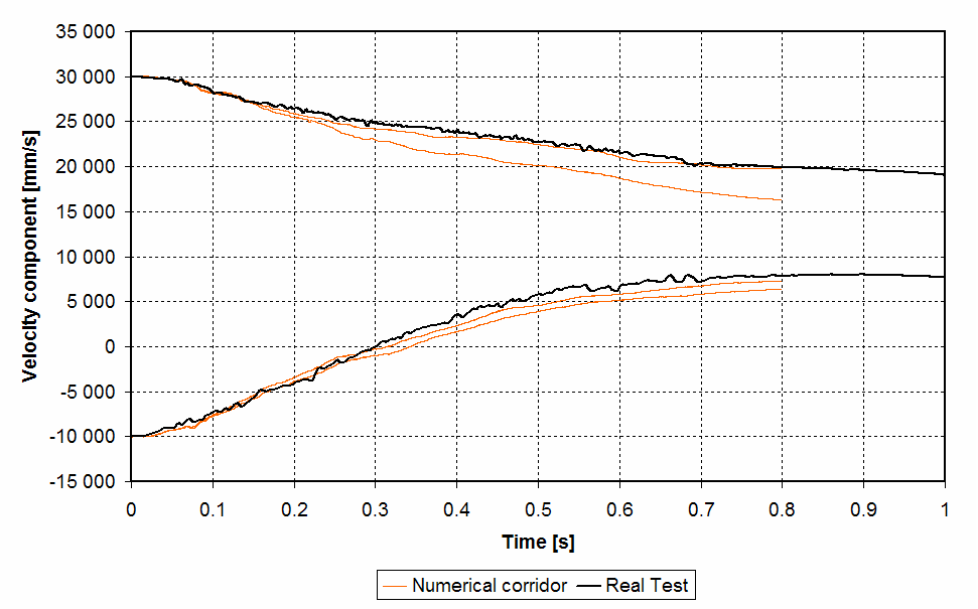

Figure A - 6 DOE T16-04-08 Velocity components

T16-05-06

	ASI	THIV	W	CM-E criteria	Total NSE
Shot 1	0.63	28.95	1.54	False	3.6
Shot 2	0.61	29.08	1.65	False	3.8
Shot 3	0.61	27.06	1.72	False	2.9
Shot 4	0.61	28.37		False	1.9
Shot 5	0.61	28.37	1.71	False	1.9
Shot 6	0.60	27.61		False	1.4
Shot 7	0.58	27.08	1.93	False	5.2
Shot 8	0.59	29.15		False	1.0
Shot 9	0.58	26.29		False	1.5
Shot 10	0.61	27.61	1.90	False	6.9
Shot 11	0.60	28.25		False	1.8
Shot 12	0.59	26.93	1.65	False	2.1
Shot 13	0.60	28.20	1.69	False	4.6
Shot 14	0.59	28.13	1.75	False	3.4
Shot 15	0.58	26.59	1.71	False	2.3
Shot 16	0.59	27.93	1.74	False	4.3
Shot 17	0.56	27.81	1.81	False	2.8
Shot 18	0.56	26.78	1.77	False	2.0
Shot 19	0.60	28.23	1.65	False	3.4
Shot 20	0.58	27.55	1.73	False	3.1
Shot 21	0.57	25.94	1.68	False	2.3
Shot 22	0.58	27.70	1.70	False	4.7
Shot 23	0.58	27.35	1.79	False	2.8
Shot 24	0.55	26.15	1.76	False	2.5
Shot 25	0.56	27.18	1.79	False	4.4
Shot 26	0.56	27.03	1.85	False	2.9
Shot 27	0.54	25.67		False	1.4

Table A - 29 - DOE T16-05-06 detailled results

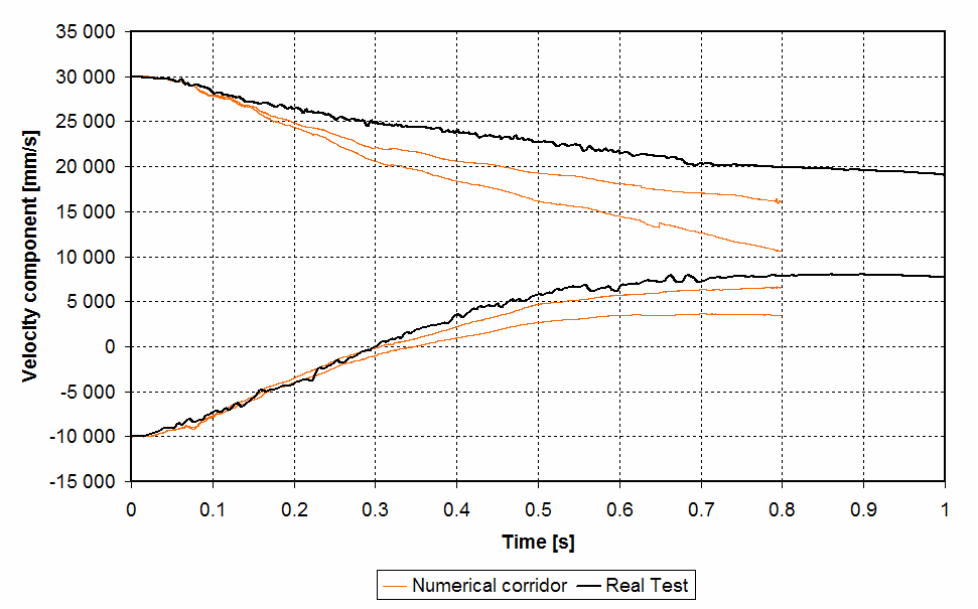

Figure A - 7 DOE T16-05-06 Velocity components

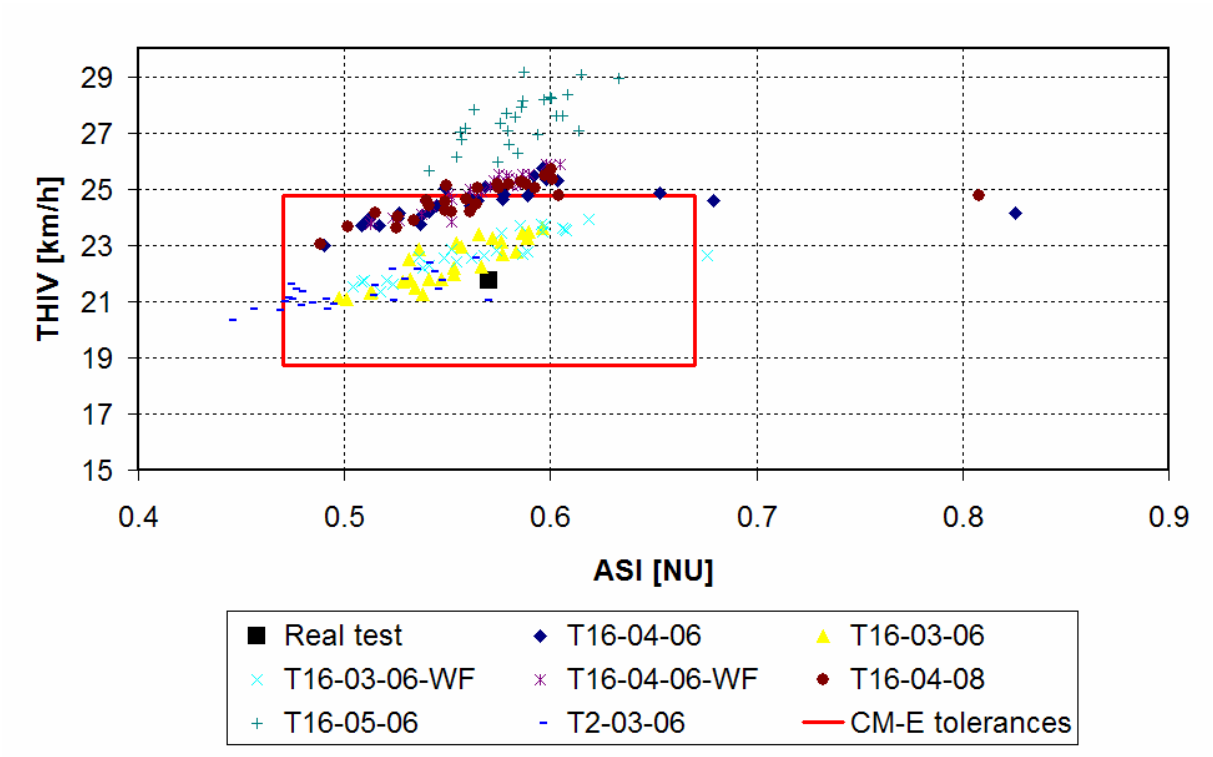

Figure A - 8 DOE comparison _ severity indices

The previous figure highlights the interest of parametric studies. The clouds comparison raises the following comments:

- Element formulation has an effect mainly on ASI
- No effect of wheel failure on ASI and THIV
- Biggest effect due to friction between vehicle/VRS on THIV

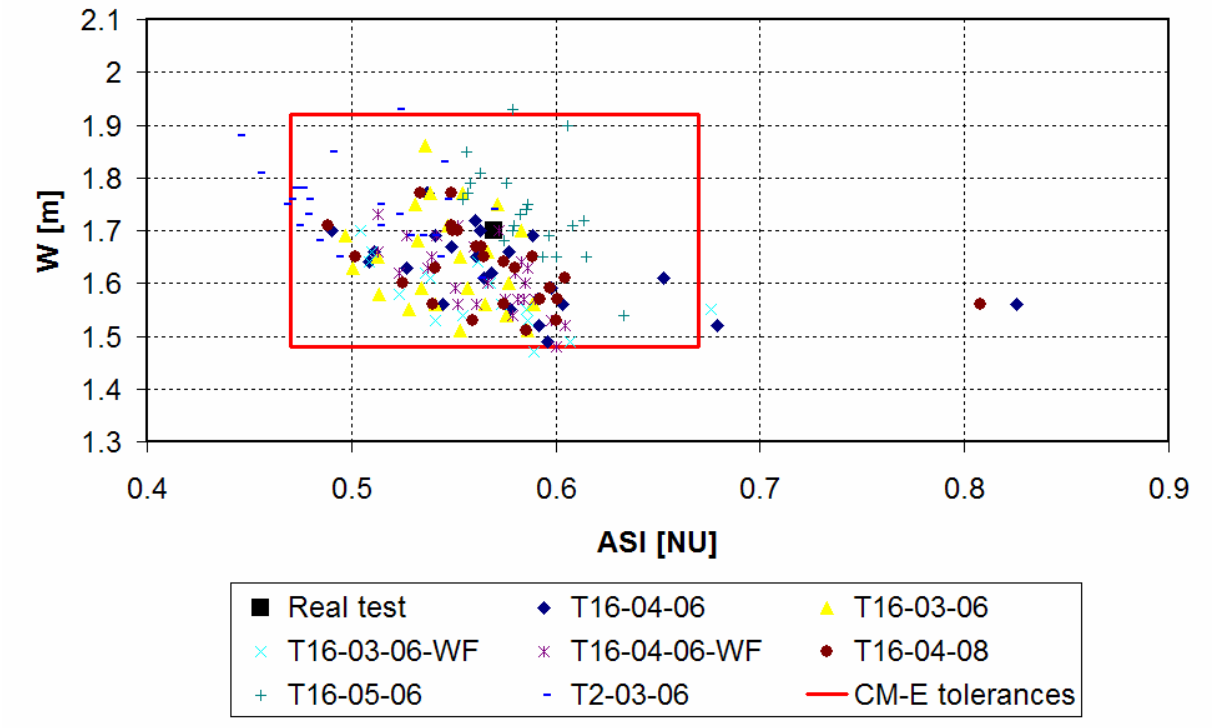

Figure A - 9 DOE comparison _ EN1317 criteria

From the above figure, one can notice that the evaluated parameters have a limited effect toward W values while the parameters evaluated in the DOE lead to an important spread on this measure.

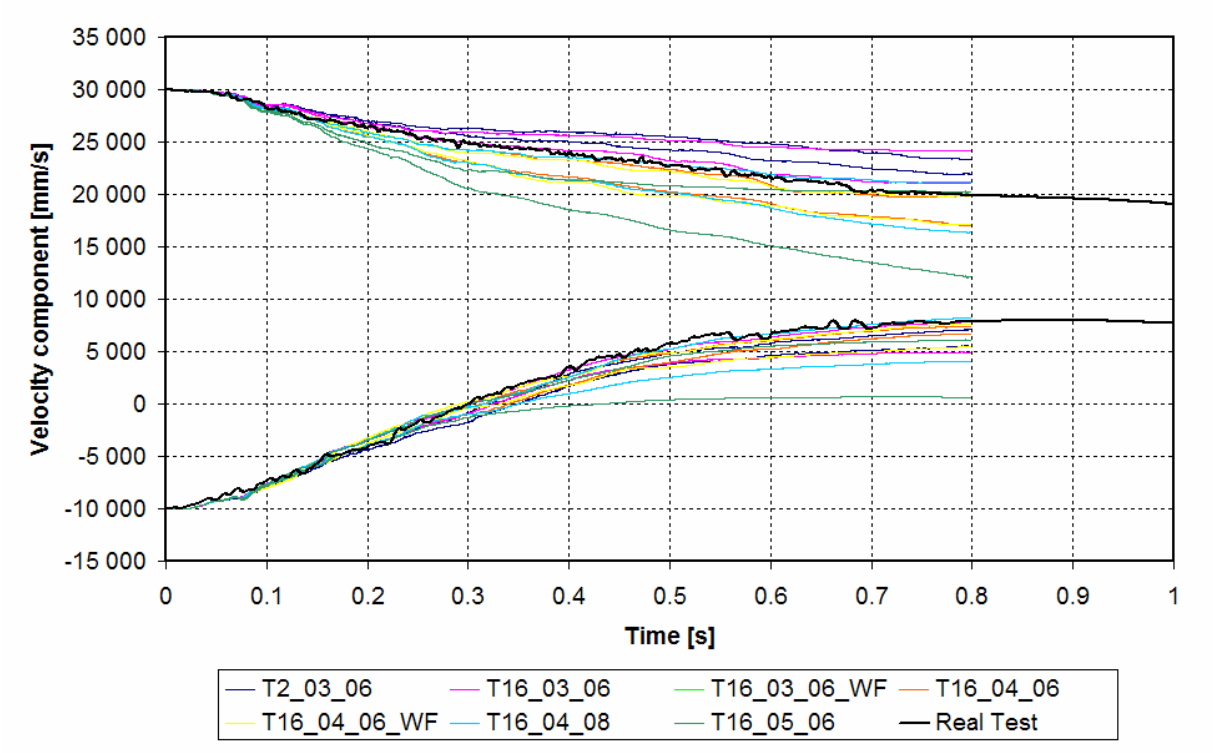

Figure A - 10 DOE comparison _ Velocity component corridors

The Vehicle/VRS friction coefficient parameter has an influence on THIV and also on the x velocity component.
On the contrary, the main variations observed for ASI and W are due to DOE itself.
Finally, it is worth noticing that the best project as regards criteria comparison is not the best concerning velocity component comparison. Furthermore, tolerances concerning criteria validation are centred on the real crash test results which are not necessarily representative of an average value of the parameters.

Appendix 4: French summary

Introduction

En France, un tiers des personnes tuées sur la route le sont lors d'un accident sur un obstacle fixe. Dans 90% des cas, ces accidents surviennent après une perte de contrôle du véhicule. Les dispositifs de retenue de véhicule (DDR) ont pour but de maintenir les véhicules en perdition sur la chaussée en limitant la sévérité de l'impact.
Ces dispositifs doivent subir des essais de chocs normatifs afin de pouvoir être installés sur le bord des routes européennes et d'évaluer leurs performances en termes de sévérité et de déflexion.
Les coûts de développement et le besoin d'optimisation des performances de ces dispositifs associés à l'augmentation de la puissance des outils de calcul ont permis le développement d'une activité de simulation numérique. La simulation de ces essais de choc présente un défit car les calculs sont effectués sur des temps longs (parfois supérieurs à la seconde) pour des modèles très longs (soixante mètres au minimum).
De plus, les tolérances existantes sur les paramètres d'essai (véhicule, masse du véhicule, vitesse d'impact, angle d'impact, point d'impact …) et les variations des caractéristiques mécaniques des matériaux constituant le dispositif ont un effet sur les performances de ce dispositifs et doivent être prises en compte lors des calculs
Les dispositifs mixtes (acier-bois) présentent une difficulté supplémentaire en raison de l'hétérogénéité du matériau et de sa sensibilité aux variables d'environnement telles que la température et l'humidité.

Ce travail a deux buts principaux :
Dans un premier temps, l'obtention d'un outil numérique fiable permettant de simuler un dispositif de retenue de véhicule mixte acier-bois soumis à un impact de véhicule dans le but de comprendre et optimiser l'utilisation du bois dans les équipements de la route.
Dans un deuxième temps, la définition d'une méthode fondée sur l'analyse des modes de ruine de la structure et la prise en compte des variations stochastiques des paramètres mécaniques qui régissent leur apparition afin d'obtenir la corrélation du modèle par rapport à une configuration d'essai de choc. Le modèle corrélé sera ensuite utilisé pour évaluer l'incidence de la modification des propriétés mécaniques du bois due aux variations des variables d'environnement.

Chapitre 1 Etat de l'art

Un dispositif de retenue de véhicule latéral, est une structure généralement assez simple dont le but est de retenir un véhicule en perdition et le renvoyer sur la chaussée dans de bonnes conditions pour son conducteur (sévérité) et pour les autres usagés (conditions sur la trajectoire de sortie).
Pour atteindre ce but, la structure va activer des modes de ruine. Un mode de ruine est une séquence d'événements (qui ne sont pas obligatoirement des ruptures) qui va caractériser le fonctionnement d'un système/

La Figure A - 11 présente la séquence d'événements menant au fonctionnement attendu d'une glissière métallique simple et double [CIR88].

Figure A - 11 Fonctionnement d'une glissière simple [CIR88]

Ce bon fonctionnement est obtenu par une déconnection entre la lisse et le support permettant à la lisse de se maintenir à une hauteur correcte pour une bonne interaction avec le véhicule.

Ce mécanisme principal peut être divisé en trois sous-mécanismes:
Plastification locale de la lisse au contact du véhicule et transfert des efforts aux supports adjacents.
Flexion des supports et création d'une charnière plastique à la base du support
Déconnection de la liaison support/lisse. Cette déconnection pouvant être obtenue de différentes manières (suivant les dispositifs) :
Rupture de vis
Déboutonnage (la tête de vis traverse la tôle)

L'activation de chacun de ces phénomènes peut être liée à, au moins, un paramètre physique pouvant être sujet à d'importantes variations.
Pour la séquence décrite ci-dessus, le tableau suivant liste les paramètres physiques associés ainsi que les plages de variation généralement observées.

Mode de ruine	Paramètre physique	Plage de variation
Plastification de la lisse	Limite élastique de l'acier Variations de section	235< < ? MPa
Flexion du support	Limite élastique de l'acier Variation de section	235< < ? MPa
Rupture de la liaison	Limite élastique de la tôle d'acier Et/ou Variations de section Et/ou Effort à rupture de la vis	235< < ? MPa 5mm (4.6 class)

Table A - 30 Modes de ruine et plages de variation

Le tableau ci-dessus illustre un des problèmes rencontrés avec le dimensionnement des DDR. La plupart des matériaux utilisés ne sont pas hautes performances et, généralement, les spécifications ne précisent que des valeurs minimales. Ainsi, pour un acier S235, il est fréquent d'obtenir, lors des analyses matériaux effectuées après les essais de choc, de trouver des limites élastiques supérieures à 300 MPa.
Ces variations fréquentes ne sont pas sans conséquences sur le fonctionnement d'un dispositif et sur ses performances. Il est donc essentiel de prendre en compte ces incertitudes lors de la conception d'un dispositif et d'essayer de faire en sortes que la séquence des événements intervenant lors d'un impact ne soit pas modifiée.
En Europe, les dispositifs, avant de pouvoir être installés sur les routes, doivent subir des essais de choc conformément aux spécifications de la norme Européenne EN1317.

Ces essais de choc permettent d'évaluer les performances d'un dispositif et des modes de ruine obtenus avec un jeu de ces paramètres.
Pour une certaine plage de variation, les modes de ruine de la structure seront inchangés et seules les performances du dispositif seront affectées. Au-delà de ces limites, les modes de ruine peuvent être modifiés et avoir une incidence sur le comportement global du véhicule. Par exemple, si la déconnection de s'opère pas (par exemple si la vis est trop résistante) alors le support peut, dans sa flexion, entrainer la lisse au sol permettant au véhicule de traverser le dispositif.
L'évaluation de ces plages n'est pas possible expérimentalement en raison du coût du matériel et des essais mais serait possible à l'aide des outils numériques.

Contexte normatif

Les essais de chocs ont été et demeurent la méthode la plus courante pour l'évaluation des performances des équipements routiers. En raison du nombre de laboratoire et afin de pouvoir comparer les dispositifs entre eux, des procédures ont été crées afin d'homogénéiser les essais et les critères d'évaluation.
La norme Européenne différentie les dispositifs par leur niveau de retenue. Celui-ci correspond à la capacité de retenue maximale du dispositif et définit le ou les essais à effectuer (voir tableau ci-après).

	Niveau de retenue	Essais d'acceptation	Conditions d'impact			
			Type de véhicule	Masse d'impact [kg]	Vitesse d'impact [km/h]	Angle d'impact [°]
faible	T1	TB 21	VL	1 300	80	8
	T2	TB 22	VL	1 300	80	15
	T3	TB 21 TB 41	VL PL[1]	1 300 10 000	80 70	20 8
Normal	N1	TB 31	VL	1 500	80	20
	N2	TB11 TB32	VL VL	900 1 500	100 110	20 20
Elevé	H1	TB 11 TB 42	VL PL	900 10 000	100 70	20 15
	H2	TB 11 TB 51	VL Bus	900 13 000	100 70	20 20
	H3	TB 11 TB 61	VL PL	900 16 000	100 80	20 20
Très élevé	H4a	TB 11 TB 71	VL PL	900 30 000	100 65	20 20
	H4b	TB 11 TB 81	VL PL	900 38 000	100 65	20 20

Table A - 31 EN1317 Définition des niveaux de retenue

Lors des essais de chocs, des critères qualitatifs et quantitatifs sont évalués afin d'évaluer les performances du dispositif.
Les performances obtenues lors des essais permettent la classification des dispositifs à la fois en ce qui concerne la et la déflexion selon les tableaux ci-dessous.

Classe de sévérité	Critères		
A	ASI ≤ 1,0		THIV ≤ 33 km/h
B	ASI ≤ 1,4	And	
C	ASI ≤ 1,9		

Table A - 32 EN1317 indices de sévérité

W classes	Valeur (m)
W1	W ≤ 0,6
W2	W ≤ 0,8
W3	W ≤ 1,0
W4	W ≤ 1,3
W5	W ≤ 1,7
W6	W ≤ 2,1
W7	W ≤ 2,5
W8	W ≤ 3,5

Table A - 33 EN1317 Largeur de fonctionnement

La performance globale d'un dispositif européen est généralement présentée par une compilation de son niveau de retenue, de son niveau de largeur de fonctionnement et de sa classe de sévérité (par exemple, N2-W3-A).

Modélisation des essais de chocs sur DDR

L'utilisation des méthodes numériques n'est pas nouvelle. [RAY97] décrit les premières utilisations de simulations numériques au début des années soixante et conclue que l'utilisation de l'analyse élément finis non linéaire a permis une amélioration sensible dans le processus de dimensionnement des équipements routiers.
A cette époque, des modèles analytiques simples composés de poutres, de masses et de ressorts ont été développés pour étudier la dynamique d'un véhicule impactant une barrière de sécurité.
Plusieurs années plus tard, en accompagnement du développement des codes de calcul et des ressources informatiques, de nouveaux modèles sont apparus. Ces modèles de véhicules n'avaient pas pour intention de représenter fidèlement un véhicule réel mais d'avoir des propriétés inertielles correctes permettant d'obtenir des signaux d'accélération comparables à ceux des essais.
De nos jours, la simulation numérique couvre deux applications distinctes:

- Le développement de nouveaux dispositifs ou l'optimisation de dispositifs existants
- La certification de produits modifiés.

Dans les deux cas, le modèle doit être prédictif. Dans le premier cas car des essais vont être effectués suite à l'analyse, et dans le deuxième cas car les produits modifiés sont appelés à être installés sur le bord des routes.

La prédictibilité concerne alors principalement la capacité à représenter le comportement global d'un véhicule au cours de l'impact et d'évaluer les critères définit dans la norme EN1317.

Cette prédictibilité est souvent remise en question car de nombreux paramètres peuvent avoir un effet sur les performances d'un dispositif.

En premier lieu, des tolérances existent sur les conditions d'impact. La Figure A - 12 présente les tolérances définie dans la norme EN1317 sur la vitesse et l'angle d'impact.

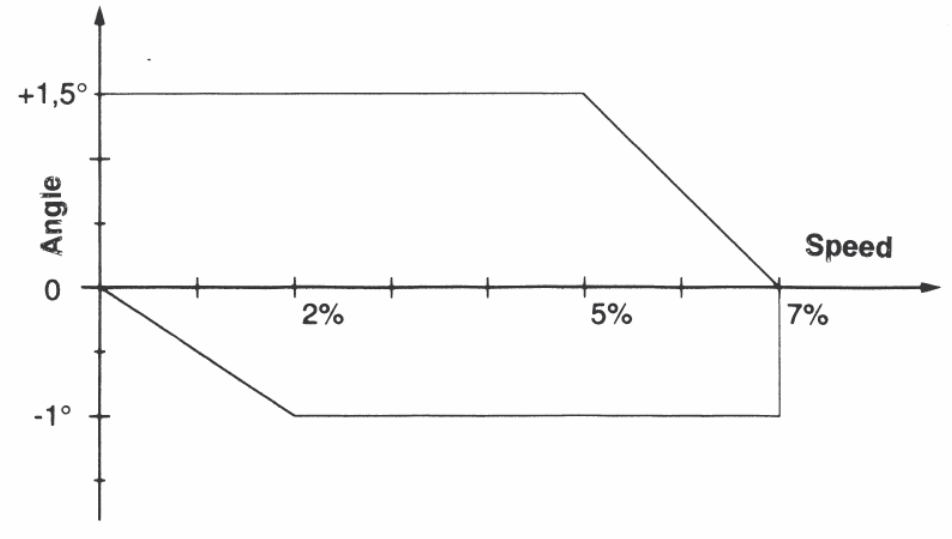

Figure A - 12 EN1317 tolérances sur l'angle et la vitesse d'impact

De même, des tolérances existent sur la masse du véhicule. Enfin, le modèle du véhicule et le point d'impact sont choisis par le laboratoire.

Le comportement d'une structure soumise à un impact de véhicule est caractérisé par ses modes de ruine dont l'activation dépend de nombreux paramètres soumis à des variations stochastiques. Lors de la mise au point d'un modèle numérique l'utilisation de valeur standard pouvant être significativement différentes des valeurs réelles

Par conséquent, il est évident qu'un seul résultat de simulation ne peut être suffisant pour la prédiction des performances d'un dispositif lors d'un essai de choc futur alors que seules les tolérances sur les conditions d'essai suffisent à la modifier significativement.
Lors d'un travail de corrélation, les conditions réelles d'essai sont connues mais un nombre important d'itérations est nécessaire afin de trouver le jeu de paramètres permettant de reproduire de manière correcte le comportement obtenu le jour de l'essai.

Enfin, la modélisation des essais de chocs sur équipements routiers présente des particularités rendant l'exercice particulièrement ardu :
Tout d'abord, la longueur du modèle (une centaine de mètres en moyenne) et la durée des chocs (de l'ordre de la seconde) nécessitent une recherche permanente du meilleur compromis entre la finesse de la modélisation et le temps de calcul.
De plus, les conditions limites (ancrages des supports, des extrémités…) et la définition même des modèles numériques peuvent avoir une incidence sur le résultat.
L'intérêt des outils numérique résulte en la possibilité de prendre en compte ces variabilités dans un premier temps pour être prédictif (en fournissant une plage de résultats possibles plutôt qu'un seul résultat) ou, dans un deuxième temps pour évaluer la robustesse d'une modification (la modification apporte-t-elle plus de sécurit que le dispositif original ?)

L'intérêt des méthodes numériques et leurs applications au domaine de l'infrastructure routière peuvent être illustrés par les nombreuses publications qui couvrent de nombreux champs; Du développement de nouveau produits [NCA09] et [NCA10-1&2], modification de produits existants [REI00], à des fins de recherche pour comparer des lois matériaux [YON05], afin d'étudier et optimiser l'absorption d'énergie [REI98] ou encore pour faire évoluer les standards normatifs [ANG09].

Dans la plupart des cas, une première étape consiste à étudier des phénomènes locaux à l'aide de modèles numériques très détaillés. Permettant de déterminer des plages de variations de certains paramètres (par exemple l'effet de la localisation du boulon dans un trou oblong sur l'effort nécessaire à déconnecter cette liaison).ou encore pour obtenir des caractéristiques équivalentes à entrer dans des macroéléments lors d'une modélisation globale.

Au niveau global (dispositif entier) les différents auteurs s'accordent sur la difficulté que présente la modélisation des liaisons boulonnées.

La corrélation de ces modèles globaux par rapports à des résultats expérimentaux est moins homogène.
Alors que les modèles locaux présentent généralement des corrélations obtenues à l'échelle du signal d'accélération, la corrélation des modèles globaux consiste à une juxtaposition d'images issues de l'essai de choc et du calcul et des comparaisons de courbes d'évolutions d'angles de rotation du véhicule en fonction du temps.

Dans de rares cas l'auteur présente des comparaisons de vitesses et encore plus rarement des comparaisons de signaux d'accélération. Dans ce dernier cas la concordance entre le signal expérimental et celui issu de la simulation devient arbitraire.

Certains auteurs [RAY96] ou [TAB00] ont propose des méthodes statistiques ou issues du traitement du signal mais, in fine, le jugement définissant si une valeur est acceptable ou non reste subjectif même si elle a le mérite d'être quantifiée.

Le groupe CEN TC226/WG1/TG5 a rédigé un document présentant des règles concernant la modélisation des véhicules dans le but de simuler des essais de chocs sur équipements routiers et sur la modélisation des équipements eux-mêmes. De plus des critères objectifs d'acceptation sont définis et des tolérances concernant la comparaison des courbes de vitesse du véhicule réel et numérique sont proposées.

L'utilisation de la simulation numérique dans le domaine des équipements de la route est de plus en plus nécessaire par les contextes économique et normatif complexes.
Une structure soumise à des chargements dynamiques est caractérisée par ses modes de ruines. Pour être fiable, un modèle numérique doit être capable de prédire l'apparition de ces modes de ruine.
L'analyse de la littérature a montré que de nombreux paramètres pilotent l'apparition de ces modes de ruines. DE nombreuses études réalisées sur des modèles locaux et corrélés sur des configurations expérimentales ont montré la très grande sensibilité de ces structures et qu'il est impossible de tous les maîtriser l'ensemble des paramètres. Des plages de variation sont proposées mais leur effet sur les performances de la structure globale ne sont jamais présentées.
En vue de modéliser les structures mixtes acier-bois, un modèle fiable du matériau bois qui, par nature est sensible aux variations de paramètres environnementaux, est nécessaire.
L'approche envisagée consiste en la réalisation d'essais de flexion dynamiques qui seront utiles pour évaluer la variation des propriétés mécaniques du bois, valider les modes de ruine d'un assemblage acier-bois et paramétrer une loi matériaux pour notre modèle numérique.
Enfin, l'effet des variations des caractéristiques mécaniques du matériau bois sur les performances d'un dispositif de retenue seront évaluées.

Chapitre 2 Essais dynamiques de flexion trois points

Matériel et méthodes

Des essais expérimentaux ont été effectués sur des éléments de structures en bois et sur des assemblages acier-bois.
Le but était de solliciter des éléments de structure identiques à ceux utilisés sur le bord des routes à des niveaux d'énergie suffisant pour provoquer la rupture des éléments.

Un total de vingt échantillons, dont les dimensions sont présentées Figure A - 13, a été testé.

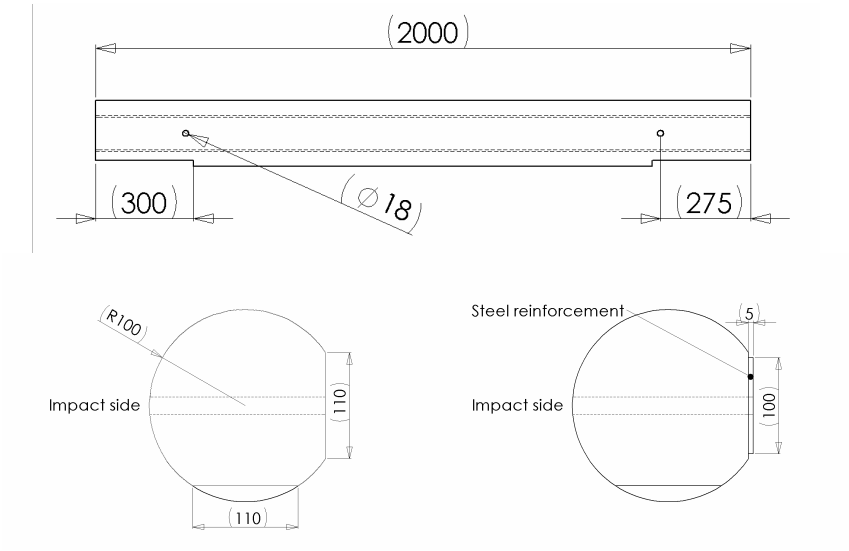

Figure A - 13 Dimensions des échantillons

Une attention particulière a été portée à l'évolution de la masse des différents échantillons au cours du temps ainsi qu'à la température ambiante et au taux d'humidité qui a été enregistré à plusieurs points de la poutre en bois.

Les tests ont été effectués sur le site de l'IFSSTAR à Bron avec un impacteur de deux tonnes mis en vitesse par une catapulte.

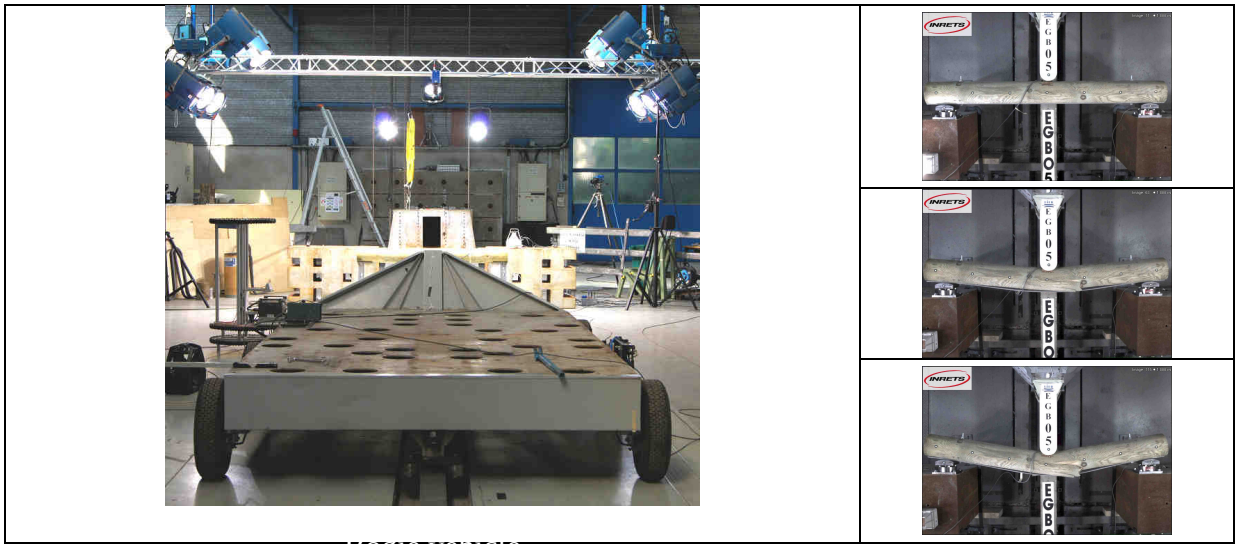

Figure A - 14 Configuration des essais

Trois niveaux de vitesse ont été choisis et chaque configuration a été testée trois fois afin d'évaluer la répétabilité.
Au total, vingt lancés ont été effectués suivant la matrice suivante:

Test	Type de structure	Vitesse d'impact
EGB 001	Bois	10 km/h
EGB 002	Bois	10 km/h
EGB 003	Bois	10 km/h
EGB 004	Bois+Acier	10 km/h
EGB 005	Bois+Acier	10 km/h
EGB 006	Bois+Acier	10 km/h
EGB 007	Bois	20 km/h
EGB 008	Bois	20 km/h
EGB 009	Bois	20 km/h
EGB 010	Bois	20 km/h
EGB 011	Bois+Acier	20 km/h
EGB 012	Bois+Acier	20 km/h
EGB 013	Bois+Acier	20 km/h
EGB 014	Bois	5 km/h
EGB 015	Bois	5 km/h
EGB 016	Bois	5 km/h
EGB 017	Bois+Acier	5 km/h
EGB 018	Bois+Acier	5 km/h
EGB 019	Bois+Acier	5 km/h
EGB 020	Bois	5 km/h

Table A - 34 Matrice d'essais

Les conditions d'impact étaient bien maîtrisées avec une très bonne répétabilité de la vitesse. La variance maximale relevée pour ce paramètre étant 4% pour les essais à faible vitesse sur échantillons acier-bois. Pour toutes les autres configurations la variance n'a jamais excédé 2%.

Les échantillons étaient prélevés dans le stock sans préparation ni contrôle préalable. Par conséquent la répartition des échantillons était arbitraire ainsi que les variances sur la masse des échantillons, leur taux d'humidité et la température.
La variance la plus importante concerne le taux d'humidité (27%) alors que la variance des autres paramètres n'excédait pas 5%.

Vitesse d'impact [km/h]		bois	Acier-bois
5	μ	-34.9	-37.4
	σ	2.4	1.5
	σ/μ	-7%	-4%
10	μ	-38.2	-44.4
	σ	3.4	5.1
	σ/μ	-9%	-12%
20	μ	-36.6	-46.7
	σ	2.7	3.1
	σ/μ	-7%	-7%

Table A - 35 Pics de décélération [mm/s²]

- Le tableau ci-dessus permet de mettre en évidence une différence significative entre les deux types de structures pour toutes les vitesses considérées.
- Cependant, aucune corrélation ne peut être trouvée entre la valeur du pic de décélération et la vitesse d'impact ni entre la variance des paramètres d'entrée et celles du pic de décélération.
- Les figures suivantes présentent les moyennes obtenues pour chaque structure pour les 3 niveaux de vitesse.

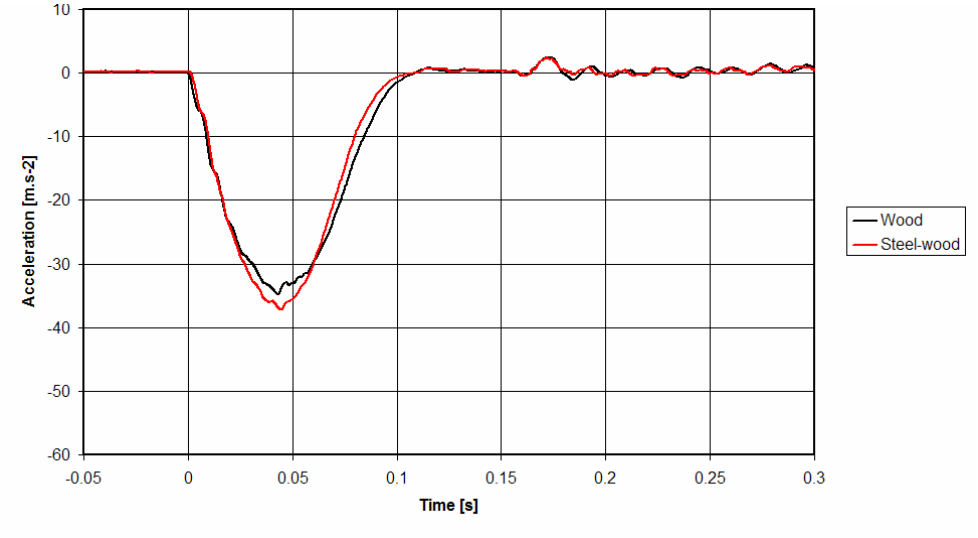

Figure A - 15 Moyennes des décélérations à 5 km/h

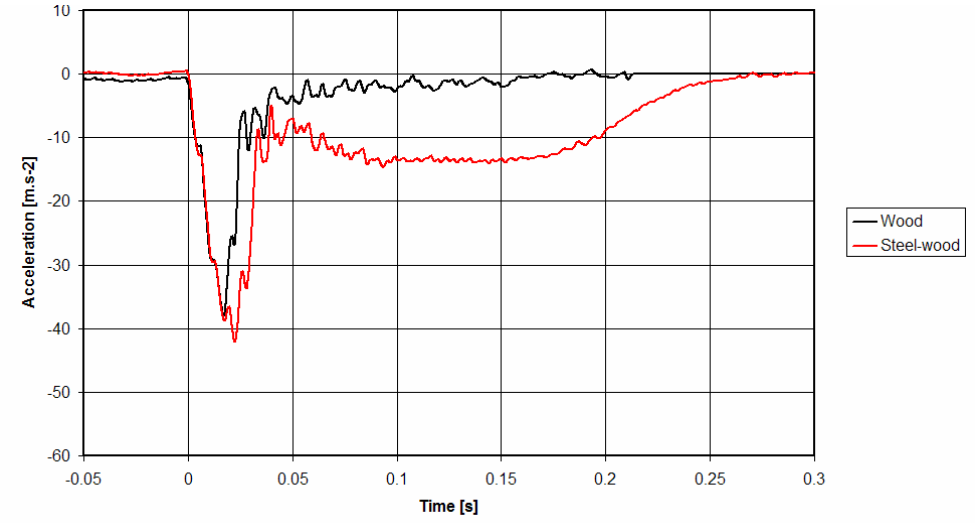

Figure A - 16 Moyennes des décélérations à 10 km/h

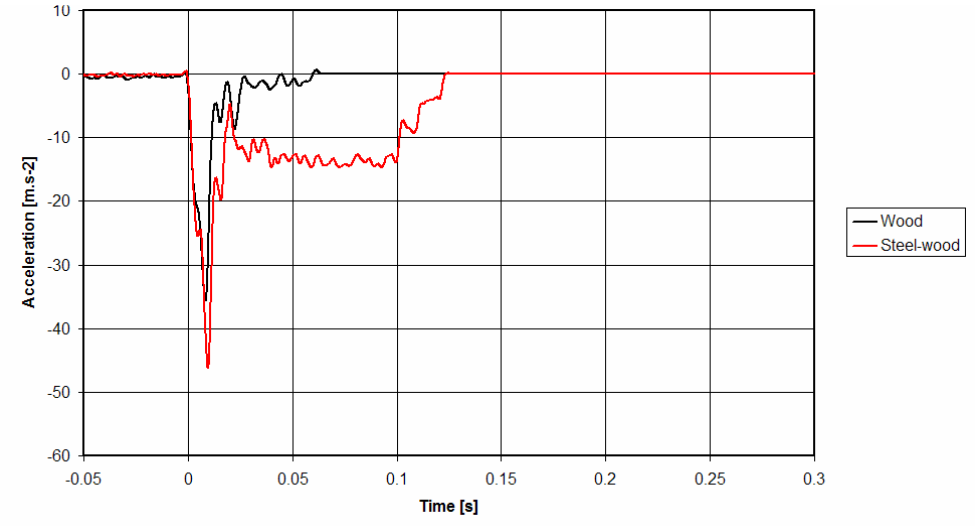

Figure A - 17 Moyennes des décélérations à 20 km/h

A 5 km/h, aucune rupture n'a été observée et les deux types structure présentent le même comportement. Pour les niveaux de vitesse supérieurs, la rupture des éléments de structure en bois permettent la plastification du renfort acier et un plateau de décélération est observé pour tous les échantillons acier-bois. Les pics de décélération pour ces deux vitesses supérieures ont des valeurs comparables alors que la largeur du pic est significativement plus faibles à 20 km/h.

Des essais dynamiques ont été effectués sur des échantillons de structure bois et acier-bois permettant l'étude des modes de ruine de ces structures soumises à des chargements dynamiques. Des courbes d'accélération ont été obtenues et seront utilisée afin de valider notre modèle numérique et la loi matériaux bois.

Chapitre 3 Simulation numérique des essais de flexion trois points

Le but de ce chapitre et de développer un modèle de la structure multi-matériaux testée et de la valider par rapport aux données expérimentales.
La configuration simple des essais effectués permet l'exploration de nombreux paramètres. Dans un premier temps, l'attention sera portée sur la convergence numérique du modèle. Dans un deuxième temps, une loi matériaux disponible dans Ls-Dyna sera évaluée dans le but de sélectionner les paramètres représentant le mieux les données expérimentales.

La loi matériaux disponible dans Ls-Dyna permet, de prendre en compte l'effet de la température et du taux d'humidité.

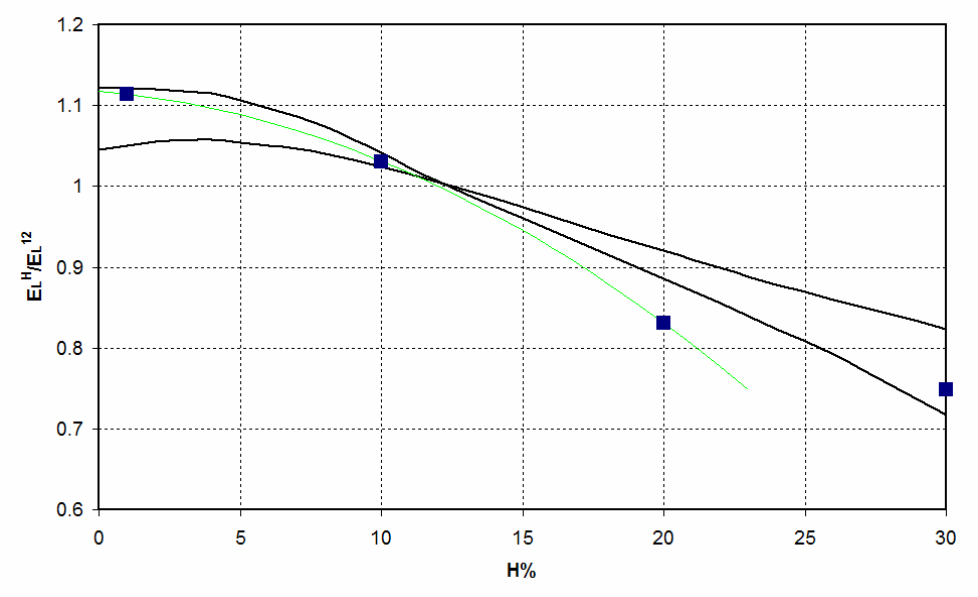

Figure A - 18 Effet du taux d'humidité

La figure ci-dessus présente en vert, le modèle implémenté, les carrés bleus correspondent aux valeurs tabulées utilisables et le corridor noir correspond à la littérature.

Cette loi permet également de prendre en compte des défauts du bois (les nœuds par exemple). L'approche utilisée consiste en l'application de facteurs de réduction appliqués aux caractéristiques mécaniques à la fois en tension et en compression selon le tableau ci-dessous.

Qualité	Qt	Qc
Bois sans défaut	1.00	1.00
Grade 1	0.80	0.93
Grade 0	0.47	0.63

Table A - 36 facteurs de réduction liés à la qualité du bois

Le tableau ci-dessous résume, pour le module élastique parallèle aux fibres, l'incidence de la température et de l'humidité :

		Température			
		1°C	**10°C**	**20°C**	**30°C**
Taux d'humidité	**1%**	17 024	16 883	16 720	16 552
	10%	16 091	15 823	15 471	15 063
	20%	13 456	13 037	12 468	11 790
	30%	12 740	12 105	11 236	10 194

Table A - 37 Module élastique parallèle en fonction de la température et de l'humidité

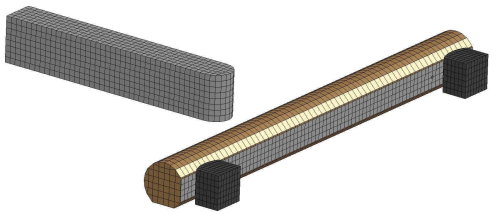

Figure A - 19 Vue générale du maillage

L'impacteur est considéré rigide et une vitesse initiale est appliquée en fonction de la configuration à simuler.les supports sont également modélisés rigides avec une condition d'encastrement avec blocage de l'ensemble des degrés de liberté.
La poutre en bois est modélisée avec des éléments brique et la loi matériaux bois décrite dans le paragraphe précédent est appliquée.
Des éléments sous-intégrés de type 1 "Constant Stress Solid" sont utilises sauf pour les configurations de référence ou des éléments à intégration complète type 2, « S/R solid » sont utilisés.
Le renfort métallique est modélisé par des coques de type 2 Belytschko-Tsay et une loi bi-linéaire élasto-plastique de type 24 (MAT_PIECEWISE_LINEAR_PLASTICITY) est appliquée.
Un effort particulier a été porté sur la modélisation de l'assemblage acier-bois. La solution retenue consiste en une représentation des vis par des éléments poutre en couplage de type Euler-Lagrange avec le matériau bois.

Model validation

Avant de valider la loi matériaux, il est apparu nécessaire de valider des aspects numériques du modèle.
Pour cela la configuration à 20 km/h a été retenue.
Deux types de maillage bois ont été étudiés : un maillage correspondant à une taille de maille standard pour des applications globales et un maillage deux fois plus fin.
Pour chaque type de structure (bois seul ou acier bois) et chaque type de maillage, une configuration de référence utilisant des éléments à intégration complète a été effectuée. Ensuite 4 coefficient de contrôle d'hourglass ont été étudiées (sans – 0.1%, 0.5% et 5%)

Pour chacune de ces configurations, 4 simulations avec les paramètres du bois correspondant aux combinaisons d'humidité et de température correspondant aux conditions expérimentales sont effectuées et moyennées.

La qualité numérique de chaque configuration est évaluée par deux critères :
L'erreur quadratique entre la moyenne de chaque configuration et sa configuration de référence (intégration complète).
Le rapport entre l'énergie d'hourglass et l'énergie interne pour le matériau bois.

Enfin, le coût en terme de temps de calcul est pris en compte, la solution retenue devant permettre la réalisation d'études paramétriques pour un modèle complet d'essai de choc sur dispositif de retenue de véhicule.

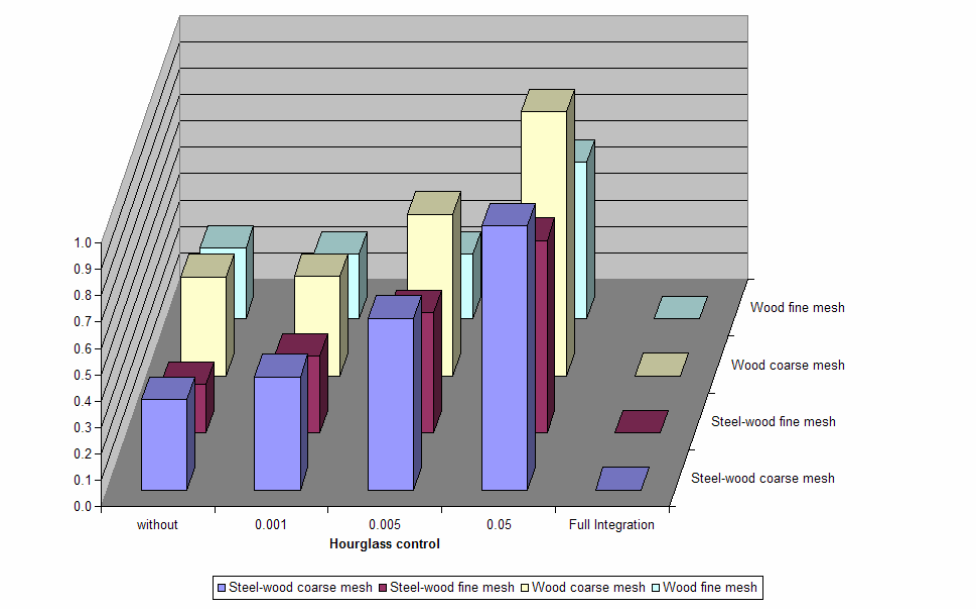

Figure A - 20 Erreur quadratique (référence Intégration complète)

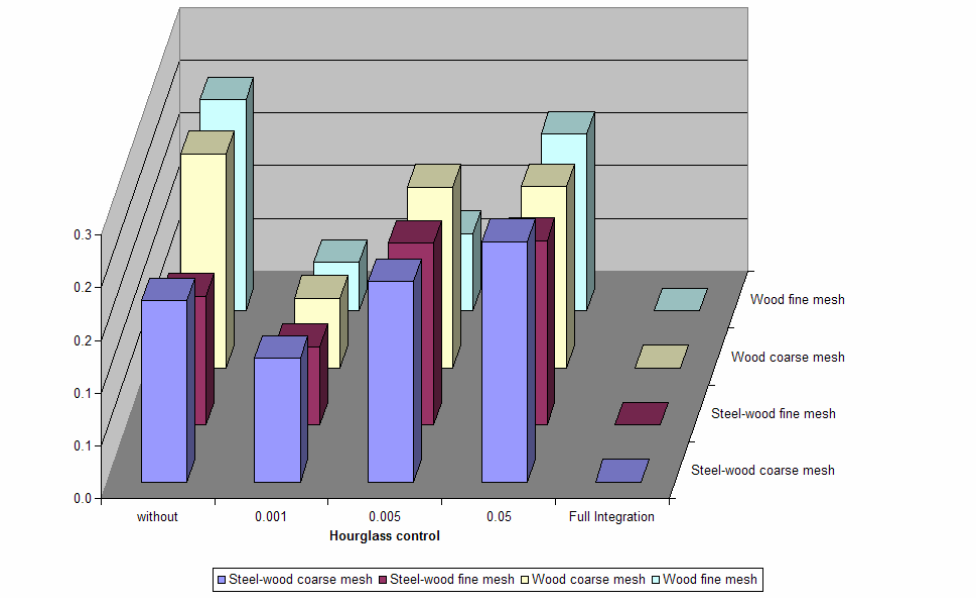

Figure A - 21 Rapport d'énergie

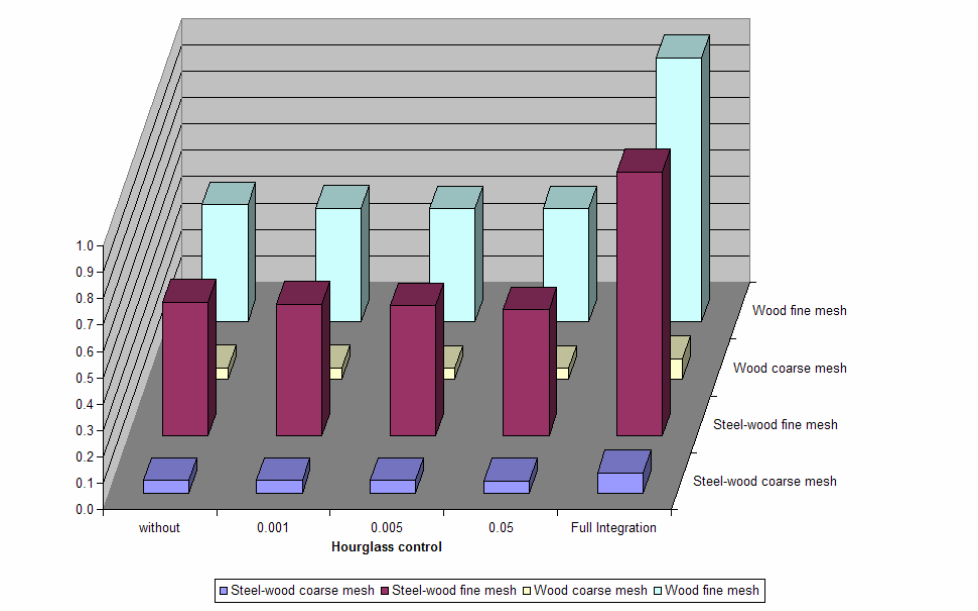

Figure A - 22 temps CPU

Les résultats démontrent que les simulations avec des éléments à intégration complète sont caractérisées par leur qualité numérique (pas d'énergie d'hourglass) mais également pas des temps de calculs rédhibitoires (Pour chaque configuration le temps de calcul est multiplié par deux).
Le maillage fin ne présente pas de meilleurs résultants que le maillage standard la seule différence notable résidant une nouvelle fois au niveau du temps de calcul.
Les simulations effectués avec des éléments sous intégrés et sans contrôle d'hourglass présentent des résultats étonnamment bons en terme de comparaison avec les simulations correspondante en intégration complète mais le critère d'énergie d'hourglass n'est pas acceptable.
Le control d'hourglass à 0.1% apparaît être un bon compromis entre le coût et la qualité numérique des résultats.

Evaluation de la loi matériau

Dans cette section, on s'intéresse à la validation de la loi matériaux et aux paramètres qui permettront de représenter les résultats expérimentaux.
Pour les deux structures, les trois niveaux de vitesse et les trois grades disponibles, quatre simulations sont effectuées (à l'instar de la section précédente pour encadrer les conditions d'humidité et de température expérimentales) et la moyenne des courbes de décélération est calculée et compare à la moyenne expérimentale correspondante.

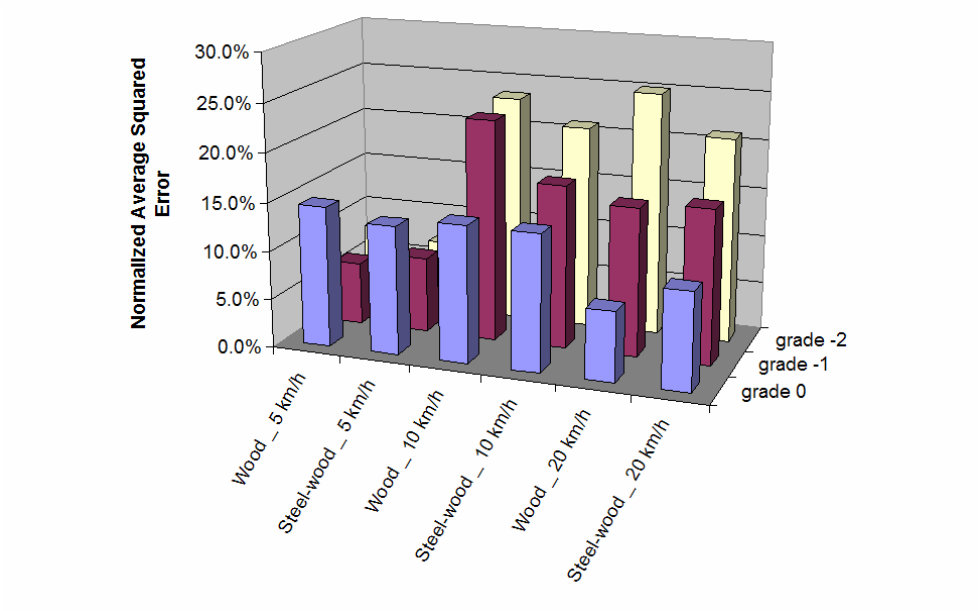

Figure A - 23 Erreur quadratique (référence expérimentale)

Le grade 0 est le grade qui représente le mieux les résultats expérimentaux notamment pour les vitesses d'impact les plus élevées.

Dans ce chapitre, des paramètres numériques ont été explorés afin d'obtenir un modèle qui combine qualité numérique et temps de calcul raisonnable.
Cette section a notamment mis en évidence que le contrôle d'hourglass avait un effet non négligeable sur les résultats des impacts simulés ici pour lesquels la distorsion des éléments situés au niveau de la rupture du bois peut piloter la dynamique globale de la séquence.
Un autre aspect important concernait la taille de maille. La taille utilisée couramment (30mm) est apparue suffisante/
Dans un deuxième temps la loi matériaux a été évaluée et le jeu de paramètre permettant de représenter les résultats expérimentaux a été défini.

Chapitre 4 Modélisation des essais de choc sur DDR

Dispositif

Le dispositif Solobois de la société SOLOSAR a été modélisé. Les caractéristiques géométriques de ce dispositif sont présentées dans la figure suivante.

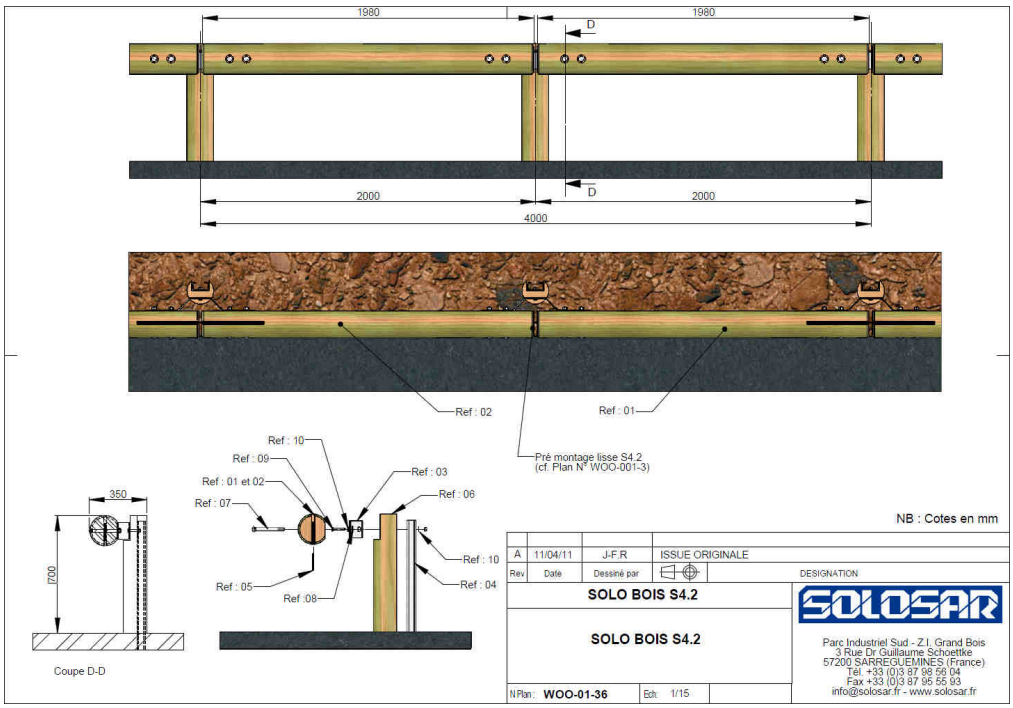

Figure A - 24 Plans du dispositif

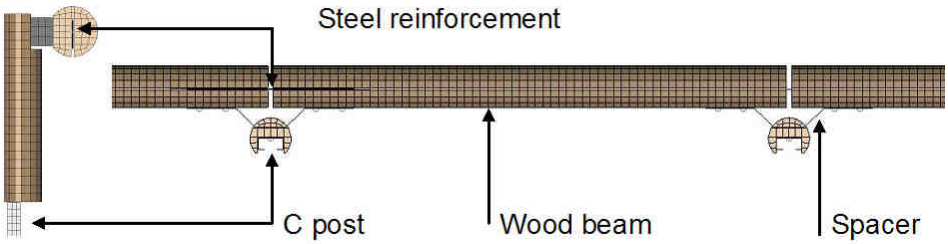

Figure A - 25 Présentation du modèle éléments finis

Le modèle numérique du dispositif a été construit en utilisant les mêmes techniques et les mêmes caractéristiques que celles utilisées dans le chapitre précédent.

Afin de valider le modèle numérique et de le corréler aux résultats obtenus lors de l'essai de choc, une méthode fondée sur l'analyse des modes de ruine et une approche paramétrique est proposée.

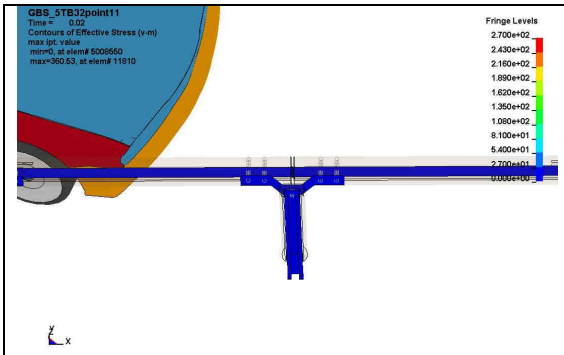	Etat initial
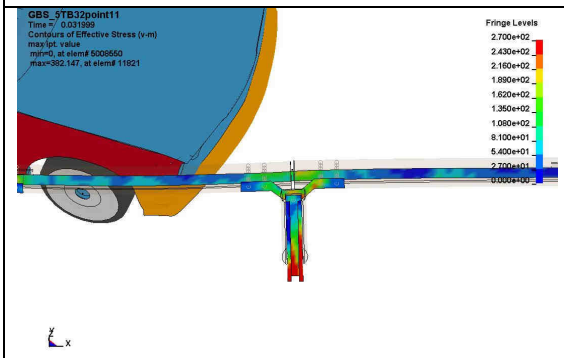	Formation d'une charnière plastique à la base du support
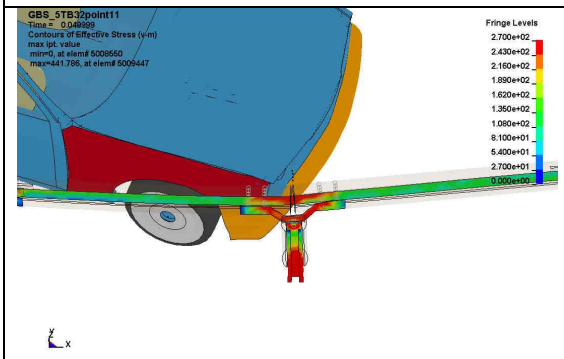	Formation d'une charnière plastque au niveau de l'articulation
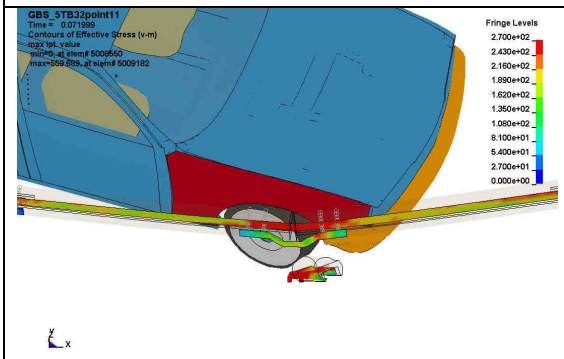	Rupture de la liaison support/lisse

Table A - 38 Identification des modes de ruine

L'analyse des modes de ruine permet l'identification de trois paramètres. Pour chaque paramètre une plage de variation est choisie et un plan d'expérience factoriel est réalisé.

Mode de ruine	Paramètre physique	Valeurs
Charnière plastique du support	Limite élastique de l'acier	240 – 270 – 300 MPa
Plastification de l'articulation	Limite élastique de l'acier	240 -270 -300 MPa
Rupture de vis	Force à rupture	33700 - 37950 – 42200 N

Table A - 39 Modes de ruine et plage de variation

Les résultats en termes de déflexion et de sévérité sont présentés dans la figure ci-dessous.
Le carré noir correspond à l'essai de choc, le rectangle rouge correspond aux tolérances définies par la norme EN1317.

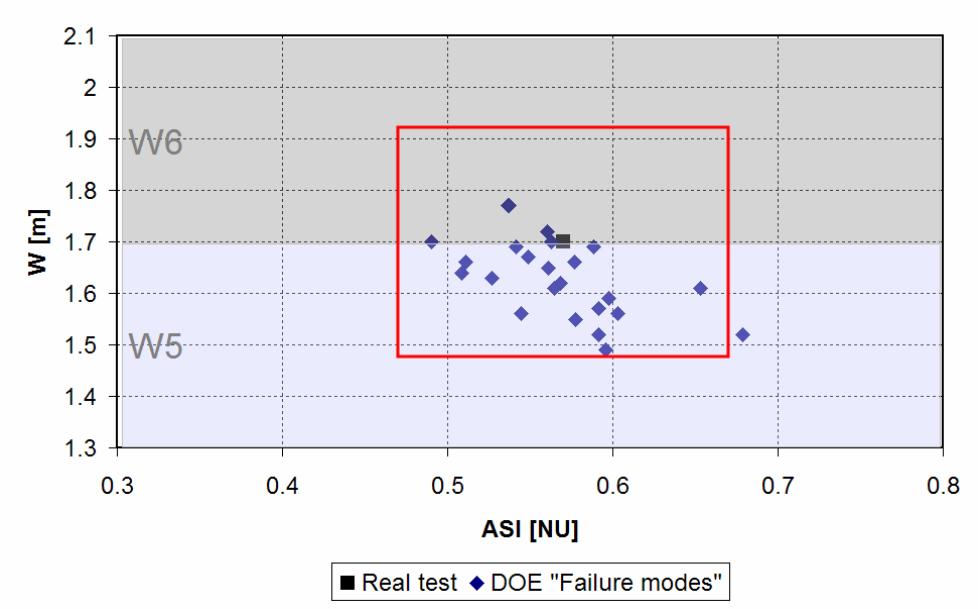

Figure A - 26 EN1317 Critères

Enfin, les composantes de la vitesse de véhicule sont calculées pour chaque simulation et compares à la courbe expérimentale ce qui permet de trouver un jeu de paramètre représentant le mieux la configuration testée.

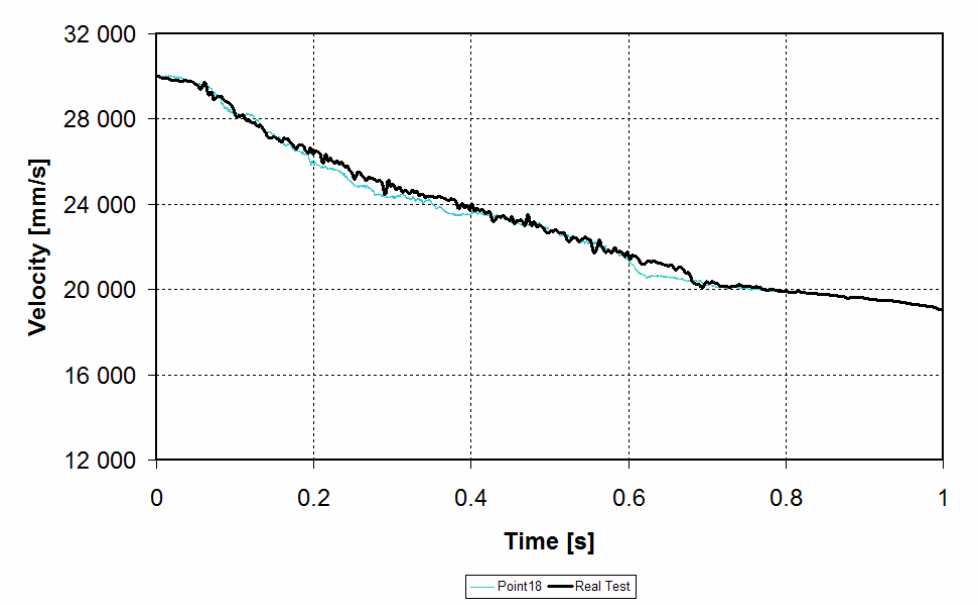

Figure A - 27 Composante X de la vitesse – Meilleure corrélation

Evaluation de l'effet de la variation des caractéristiques mécaniques du bois

La configuration retenue dans le paragraphe précédant permet de satisfaire l'ensemble des critères de validation définis par le TG5.
Le modèle peut maintenant être utilisé pour évaluer l'incidence des modifications des caractéristiques mécaniques du bois liées aux modifications des conditions de température et d'humidité.
Un plan d'expérience factoriel sur l'ensemble des 16 combinaisons offertes par la loi disponible dans LS-Dyna est effectué et les résultats sont présentés sur la figure suivante.

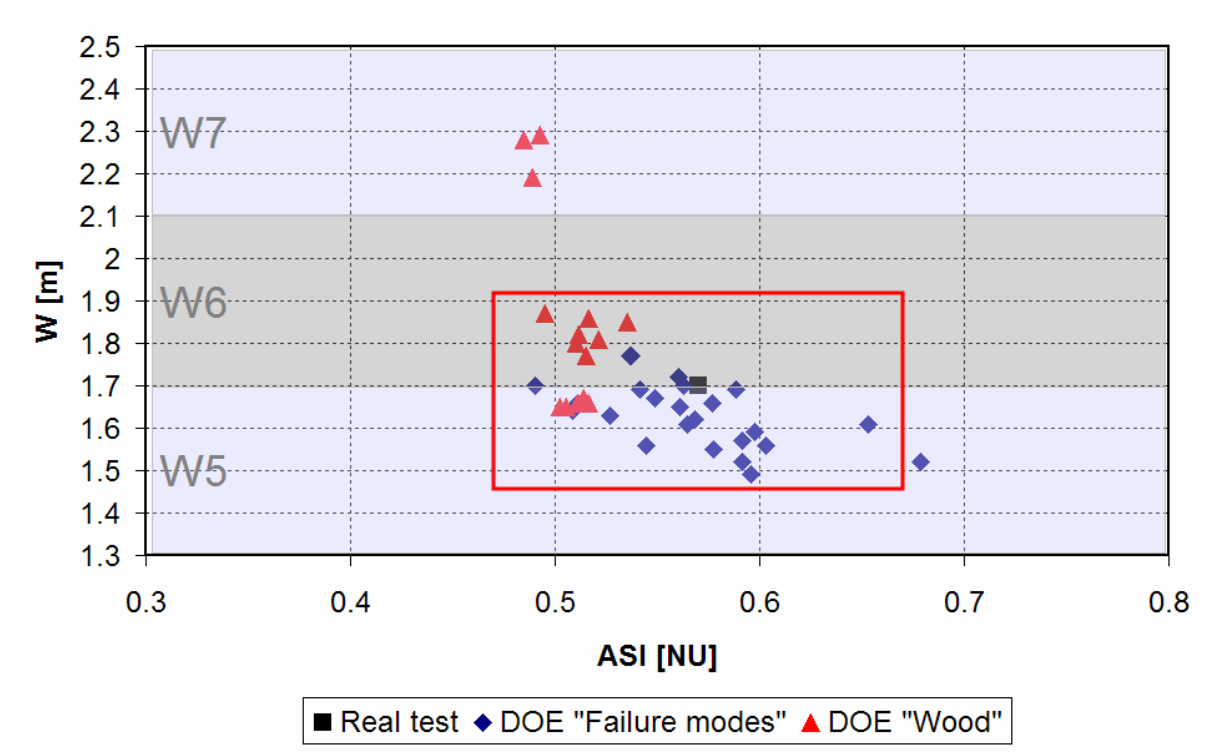

Figure A - 28 Plan d'expérience BOIS – Critères EN1317

Bien que la variation des propriétés mécaniques soit d'environ 20% l'effet obtenu sur la sévérité est très faible (3%)/
L'effet le plus important est sur la mesure de la largeur de fonctionnement. En effet, le comportement fragile observé pour les températures et taux d'humidité faibles provoquent des ruptures de poutres ayant une incidence directe sur la mesure.

La redirection d'un véhicule lors d'un essai de choc sur un dispositif de retenue de véhicule est obtenue grâce à une séquence d'événement appelés modes de ruine. Ces modes de ruine sont facilement identifiables sur les films à haute vitesse ou encore grâce à une étude numérique.
L'apparition d'un mode de ruine est généralement liée à un paramètre physique sujet à des variations stochastiques. Les matériaux utilisés pour les équipements routiers présentent habituellement des variations très importantes de leurs caractéristiques mécaniques.
C'est la raison pour laquelle les simulations effectuées avec des valeurs standard donnent lieu à des corrélations médiocres.
L'approche paramétrique présentée dans ce chapitre est une méthode pour identifier le jeu de paramètre permettant l'obtention d'une bonne corrélation avec l'essai de choc réel.
De plus, l'approche paramétrique permet l'évaluation de la robustesse d'un dispositif qui ne peut pas être évaluée par des essais de choc pour des raisons économique d'une part et d'autre part car l'ensemble des paramètres ne peut être contrôlé.
Enfin, cette méthode peut être appliquée pour évaluer l'incidence d'autres paramètres.
Par exemple, cette approche a été utilisée afin d'évaluer l'incidence de la variation des caractéristiques mécaniques du bois qui s'est avérée très limitée.
Les simulations effectuées avec des valeurs basses de la température et du taux d'humidité font apparaître un comportement fragile du vois et la rupture des poutres de bois affecte la mesure de la largeur de fonctionnement sans pour autant altérer le fonctionnement du dispositif et l'efficacité de la redirection.

Conclusion

L'utilisation de la simulation numérique dans le cadre de la sécurité routière a augmenté durant les dix dernières années et son utilisation dans le processus de certification est actuellement en discussion au niveau Européen.
De nos jours, les modèles numériques sont supposés être prédictifs.
Une bonne prédiction de peut pas être obtenue sans une approche paramétrique prenant en compte les paramètres connus pour présenter une variation stochastique tels que les caractéristiques mécaniques des matériaux ou même les conditions d'impact.
La pertinence d'une telle approche repose sur la connaissance de la plage de variation de ces paramètres.
Ce travail s'est intéressé spécifiquement aux dispositifs de retenue de véhicule mixte acier-bois. Ces dispositifs présentent un intérêt esthétique mais souffrent de la réputation du bois d'être hétérogène, sensible aux variables d'environnement et, donc, peu fiable.
Le but était donc de développer un modèle fiable incluant la modélisation du bois comme un matériau anisotrope, son couplage avec l'acier ainsi que ses variations de propriétés mécaniques liées à son hétérogénéité et sa sensibilité aux variables d'environnement.
Des essais dynamiques de flexion trois point ont été effectués à trois niveaux de vitesse sur des éléments de structure de dispositif de retenue.
Pendant ces essais une attention particulière a été portée sur la mesure des paramètres de température et de taux d'humidité du bois.
Ces essais ont permis d'obtenir des courbes de décélération de l'impacteur nécessaire à la validation des modèles numériques.
Ces essais expérimentaux ont été modélisés. Etant donnée la simplicité de la configuration, la taille du modèle obtenu a permis d'explorer de nombreux paramètres numériques (taille de maille, formulation d'élément, contrôle d'hourglass, contrôle du pas de temps). Des améliorations ont également pu été apportées au niveau de la modélisation de l'assemblage bois-métal. Enfin, ces configurations ont permis la validation de la loi matériau bois disponible dans Ls-Dyna et l'identification d'un jeu de paramètres représentant le mieux le bois utilisé durant les expérimentations.
Un modèle d'un dispositif de retenue de véhicules mixte a ensuite été réalisé. La validation de ce modèle par rapport à des résultats d'essais de choc a été effectuée en suivant une approche paramétrique fondée sur l'analyse des modes de ruine de la structure et sur la variation des paramètres physiques associés.
Le modèle validé a ensuite été utilisé afin d'étudier l'effet de la variabilité du bois sur les performances du dispositif.
Pour le dispositif modélisé, l'utilisation du bois peut être qualifiée de « sûre » car les variations des caractéristiques mécaniques du bois ont un effet très limité sur les performances du dispositif. Seule la mesure de la largeur de fonctionnement est affectée par le comportement fragile du bois qui apparaît pour les valeurs faibles de température et de taux d'humidité.
Une première perspective de ce travail est l'intégration de cette approche dans le processus de certification de produits modifiés par simulation numérique. En effet, la réalisation d'études paramétriques permettrait de comparer des nuages de points entre le dispositif initial et le dispositif modifié et offrirait la possibilité de définir des critères d'acceptation des modifications.
Une deuxième perspective consiste en l'optimisation de l'utilisation du bois dans les dispositifs de retenue de véhicule. Les méthodes proposées dans ce travail pourraient être appliquées à d'autres dispositifs et le lien entre les largeurs de fonctionnement et les caractéristiques dimensionnelles des poutres en bois pourrait être étudié. La réduction des caractéristiques inertielles sans modification de l'aspect esthétique, couplée à l'étude de la position du renfort métallique permettrait l'optimisation des performances de ces dispositifs et une meilleure utilisation du bois.

Appendix 5: List of publications

International journal peer reviewed

C. Goubel, M. Massenzio & S. Ronel (2011): Wood–steel structure for roadside safety barriers, International Journal of Crashworthiness, DOI:10.1080/13588265.2011.625678

C. Goubel, M. Massenzio & S. Ronel: Consideration of wood mechanical properties variation in roadside safety barriers performances evaluation, International Journal of Crashworthiness (On going: Submitted)

International conferences

C. Goubel, E. Di Pasquale, M. Massenzio, S. Ronel, Comparison of crash tests and simulations for various vehicle restraint systems, 7th European LS-DYNA Users Conference, May 14-15, 2009, Salzburg, Austria

C. Goubel, M. Massenzio & S. Ronel, Wood–steel structure for roadside safety barriers, International Crashworthiness Conference, September 22-24, 2010, Washington DC, USA

C. Goubel, M. Massenzio, S. Ronel, Wood-steel structure for vehicle restraint systems, 8th European LS-DYNA Users Conference, May 23-24, 2011, Strasbourg, France

C. Goubel, E. Di Pasquale, Robust prediction and validation from vehicle restraining systems simulations, 3rd International Conference on Impact Loading of Lightweight Structures, June 28th-July 1st, 2001, Valenciennes, France

C. Goubel, M. Massenzio, S. Ronel, Consideration of wood mechanical properties variation in vehicle restraining systems design, 3rd International Conference on Impact Loading of Lightweight Structures, June 28th-July 1st, 2001, Valenciennes, France

C. Goubel, M. Massenzio & S. Ronel: Consideration of wood mechanical properties variation in roadside safety barriers performances evaluation, International Crashworthiness Conference, July 18-20, 2012, Milan, Italy